



**BACHELOR THESIS – ME141501**

**DESIGN DEVELOPMENT OF WAVE ENERGY  
CONVERSION SYSTEM HEXAGONAL PONTON**

**AZZAHRA NIRWANA ISLAMI**  
**NRP: 04211541000049**

**Supervisor:**  
**Irfan Syarif Arief, S.T., M.T.**  
**Achmad Baidowi, S.T., M.T.**

**DEPARTMENT OF MARINE ENGINEERING**  
**FACULTY OF MARINE TECHNOLOGY**  
**INSTITUT TEKNOLOGI SEPULUH NOPEMBER**  
**SURABAYA**  
**2019**





**BACHELOR THESIS – ME141501**

**DESIGN DEVELOPMENT OF WAVE ENERGY  
CONVERSION SYSTEM WITH HEXAGONAL PONTON**

**AZZAHRA NIRWANA ISLAMI**  
**NRP: 04211541000049**

**Supervisor:**

**Irfan Syarif Arief, S.T., M.T.**

**Achmad Baidowi, S.T., M.T.**

**DEPARTMENT OF MARINE ENGINEERING  
FACULTY OF MARINE TECHNOLOGY  
INSTITUT TEKNOLOGI SEPULUH NOPEMBER  
SURABAYA  
2019**

“This page is intentionally left blank”

**ENDORSEMENT PAGE**

**DESIGN DEVELOPMENT OF WAVE ENERGY CONVERSION  
SYSTEM WITH HEXAGONAL PONTON**

**BACHELOR THESIS**

Submitted to Comply the Requirement to Obtain a Bachelor of  
Engineering Degree  
On

Marine Manufacturing & Design (MMD)  
Bachelor Program Department of Marine Engineering  
Faculty of Marine Technology  
Institut Teknologi Sepuluh Nopember

Prepared by:

**AZZAHRA NIRWANA ISLAMI**  
NRP. 04211541000049

Approved by Supervisor:

**Irfan Syarif Arief, S.T., M.T.**

(  )

**Achmad Baidowi, S.T., M.T.**

(  )

“This page is intentionally left blank”

**ENDORSEMENT PAGE**

**DESIGN DEVELOPMENT OF WAVE ENERGY CONVERSION  
SYSTEM WITH HEXAGONAL PONTON  
BACHELOR THESIS**

Submitted to Comply the Requirement to Obtain a Bachelor of  
Engineering Degree

On

Marine Manufacturing & Design (MMD)  
Bachelor Program Department of Marine Engineering  
Faculty of Marine Technology  
Institut Teknologi Sepuluh Nopember

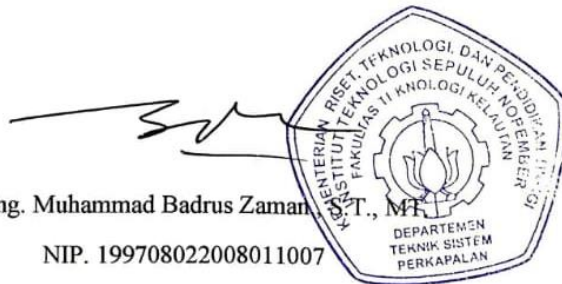
Prepared by:

**AZZAHRA NIRWANA ISLAMI**  
NRP. 04211541000049

Approved by

Head of Department of Marine Engineering

Dr. Eng. Muhammad Badrus Zaman  
NIP. 199708022008011007



“This page is intentionally left blank”



**ENDORSEMENT PAGE**

**DESIGN DEVELOPMENT OF WAVE ENERGY CONVERSION  
SYSTEM WITH HEXAGONAL PONTON  
BACHELOR THESIS**

Submitted to Comply the Requirement to Obtain a Bachelor of  
Engineering Degree

On

Marine Manufacturing & Design (MMD)  
Bachelor Program Department of Marine Engineering  
Faculty of Marine Technology  
Institut Teknologi Sepuluh Nopember

Prepared by:

**AZZAHRA NIRWANA ISLAMI**  
NRP. 04211541000049

Approved by

Representative of Hochschule Wismar in Indonesia



Dr.-Ing. Wolfgang Busse

“This page is intentionally left blank”

# DESIGN DEVELOPMENT OF WAVE ENERGY CONVERSION SYSTEM WITH HEXAGONAL PONTON

**Name** : Azzahra Nirwana Islami  
**Reg. Number** : 04211541000049  
**Department** : Marine Engineering  
**Supervisor** : Irfan Syarif Arief, S.T., M.T.  
Achmad Baidowi, S.T., M.T.

## ABSTRACT

The wave energy conversion system is one of the technology innovative used in the researches of alternative power plant at sea. It receives environmental loads such as wave, wind, and current during its operation. In order to be able to rotate the pendulum and produce electricity, it is designed with a hexagonal shaped ponton with three floaters on its sides to increase the rotational motion of the ponton. These floaters are connected to the ponton by an arm, identically distance from one another. Mooring system used in this research is designed to allow it to still move and rotate the pendulum while keeping the platform from capsizing. This research is discussing about the difference of motion response between three variations of wave energy conversion system designs, Variation 1 that is designed with floaters, Variation 2 with shortened floater arms, and Variation 3 which have no floaters, by comparing their RAOs (Response Amplitude Operator), to figure out which design is the most responsive when collinear load from heading  $0^\circ$ ,  $30^\circ$ ,  $60^\circ$ ,  $90^\circ$ , and  $120^\circ$  is acting on it. This research reveals that model Variation 1 is the most optimal because it has relatively higher values of RAOs, and the motion response of the ponton is still apparent after mooring system is installed. The highest RAO in free floating condition for 6 degree of freedom surge, sway, heave, pitch, roll, and yaw are 1,949 m/m frequency 0,1 Rad/s heading  $0^\circ$ , 1,6 m/m frequency 1,7 Rad/s heading  $60^\circ$ , 0,998 m/m frequency 0,1 Rad/s heading  $0^\circ$ , 22,13 Deg/m frequency 1,8 Rad/s heading  $60^\circ$ , 21,7 Deg/m frequency 2 Rad/s heading  $0^\circ$ , and 77,212 deg/m frequency 1,8 deg/m heading  $0^\circ$  consecutively. The furthest excursion is at 5,1 meters along x-axis  $0^\circ$  load, while the shortest excursion is 1,5 meters along y-axis  $120^\circ$  load. The highest Roll motion reached  $62,5^\circ$  along the x-axis  $90^\circ$  load while pitch motion reached  $15,5^\circ$  along y-axis  $120^\circ$  load.

**Keywords**—*Hexagonal Ponton, Motion, RAO, Wave Energy Conversion System.*

“This page is intentionally left blank”

## PENGEMBANGAN DESAIN PEMBANGKIT LISTRIK GELOMBANG LAUT DENGAN PONTON BERBENTUK HEXAGON

**Nama** : Azzahra Nirwana Islami  
**NRP** : 0421154100049  
**Departemen** : Teknik Sistem Perkapalan  
**Pembimbing 1** : Irfan Syarif Arief, S.T., M. T.  
**Pembimbing 2** : Achmad Baidowi, S.T., M.T.

### ABSTRAK

Pembangkit Listrik Gelombang Laut adalah salah satu teknologi inovatif yang digunakan dalam penelitian pembangkit listrik alternatif di laut. Ia menerima beban lingkungan seperti gelombang, angin, dan arus ketika beroperasi. Agar dapat memutar pendulum dan menghasilkan listrik, ia dirancang dengan ponton berbentuk heksagonal yang memiliki tiga *floaters* di sisinya untuk meningkatkan gerakan rotasi ponton. *Floater* tersebut terhubung ke ponton pada sebuah lengan, yang berjarak simetris antara satu dengan yang lainnya. Sistem tambat yang digunakan dalam penelitian ini dirancang untuk memungkinkan ponton tetap bergerak dan memutar pendulum sambil menjaga agar ia tidak tenggelam terbawa arus atau terhempas gelombang. Penelitian ini membahas tentang perbedaan respons gerak antara tiga variasi desain pembangkit listrik gelombang laut, Variasi 1 yang dirancang dengan *floaters*, Variasi 2 dengan panjang lengan *floater* yang dikurangi, dan Variasi 3 yang tidak memiliki *floaters*, dengan membandingkan RAO (*Respon Amplitude Operator*) mereka, untuk mengetahui desain mana yang paling responsif ketika beban *collinear* dari arah  $0^\circ$ ,  $30^\circ$ ,  $60^\circ$ ,  $90^\circ$ , dan  $120^\circ$  mengenainya. Penelitian ini mengungkapkan bahwa model Variasi 1 adalah yang paling optimal karena ia memiliki nilai RAO yang relatif lebih tinggi, dan respons gerak ponton pun masih terlihat setelah sistem tambat dipasang. RAO tertinggi dalam kondisi mengambang bebas untuk 6 *Degree of Freedom*, *Surge*, *Sway*, *Heave*, *Pitch*, *Roll*, dan *Yaw* masing-masing adalah 1.949 m/m frekuensi 0,1 Rad/s arah beban  $0^\circ$ , 1,6 m/m frekuensi 1,7 Rad/s arah beban  $60^\circ$ , 0,998 m/m frekuensi 0,1 Rad / s arah beban  $0^\circ$ , 22,13 Deg/m frekuensi 1,8 Rad/s arah beban  $60^\circ$ , 21,7 Deg/m frekuensi 2 Rad/s arah beban  $0^\circ$ , dan 77.212 deg/m frekuensi 1,8 deg/m arah beban  $0^\circ$ . Ekskursi ponton yang terbesar adalah sejauh 5,1 meter sepanjang sumbu x dari arah beban  $0^\circ$ , sedangkan ekskursi terkecil adalah 1,5 meter sepanjang sumbu y arah beban  $120^\circ$ . Gerakan *Roll* tertinggi mencapai  $62,5^\circ$  arah beban  $90^\circ$ , sementara gerakan *pitch* mencapai  $15,5^\circ$  arah beban  $120^\circ$ .

**Kata kunci-** *Pembangkit Listrik Tenaga Gelombang, Ponton Heksagon, Respon Gerak.*

“This page is intentionally left blank”

## PREFACE

The author would like to show gratitude to Allah SubhaanAllahu Ta'aalaa, for the knowledge, time, strength, and willingness to complete the study and write this bachelor thesis. May this research be useful in the future.

The author would like to say her warmest gratitude to everyone who helped the writer throughout this journey.

1. Author's dearest parents and brothers, who have been giving abundant support and motivation for the author.
2. Bapak Irfan Syarief Arief, S.T., M.T. as the head of MMD Lab for providing learning facilities for the author.
3. Bapak Achmad Baidowi, S.T., M.T. as the writer's supervisor for the patience in giving guidance for the author.
4. Favi Ainin for the kindness to tutor the author during her busy time.
5. Author's dearest friends who have been supporting the author in her hardest times.
6. Fellow MMD Staffs who have been very supportive to the author.

This research remains away from perfection, therefore, any critique and suggestions are welcomed in hopes for improvements in the future. May Allah bless everyone who is involved with this research.

“This page is intentionally left blank”



# Table of Contents

<b>ENDORSEMENT PAGE</b> .....	i
<b>ENDORSEMENT PAGE</b> .....	<b>Error! Bookmark not defined.</b>
<b>ENDORSEMENT PAGE</b> .....	iii
<b>ABSTRACT</b> .....	vii
<b>ABSTRAK</b> .....	ix
<b>PREFACE</b> .....	xi
<b>Table of Contents</b> .....	xiii
<b>List of Table</b> .....	xvii
<b>List of Figures</b> .....	xix
<b>Chapter 1</b> .....	1
<b>Introduction</b> .....	1
<b>1.1 Background</b> .....	1
<b>1.2 Problem Identification</b> .....	2
<b>1.3 Research Objectives</b> .....	2
<b>1.4 Research Limitation</b> .....	2
<b>1.5 Benefit of Research</b> .....	2
<b>Chapter 2</b> .....	3
<b>Study Literature</b> .....	3
<b>2.1 Wave Energy</b> .....	3
<b>2.2 Wave Generated Power Plant</b> .....	4
<b>2.3 Previous Research</b> .....	5
<b>2.4 Theory of Floating Structures and Motion Response</b> .....	7
<b>2.4.1 Floating Structure Stability</b> .....	7
<b>2.4.2 Six Degrees of Freedom</b> .....	7
<b>2.5 Response Amplitude Operator (RAO)</b> .....	8
<b>2.6 Response of Floating Structures to Irregular Waves</b> .....	9
<b>2.7 Spectrum of Wave</b> .....	10
<b>2.8 Joint North Sea Wave Project (JONSWAP) Spectrum</b> .....	11
<b>2.9 Environmental Loads</b> .....	11
<b>2.10 Mooring Configuration for Floating Structures</b> .....	11

2.10.3	<b>Spread Mooring</b> .....	13
2.10.4	<b>Determining Length of Mooring Line</b> .....	14
2.10.5	<b>Excursion</b> .....	14
2.11	<b>MOSES</b> .....	15
<b>Chapter 3</b>	.....	17
<b>Research Methodology</b>	.....	17
3.1	<b>Problem Identification</b> .....	18
3.2	<b>Literature Study</b> .....	18
3.3	<b>3D Numerical Model of the Ponton</b> .....	18
3.4	<b>Simulation using MOSES</b> .....	19
3.4.1	<b>Input of Parameters</b> .....	19
3.4.2	<b>Sea Keeping Simulation</b> .....	20
<b>Chapter 4</b>	.....	23
<b>Data Analysis</b>	.....	23
4.1	<b>Data of Ponton for 3D Numerical Modelling</b> .....	23
4.1.1	<b>The Main Dimension of Ponton</b> .....	23
4.2	<b>3D Numerical Modelling of Ponton</b> .....	23
4.2.1	<b>Design Variation 1</b> .....	23
4.2.2	<b>Design Variation 2</b> .....	25
4.2.3	<b>Design Variation 3</b> .....	26
4.3	<b>Modelling in Moses</b> .....	27
4.4	<b>Motion Response Analysis</b> .....	28
4.4.1	<b>Motion Analysis of Variation 1</b> .....	29
4.4.2	<b>Motion Response Analysis of Model Variation 3</b> .....	41
4.5	<b>Mooring System Analysis</b> .....	47
4.5.1	<b>Analysis of Ponton Excursion</b> .....	48
4.5.2	<b>Analysis of Ponton Motion</b> .....	49
4.5.3	<b>Analysis of Mooring Line Tension</b> .....	50
4.5.4	<b>Safety Factor Calculation</b> .....	50
<b>Chapter 5</b>	.....	51

**Conclusions and Suggestion..... 51**  
    **5.1 Conclusion..... 51**  
    **5.2 Suggestion ..... 51**  
**References ..... 53**  
**AUTHOR BIOGRAPHY ..... 99**

“This page is intentionally left blank”

## List of Table

Table 3.1. Parameter input for Seakeeping Simulation.....	20
Table 4.2. Principal Dimension of the unit .....	23
Table 4.3. Calculation from modelling Variation 1 in Solidwork.....	24
Table 4. 4. Calculation from modelling Variation 2 in Solidwork.....	26
Table 4.5. Calculation from modelling Variation 3 in Solidwork.....	27
Table 4.6 Excursion Analysis of Ponton with mooring system. ....	48
Table 4.7. Motion Analysis of Ponton with mooring system.....	49
Table 4.8 Data of Mooring Line Effective Tension at End A and B.....	50

“This page is intentionally left blank”

## List of Figures

Figure 2.1. The comparison of alternative energy power output .....	3
Figure 2.2. diagram of an oscillating water column. ....	4
Figure 2.3. Diagram of Overtopping Devices (OTD) .....	5
Figure 2.4. Wave Activated Bodies (WAB). ....	5
Figure 2.5 Prototype of Tripod Ponton in Tanjung Bumi .....	6
Figure 2.6 Model of Tripod Ponton in wave tank of Indonesian Hydrodynamics Laboratory. .....	6
Figure 2.7. Floating structure stability.....	7
Figure 2.8. Diagram of six degrees of freedom on a ship. ....	8
Figure 2.9. common spectrum of wave .....	10
Figure 2.10. Wave Spectrums .....	11
Figure 2.11. Catenary mooring system configuration.....	12
Figure 2.12. Taut leg mooring .....	13
Figure 2.13. spread mooring.....	14
Figure 4.14. Perspective view of Design variation 1 in Solidwork.....	23
Figure 4.15. Perspective view of Design variation 1 in Maxsurf.....	24
Figure 4.16. Perspective view of Design variation 2 in Solidwork.....	25
Figure 4.17. Perspective view of Design variation 2 in Maxsurf.....	25
Figure 4.18. Perspective view of Design variation 3 in Solidwork.....	26
Figure 4.19. Perspective view of Design variation 2 in Maxsurf.....	27
Figure 4.20. Trimesh of variation 1 model in Moses.....	28
Figure 4.21 Load headings toward the pontoon.....	28
Figure 4.22. Surge RAO of variation 1 in free floating condition. ....	29
Figure 4.23. Sway RAO of variation 1 in free floating condition. ....	30
Figure 4.24. Heave RAO of variation 1 in free floating condition.....	31
Figure 4.25. Roll RAO of variation 1 in free floating condition. ....	32
Figure 4.26. Pitch RAO of variation 1 in free floating condition.....	33
Figure 4.27. Yaw RAO of variation 1 in free floating condition. ....	34
Figure 4.28. Surge RAO of variation 2 in free floating condition. ....	35
Figure 4.29. Sway RAO of variation 2 in free floating condition. ....	36
Figure 4.30. Heave RAO of variation 2 in free floating condition.....	37
Figure 4.31. Pitch RAO of variation 2 in free floating condition.....	38
Figure 4.32. Roll RAO of variation 2 in free floating condition. ....	39
Figure 4.33. Yaw RAO of variation 2 in free floating condition. ....	40
Figure 4.34. Surge motion RAO of model variation 3 in free floating condition.....	41
Figure 4.35. Sway RAO of variation 3 in free floating condition. ....	42
Figure 4.36. Heave RAO of variation 3 in free floating condition.....	43
Figure 4.37. Pitch RAO of variation 3 in free floating condition.....	44
Figure 4.38. Roll RAO of variation 3 in free floating condition. ....	45

Figure 4.39. Sway RAO of variation 3 in free floating condition. ....	46
Figure 4.40. 3D view of mooring simulation. ....	47
Figure 4.41. Single Point Mooring system perspective view. ....	47
Figure 4.42. Excursion along X and Y axis of Ponton with mooring system. ....	48
Figure 4. 43. Rotational motion along X and Y axis of Ponton with mooring system. ....	49



“This page is intentionally left blank”



# Chapter 1

## Introduction

### 1.1 Background

Fossil fuels such as crude oil, coal, and natural gases have been the main resource used for energy and power plant. Although the industry has already been established, there are still many negative effects due to the excessive extraction of these natural resources (Santos, 2013). Other than being an unrenovable resource, the production process using these resources are still very harmful to the environment and also human despite the advance technologies that are available. To prevent more fatal damages, researches for alternative renewable energy source have been going on for many years. Numbers of alternative renewable resources such as water, wind, solar energy and many more have been found. These alternative energies are now being used around the world depending on the available potential on each region. (Santos, 2013)

There are three types of ocean energy potentials, the tidal power, the wave energy, and the ocean thermal energy. One of the already existing ocean energy power plant is the wave generated power plant with pendulum system invented and developed by Zamrisyaf, a researcher at the centre of research and development of *Perusahaan Lisrik Negara (PLN)* together with *Institut Teknologi Sepuluh Nopember (ITS)* Surabaya since 2002 (Wardhana, 2013).

This power plant operates by utilizes a ponton that acts as a floating structure. This ponton is carrying the pendulums that are integrated to a dynamo. The pendulums are assisted with a double freewheel transmission equipment to make the dynamo rotates, thus, electricity is produced. Due to the dependency of the energy produced to the movement of the pendulums, the design of ponton, angle of slope of the ponton hull, type of wave and environmental factors of where the ponton is installed are the most affective factors on the movement of the ponton (Wardhana, 2013).

Mooring system installation is required to keep the power plant unit stays in its appropriate working station and also to prevent it from exceeding the maximum excursion of the ponton, thus, the flexibility in certain mode of motion required to improve the energy extraction is provided and the operability of the unit can be maintained or even increased. Therefore, analysis needs to be conducted in order to find the most suitable mooring system configuration that can be easily and safely installed whilst maintaining high operability of the wave generated power plant with pendulum system. The analysis is done using MOSES to find out the effect of installing mooring system to the movement of the wave generated power plant with pendulum system.

## **1.2 Problem Identification**

Based on the background above, the problem identification that will be used in the research is as listed below:

1. What is the most effective design for the wave energy conversion system?
2. How is the effect of mooring system on the motion of wave energy conversion system?

## **1.3 Research Objectives**

Based on the problem identification above, the objection of this research is as listed below:

1. To find the most effective design for the wave energy conversion system.
2. To find the effect of mooring system on the motion of the wave energy conversion system.

## **1.4 Research Limitation**

The limitation of this research is as listed below:

1. The simulation is conducted using MOSES by only observing three degrees of freedom of the ponton, they are the heave, roll, and surge.
2. The dimension and shape of the ponton for the simulation is fixed.
3. The simulation is conducted for shallow water only.
4. The analysis for the pendulum system is not included.

## **1.5 Benefit of Research**

This research will be giving information about the effect of mooring system configuration on the movement of the wave generated power plant with pendulum system. This information is expected to become a useful and valid reference for further development of other alternative ocean energy converters, also to give solutions when identifying the requirements and designing its mooring system.

## Chapter 2 Study Literature

### 2.1 Wave Energy

Energy is the main support to human adaptation. As the population on earth keeps on increasing, the demand for energy is only getting higher. The dependency on fossil fuels has become harmful because of the continuous extraction and the unsustainability of the fossil fuel. Therefore, alternative energy from a renewable resource is in high demand. Wave energy is one of them. Wave energy is divided into three different categories, the ocean wave energy, ocean current energy, and ocean thermal energy (Wardhana, 2013).

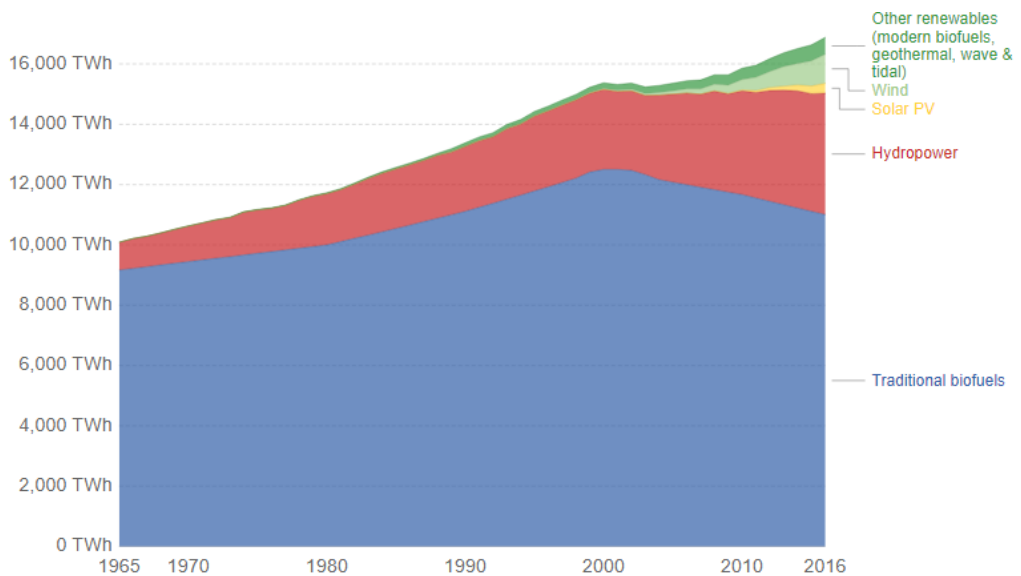


Figure 2.1. The comparison of alternative energy power output  
(source: Global Energy Production by Source – Vaclav Smil (2017), BP Statistical Review of Global Energy)

Based on the figure above, the power produced by a number of alternative resources is topped by modern biofuels, geothermal, waves and tidal. This statistic also shows that the ocean energy potential to produce electricity such as the wave generated power plant is very beneficial to many and should always be developed. According to London-based Carbon Trust, wave energy can realistically provide over 2,000 terawatts (TWh) of electricity per year or approximately 10% of global energy needs (Alam, 2014). However, according to the Electric Power Research Institute (EPRI) of Palo Alto, CA, a realistic estimate of ocean wave energy potential in the United States alone indicates approximately 6% of total energy needs with a wholesale market value eventually

reaching billions of dollar per year. This shows how big of a potential wave energy is. The wave energy is also depending on the location at which it is installed (Smil, 2017).

## 2.2 Wave Generated Power Plant

Technology of wave converters are needed to support the potential of ocean wave energy. The wave generated power plant utilizes the ocean wave to rotate a generator and produce electricity. Any devices that converts ocean wave into a source of electricity is called the Wave Energy Converter (WEC). Numbers of WECs have already been developed, currently there are the submerged pressure differential, the overtopping device, the oscillating water column, and many more to mention. Wave energy is substantial as a resource. However, the commercial utilization of wave energy is still very low. There are three major types of wave energy conversion devices based on how they interact with the ocean wave.

The first one is the Oscillating Water Columns (OWC). OWCs are devices that involve a structure on the shoreline in which the waves enter and leave a static chamber. The motion of the water pushes air up when it enters and pulls air back as it leaves. This oscillation of air pressure rotates the integrated turbine to generate electricity (Igesias et al, 2013).

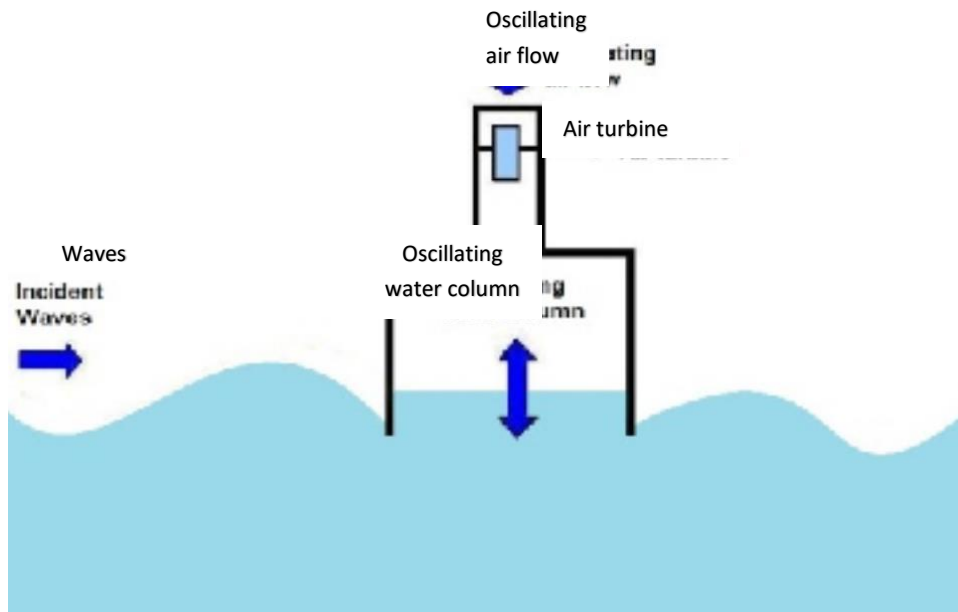


Figure 2.2. diagram of an oscillating water column.

(source: Numerical Analysis of an Oscillating Water Column Converter Considering a Physical Constraint in the Chimney Outlet, 2014)

The second one is the Overtopping Devices (OTD) that consist of a structure that elevates the wave into a reservoir placed above the sea level. The energy is then extracted by using the difference in water level between the reservoir and the sea. The difference of the water level is measured using a low head Kaplan turbine.

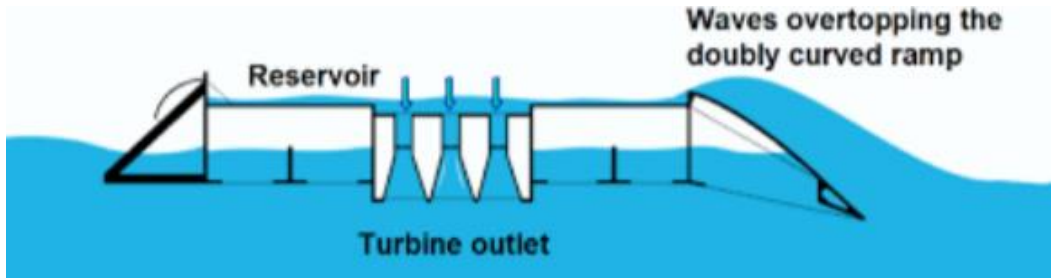


Figure 2.3. Diagram of Overtopping Devices (OTD)  
(source: wavedragon, 2013)

The last one is the wave activated bodies (WAB) that directly utilizes the motion of the ocean surface. They generally involve floating structures that moves up and down due to the buoyancy force of waves. The energy is extracted from the relative motions of the structures relative to its fixed reference by using a hydraulic system to compress oil, that is then used to drive the generator to produce electricity.

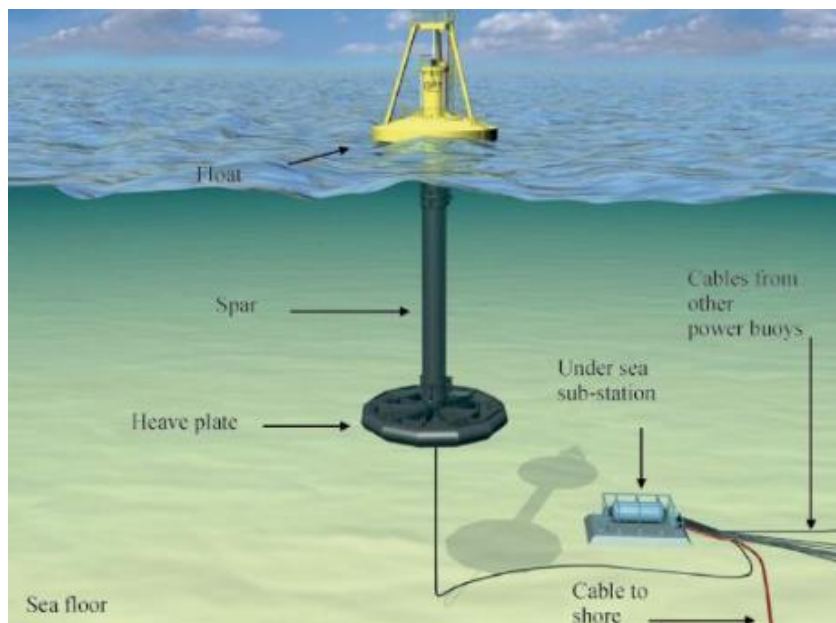


Figure 2.4. Wave Activated Bodies (WAB).  
(source: A review on front end conversion in ocean wave energy converters, 2015)

The most common energy extraction methods for nearshore devices are the OWs and OTDs compared to the WABs. OWCs or overtopping are mostly used by shoreline installed devices as their operating principle.

### 2.3 Previous Research

The previous research of wave energy conversion system called the Tripod Ponton used octagonal ponton. The prototype was installed at the shore of Tanjung Bumi,

Madura, East Java. Tripod Ponton was built with three pontons connected to a rigid triangular deck. The octagonal ponton was designed to allow higher amplitude of motion response. The diameter of this unit is 3 meters and the draft is 1,5 meters. Although the full scaled prototype was built for sea trial, an experiment was carried out at the Indonesian Hydrodynamics Laboratory in order to gain more reliable data and validation. The experiment used a model and hydrodynamics parameters with scale of 1:10 calculated with Froud scaling. The prototype and model of the unit is as shown in Figure below (Mukhtasor, 2016).



Figure 2.5 Prototype of Tripod Ponton in Tanjung Bumi

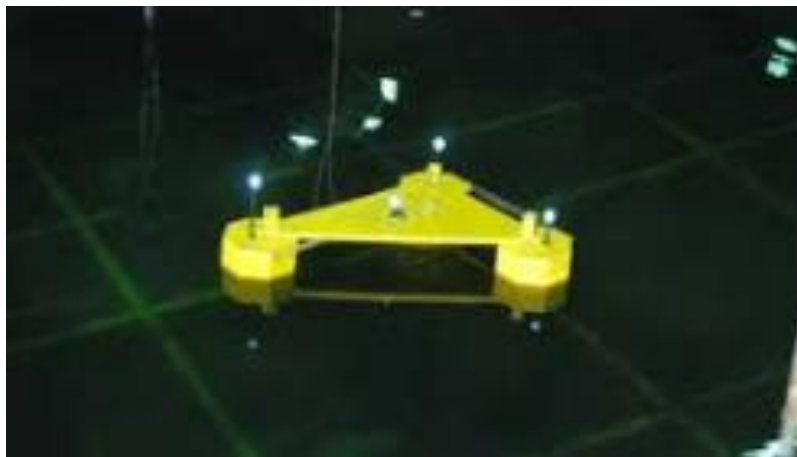


Figure 2.6 Model of Tripod Ponton in wave tank of Indonesian Hydrodynamics Laboratory.

The experiment was conducted in the wave tank. Three LED lights were attached to track the movement of the model as regular wave is generated during experiment. The motion response is then mapped and translated into x-y-z coordinates to be analysed and translated into roll, pitch, and yaw motion response. Based on the results of the test and experiment, it is found that the motion response was more effected by wave height than wave period, however, the understanding of the whole system remained limited (Mukhtasor, 2016).



## 2.4 Theory of Floating Structures and Motion Response

The floating structures comes in various shape and utilities, for example, a ship that have been used as a transportation device. A ponton is an example of floating structures that do not have a prime mover just like a ship would, therefore, its motion will heavily be affected by environmental forces such as waves and winds. According to the law of Archimedes, a floating structure will have the same amount of buoyancy and amount of water displaced from the environment. The amount of force of gravity must be at least equal or less than the amount of the force of buoyancy, therefore, the structure will be able to maintain its stability to stay above the water.

The stability is the ability of a floating structure to go back to its initial position after experiencing disturbance from internal or external factors, for example, the environmental load (Wave and wind). There are two types of stability, the horizontal stability and the longitudinal stability. The horizontal stability means that the structure is experiencing a trim while the longitudinal stability means that the structure is experiencing a rolling. There are three important aspect to be considered as part of the stability, they are the centre of gravity, centre of buoyancy, and the metacentric point.

### 2.4.1 Floating Structure Stability

Stability of a floating body to resist the overwhelming forces and return to its original position after the disturbing forces is gone (Madland, 2012). According to law of Archimedes, when a floating structure is floating in calm waters, the value of force of gravity and buoyancy will be equal. There are many points that affects the stability such as the centre of gravity (G), centre of buoyancy (B), metacentric point (Z) and many more.

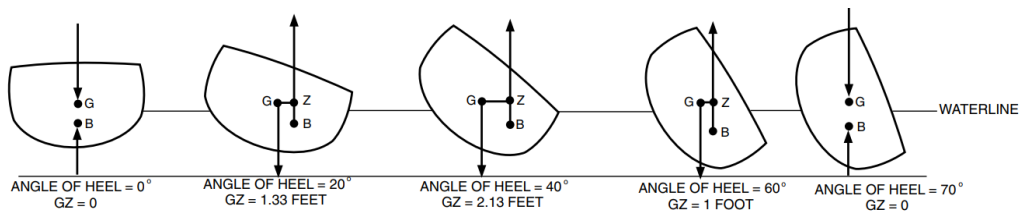


Figure 2.7. Floating structure stability.  
(Source: ship stability and buoyancy)

As seen in the figure 2.7 above, G will always stay in its position while B shifted when there is a force acting upon the body of the floating structure. This proves that the platform will move to its initial position once the effect of external forces upon the floating structure body is gone.

### 2.4.2 Six Degrees of Freedom

A floating structure is considered to be a free moving structure even though it is secured to the bottom of the water/sea. Since the body of the structure remains rigid to the movement of the waves, the floating structure will have six degrees of freedom.

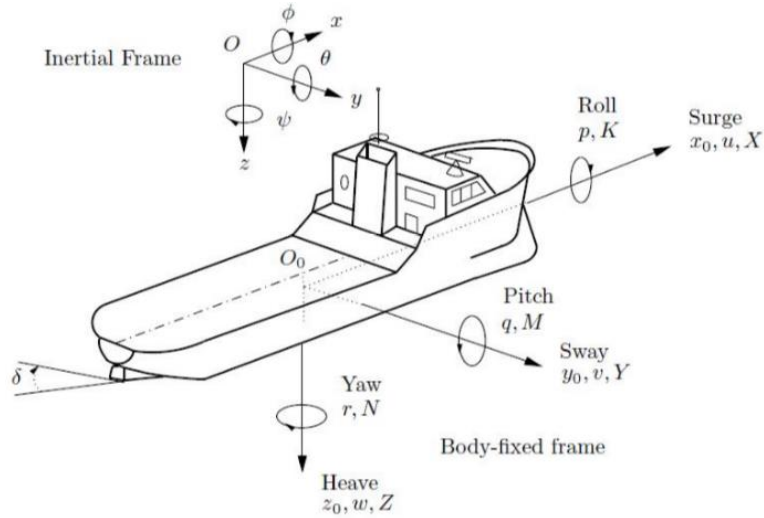


Figure 2.8. Diagram of six degrees of freedom on a ship.  
(source: Universidad Politecnica Madrid, 2019)

As seen in the figure above, a floating structure on a surface of the water will experience those six movement that are divided into two categories, the translational that includes the surge, yaw, and sway, and the rotational motions that includes the pitch, heave, and roll (Madland, 2012). In this research, motion response in all six degrees of freedom will be analysed both in free floating and moored condition.

## 2.5 Response Amplitude Operator (RAO)

Response Amplitude Operator (RAO) or also called Transfer function is the function of structure response when affected by wave load towards the structure. Therefore, the function can be written as the ration between the structure respond amplitude to the wave amplitude. Structure respond amplitude can be in a form of motions, vibration, or tension. RAO can be determined by using the equation below:

$$RAO(\omega) = \frac{X_p(\omega)}{\eta(\omega)}$$

Where:

$X_p(\omega)$  = amplitude of the structure

$\eta(\omega)$  = amplitude of wave

RAO is then represented in a form of response curve. The response curve of a floating structure is divided into three different areas, the sub critical, critical, and the super critical area (Fajar, 2018).

### A. Sub-critical Area

The sub-critical area has low frequency section and long period of wave. The floating structure will follow the contour of the long wave elevation, therefore, the amplitude

of motion and amplitude of wave will be identical. This condition is also called contouring.

#### B. Critical Area

The critical area shows an increase in amplitude of motion compared to the amplitude of wave, and the turning point of the curve is at its natural frequency which is located within the resonance area, which means that there is an increase in the motion response

#### C. Super Critical Area

The super critical area shows the highest frequency or short period of wave. The higher the frequency, the denser the wave will be, which means that the distance between the turning point of the curve is also getting shorter. The motion response in this area is decreasing and the condition is called platforming.

The analysis of RAO graphs will generate information about the behaviour of the floating structure that can be used for other analysis. The list of information can also be used as the validation of the advisability of the selected mooring system for the wave generated power plant with pendulum system.

## 2.6 Response of Floating Structures to Irregular Waves

Random waves are superposition of unlimited sinusoidal waves components. Each of wave components have their own level of energy that are accumulated in a form of wave energy spectrum (Djatkiko,2012). Response of floating structures such as ships caused by irregular waves excitation is already introduced by St. Denis and Pierson (1953), where these responses can be calculated as a reaction due to sinusoidal waves excitations with certain value of amplitude and frequency. The calculation is done by taking a constant value of amplitude while varying the value of frequency within a certain interval. Structure response on irregular wave can be done by transforming wave spectrum into response spectrum, where response spectrum is defined as the density of energy caused by waves on the structure.

The structure response on irregular wave can be determined by transforming wave spectrum into response spectrum. The equation of this transformation is as written below.

$$S_R = [RAO(\omega)]^2 S(\omega) \text{deg/m}$$

Where:

$S_R$  = response spectrum

$RAO(\omega)$  = transfer function

$\omega$  = wave frequency (Rad/sec)

## 2.7 Spectrum of Wave

Wave spectrum the selection of wave energy spectrum to determine the real sea condition that is being researched on. The method used is by transforming records of irregular waves within time domain into wave energy spectra within frequency domain by using Fehrer's mathematics algorithm, or known as the FFT (Fast Fourier Transform). The results derived from FFT is the plotted into wave energy density spectra versus wave frequency graph. Wave spectrum is needed in the process of designing a ship (floating structure) to predict the high of the wave caused by the movement of the ship during operation (Charizzaka, 2016).

There are numbers of different wave spectrum derived from numerous experiments on different sea conditions. The mostly used wave spectrum used in calculations are the Pierson-Moskowitz model (1964), ISSC (1964), Scott (1965), Bretsneider (1969), JONSWAP (1973), ITTC (1975), Wang (1991). (Djatkiko, 2012)

The spectrum of wave represents the distribution of wave energy as the function of wave frequency. The wave amplitude energy density spectrum is the representation of continual frequency domain that shows the variation of density of wave energy with the frequency. The ordinate of the spectral is symbolised using  $S_{\zeta}(\omega)$ , where  $\zeta$  is the mean of wave amplitude calculation. The wave spectral density can be seen in the figure below. (Fajar, 2018)

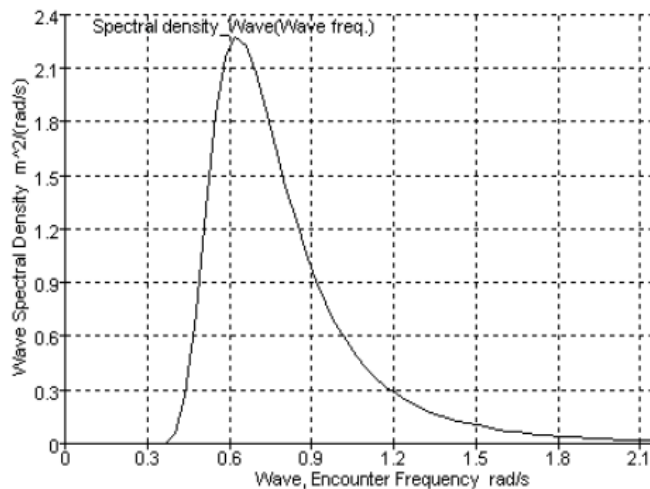


Figure 2.9. common spectrum of wave  
(source: MOSES manual)

The spectral shown in the figure above indicated the sea condition that is crucial in determining the floating structure response at the sea.

## 2.8 Joint North Sea Wave Project (JONSWAP) Spectrum

JONSWAP wave spectrum as seen in Figure 2.10 below is used in this research because it suits the condition of Indonesian ocean the most compared to the other type of spectrum. The equation of JONSWAP is determined by transforming Pierson-Moskowitz spectrum (DNV RP- C205, 2010).

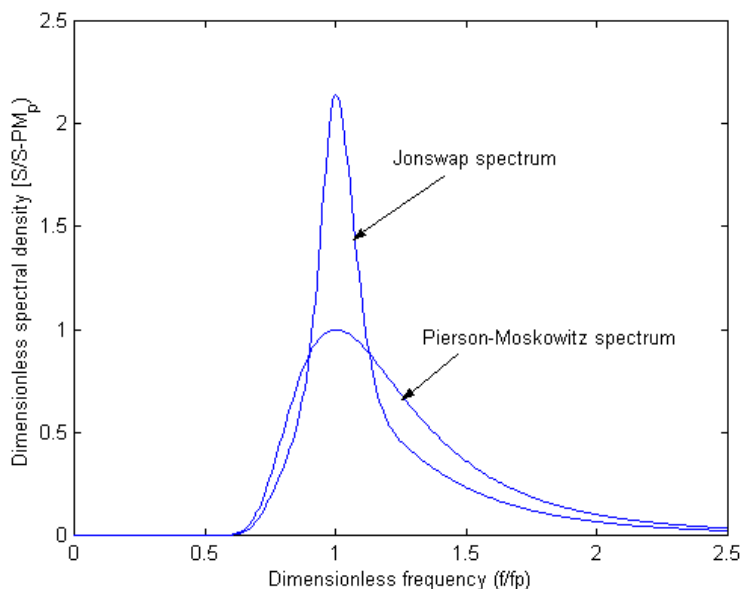


Figure 2.10. Wave Spectrums  
(source: Moses Manual)

## 2.9 Environmental Loads

The environmental loads are caused by natural phenomenon such as the wind, waves, current, and other external forces that can affect the movement of the platform of a floating structure. Environmental loads can also be caused by natural disasters such as earthquakes, cyclonic storms such as hurricanes, typhoons, and tornados, as well as flooding. They are difficult to predict and they can cause severe damages to the affected structure. Therefore, these loads are very crucial to be included in the analysis of this research for reliability purposes (Fajar, 2018).

## 2.10 Mooring Configuration for Floating Structures

Mooring is a set of equipment with permanent structure that is use to make sure the structure will not get swept away by the waves. Mooring can be in a form of a quay, jetty, anchor buoy, wharf, and mooring buoy. The wave energy conversion system in this research needs to have as many motion responses as possible to allow the pendulums to keep moving, thus, electricity is guaranteed to be produced continuously. However, there

are many factors affecting the operability of the unit, one of the critical one is the environmental loads, the wind and the wave (Charizzaka, 2016).

These environmental loads can be unpredictable and can change drastically in a short period of time. If the wind suddenly gets fast, the wave on the surface will also get affected and create big waves. Such a condition could possibly cause damage to the unit due to excessive excursion of the ponton. Parts of the unit could be damaged and the unit could also sink due to the extreme weather. Therefore, mooring system is still mandatory to secure the unit to stay within its safe working area.

In this research, the mooring system will be installed on the ponton of the wave energy conversion system to figure out the operability of the structure when moored. Besides the environmental loads, other main segment that could be analysed in this research are the type of mooring system, the material and arrangement of the mooring line, and the type of anchor that are suitable for the wave generated power plant with pendulum system and able to maintain a certain level of operability.

### 2.10.1 Catenary Mooring

In shallow to deep water, is the catenary mooring. The catenary mooring as seen in Figure 2.11 below arrives at the seabed horizontally subjecting the anchor to horizontal forces. In a catenary mooring, most of the restoring forces are generated by the weight of the mooring line. It derives its compliance from the change in suspended line weight. Most semisubmersible drilling rigs are fitted with catenary mooring systems. Floating wave energy converter units that are moored by free hanging catenary mooring might not have sufficient extension without excessive loads when the tidal range is large and there would be restraining stiffness affecting the motion of the unit (Santos, 2013).

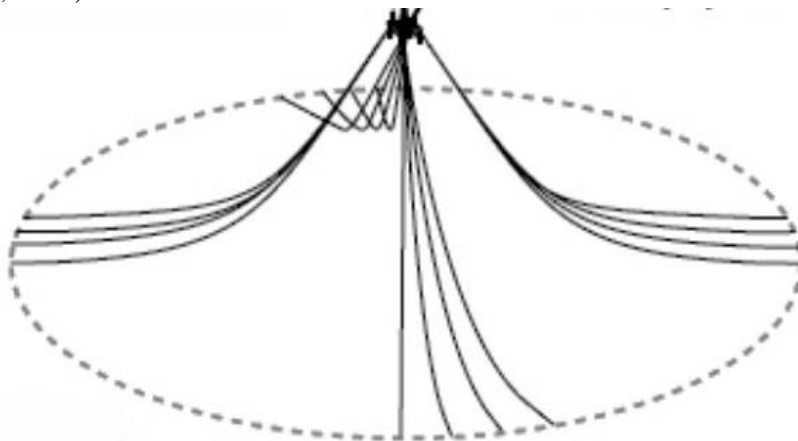


Figure 2.11. Catenary mooring system configuration.  
(source: ABC Moorings)

### 2.10.2 Taut Leg Mooring

In deep, the weight of the mooring line becomes a limiting factor in the design of a floater. To overcome this problem synthetic ropes in the mooring line (less weight) and/or a taut leg mooring system can be applied. The taut leg mooring arrives at the seabed at an angle, meaning the anchor point has to resist both horizontal and vertical forces. The restoring forces are generated by the elasticity of the mooring line. An advantage of a taut leg mooring over the catenary mooring is that the footprint of the taut leg mooring is smaller than the footprint of the catenary mooring.

A taut mooring leg, as seen in Figure 2.12 below, will usually have an angle of between 30 and 45 degrees to horizontal at the vessel and exhibit fairly linear load-excursion characteristics. Another advantage is the better load sharing between adjacent lines than the array of catenary. A taut mooring also has much shorter lines than a catenary system at similar depth. Crowded seafloor conditions gives challenges and the synthetics/taut systems have been used to reduce the risk of steel mooring components suspended over pipelines or subsea equipment. Polyester taut leg mooring systems are expected to be suitable for water depths up to 3000m (Santos, 2013).

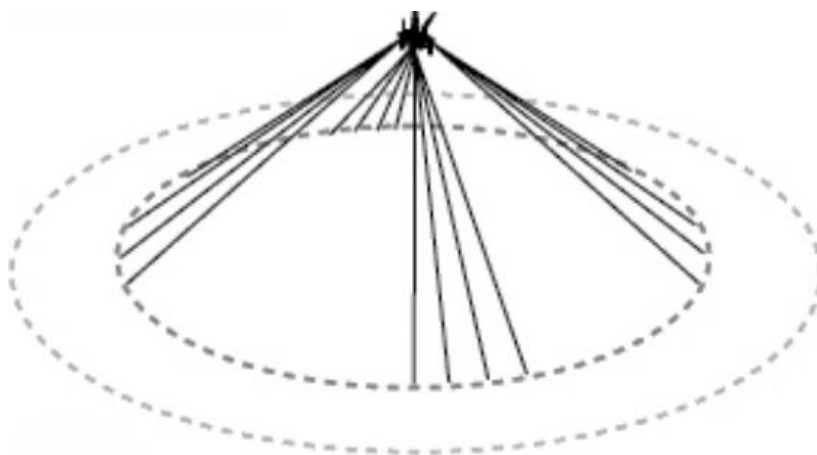


Figure 2.12. Taut leg mooring  
(source: ABC Moorings)

### 2.10.3 Spread Mooring

The spread mooring system, as seen in Figure 2.13 below, will not allow the ship (floating structure) to move rotationally when there are only little environmental loads working on the ship. It usually consists of mooring lines and legs and is installed on the bow and stern of the ship. the bigger the environmental load is, the more mooring line is added. It has a low maintenance due to its simple configuration and it is applicable to all type of ship while considering the facility on deck (Santos, 2013).

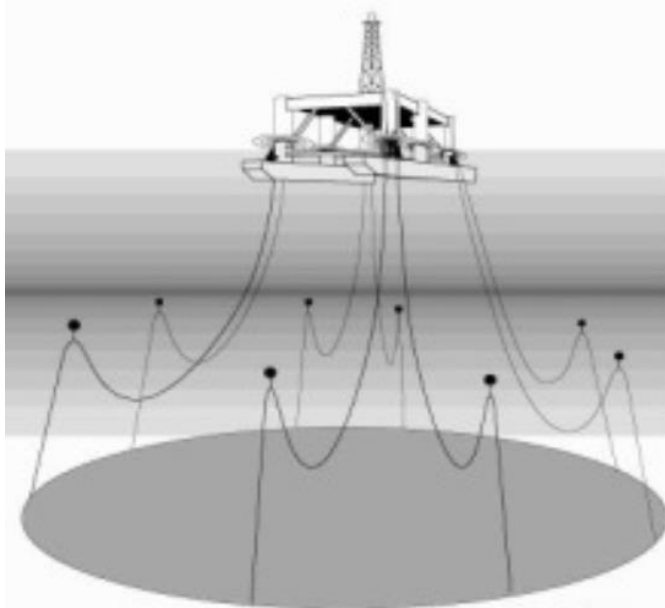


Figure 2.13. spread mooring.  
(source: ABC Moorings)

#### 2.10.4 Determining Length of Mooring Line

The length of mooring line is crucial for the positioning of the floating structure. The length of mooring line can be calculated to determine the minimum length that is appropriate to the configuration of the mooring system to the floating structure itself. The equation to determine the minimum length of mooring line is as written below (Suwandi, 2018):

$$\frac{l}{h} = \sqrt{\frac{2F_H}{Ph}} + 1 \quad [10]$$

Where:

$l$  = minimum distance from chain line

$h$  = water depth

$Ph$  = weight of chain line/m under water

$F_H$  = chain line horizontal force upon fairlead (10% MBL)

#### 2.10.5 Excursion

Excursion is the shifting of floating structure position caused by natural loads such as wind, current, and waves that are acting upon it. The tolerable maximum excursion can be calculated based on the equation written below (Fitria, 2018):

If,



$S_{lfmax} > S_{wfmax}$ , then:

$$S_{max} = S_{mean} + S_{lfmax} + S_{wfsig}$$

If,  $S_{lfmax} < S_{wfmax}$ , then:

$$S_{max} = S_{mean} + S_{lfmax} + S_{wfsig}$$

Where:

$S_{max}$	= maximum vessel excursion
$S_{mean}$	= mean vessel excursion
$S_{lfmax}$	= maximum low frequency motion
$S_{wfmax}$	= maximum wave frequency motion
$S_{wfsig}$	= significant wave frequency motion

## 2.11 MOSES

Moses or Ultramarine's MOSES software is a software utilizes for offshore floating structure design optimization. It consists of numbers of simulation, the Launch, mooring, ballasting, stability, seakeeping, upending, lowering, loadout, deck installation, in-place analysis, and transportation (Fajar, 2018). The type of structures that can be analysed also varies, starting from fixed platforms, compliant towers, wind turbines, and many more. There are three steps to the analysis done in this research. the steps are as written below:

### 2.11.1 Pre-Processor

The pre-processor is the early step which includes inputting the principle data of the structure for meshing process. Then the parameters to be analysed is also inputted.

### 2.11.2 Processor

The processor step involves data calculation using equations and iterations that were decided.

### 2.11.3 Post Processor

In the post processor step, results of the calculation is displayed in the form of graphs, figures, and animation.

“This page is intentionally left blank”

### Chapter 3 Research Methodology

The methodology represents the steps of completion of this research. MOSES integrated simulation process is used to gather analytical data needed for this research. The step of the methodology is as shown in the figure below.

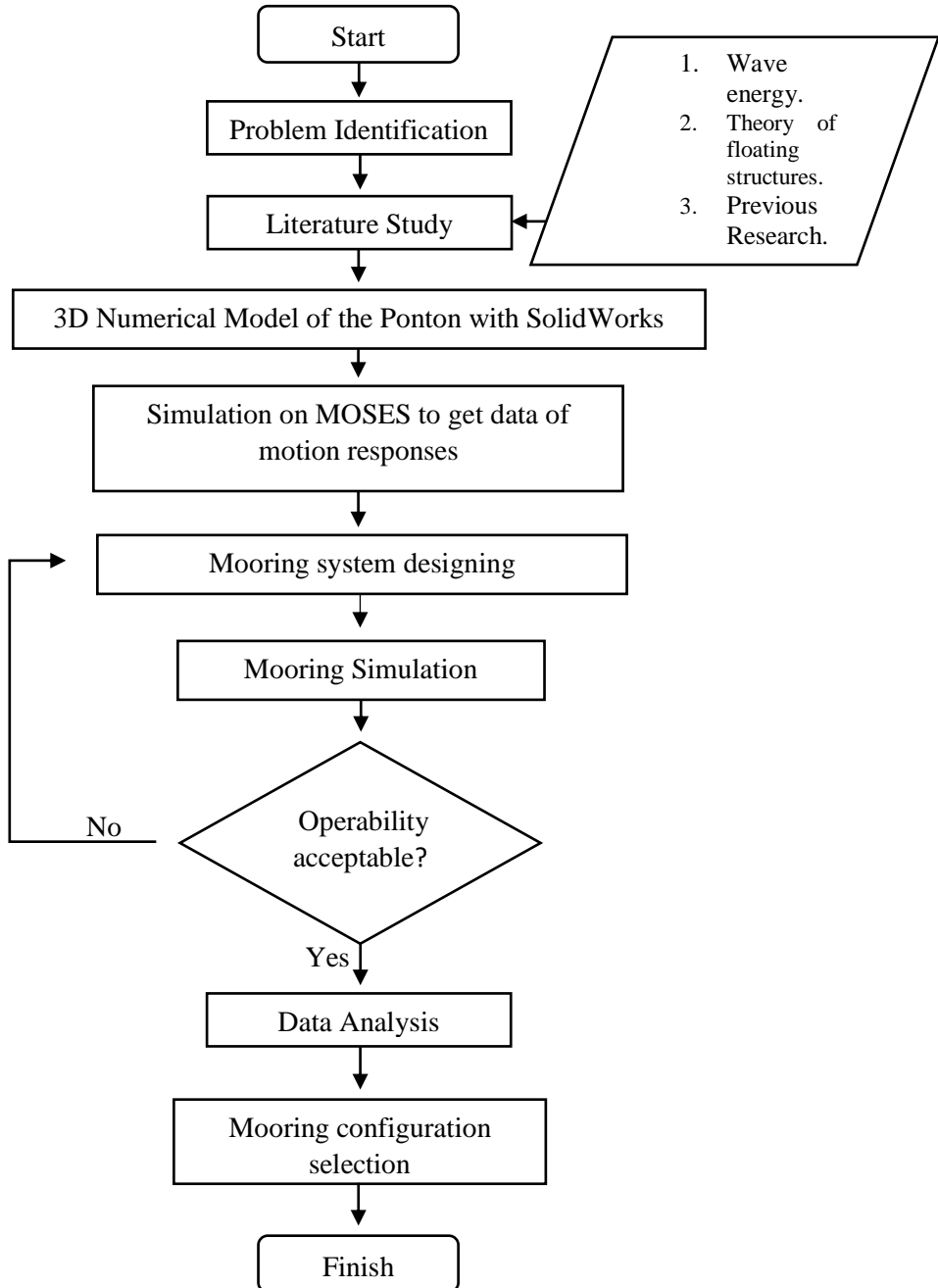


Figure 3. 1 Research methodology

### 3.1 Problem Identification

The designing of wave energy conversion system with hexagonal ponton is done with the floater arms distance variation to determine the best design that will produce more rotational motion and less translational motion so that the pendulum will have more ability to rotate the generator to produce electricity. On the other hand, the designing of mooring system for the wave energy conversion system is done based on the need in optimizing the operability of the unit while considering the natural loads acting upon the ponton.

### 3.2 Literature Study

Literature study is an approach to a summary of the basic theory and references needed for the research. The theories are gathered from various sources such as papers, journals, previous researches, and other study materials that might be useful for the research. The literature study is mostly related to theory of wave generated power plant, mooring system, and MOSES: Integrated Offshore Simulation Software. The material that refers to this research is as the following:

1. Wave energy
2. Wave generated power plant
3. Theory of floating structure
4. Stability of floating structures
5. Motion response of a floating structure
6. Mooring system

### 3.3 3D Numerical Model of the Ponton

The numerical modelling of the ponton for the motion analysis in MOSES is done in two step. The first step is to make the model in SolidWorks to determine the centre of gravity (CG), moment of inertia, mass and volume of the ponton model. These properties are obtained from the mass properties option in Solidworks as shown in Figure 3.2 below. Solidwork 2014 was used in this research.

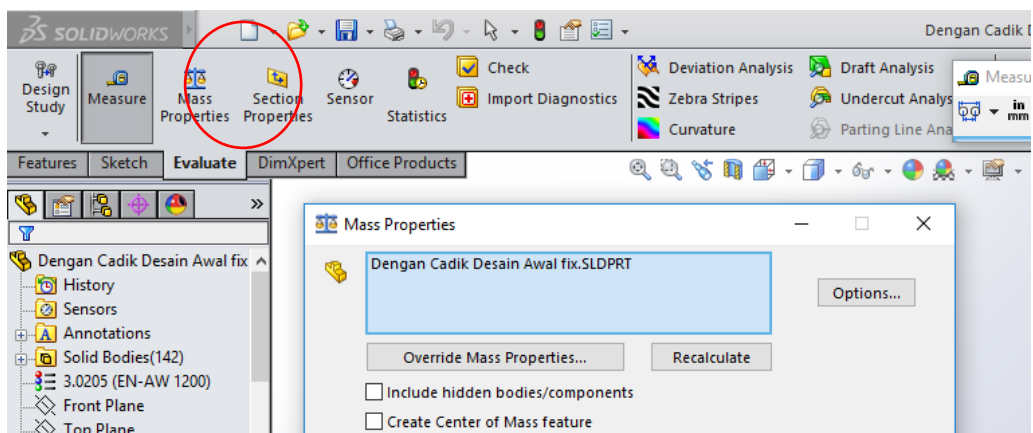


Figure 3. 2 Mass Properties option in Solidwork.

The second step is to make the 3D modelling in Maxsurf Modeller Advanced. the modelling in maxsurf is done to obtain the hydrostatic properties of the ponton such as the draft and zero point of the model. The 3D model from Maxsurf is then exported as File.DAT or File.dat by opening the file in Moses Modeller and save it as Moses Trimesh Model as shown in Figure 3.3 below to later be used in the sea keeping simulation in MOSES. Generate Trimesh command can be found in the Trimesh option of Surfaces.

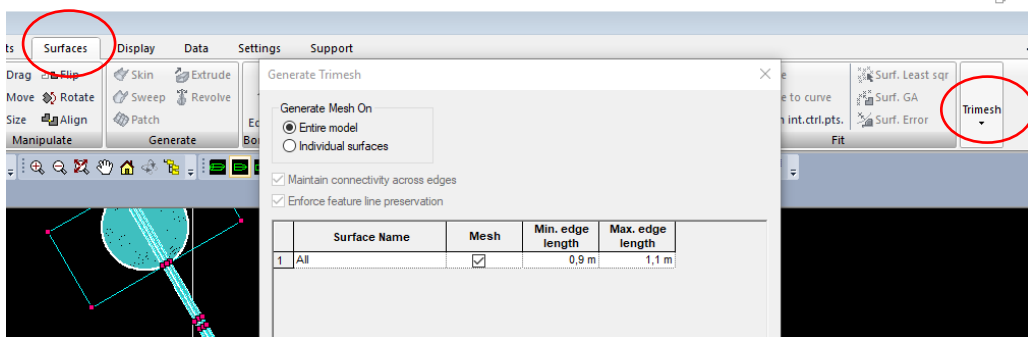


Figure 3. 3 Trimeshing in Moses Modeller.

The hydrostatic data of the model shown in Figure 3.4 below can be determined by going to the Calculate Hydrostatic option in Data tab.

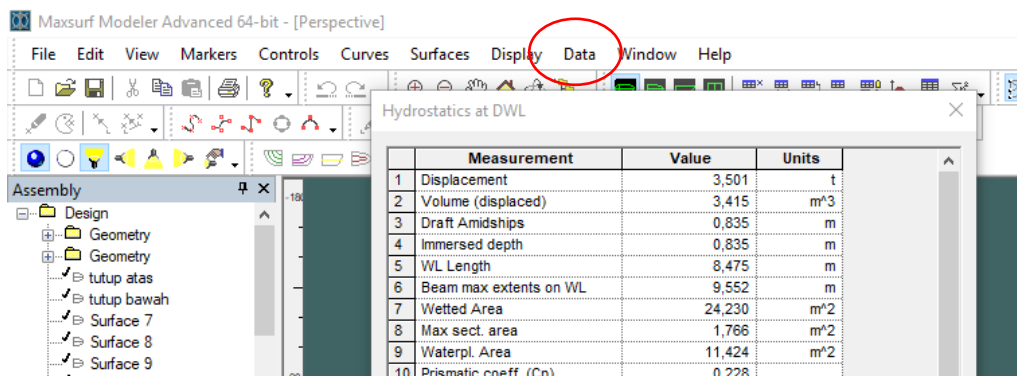


Figure 3. 4 Hydrostatic Data of the model in Maxsurf Modeller Advanced.

### 3.4 Simulation using MOSES

Simulation in MOSES is done to gather data of Response Amplitude Operator (RAO) of the ponton. The simulation is conducted by coding in Moses Editor. The steps are as the following:

#### 3.4.1 Input of Parameters

The input parameters needed for the simulation in MOSES is divided into few categories, the hydrostatic input and environmental parameters input. The hydrostatic input includes the wave spectrum, draft, center of gravity, and radius of gyration of the ponton, while the environmental parameter input includes sea current, wind speed, water

depth, and wave height significant. There should be at least one spectrum input, in this research, the JONSWAP spectrum is used. Speed of vessel is 0 m/s because the ponton is in a free-floating position.

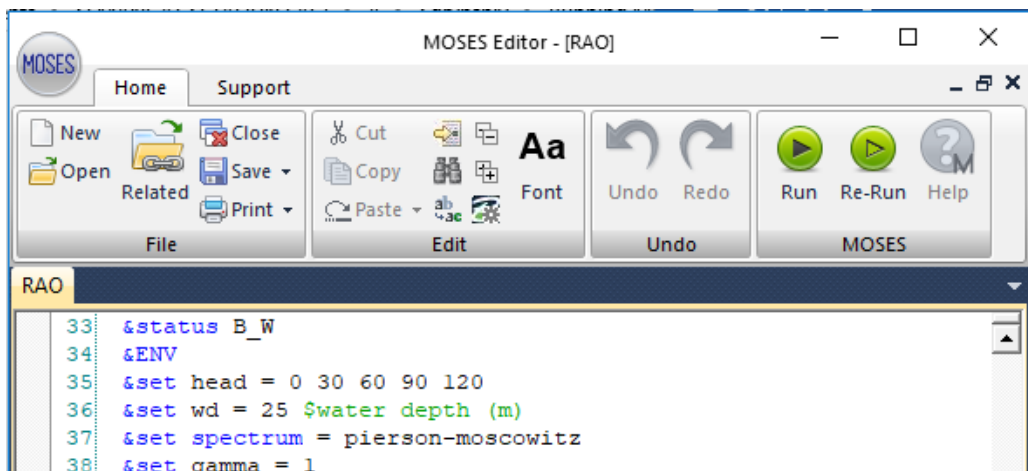
The environmental loads such as water depth, speed and direction of wind, and wave properties must be according to the existing data from the location at which the ponton is placed. The hydrostatic input should also match the data derived from the process of 3D modelling in Maxsurf Modeller Advanced and Solidworks. The input parameter for seakeeping analysis in MOSES is as seen in the table 3.1 below.

Table 3.1. Parameter input for Seakeeping Simulation.

No.	Input	Value	Units
1.	Wave Spectrum	JONSWAP	-
2.	Wave Height Significant	2,364	Meters
3.	Sea Current	0,49	m/s
4.	Period	7,74	Second
5.	Water Depth	25	meters
6.	Wind Speed	16	m/s
7.	Vessel Draft	0,837	Meters
8.	Gamma	1	Meter
9.	Wave Heading	0-120	Degrees

### 3.4.2 Sea Keeping Simulation

Once the parameters are determined and the input File.DAT/dat is ready, the seakeeping simulation by coding in Moses Editor can be started. The coding file.CIF and File.DAT shall be placed in the same folder as shown in Figure 3.5 and 3.6 consecutively below.



```

33 &set B_W
34 &ENV
35 &set head = 0 30 60 90 120
36 &set wd = 25 $water depth (m)
37 &set spectrum = pierson-moscowitz
38 &set gamma = 1

```

Figure 3.5 Coding in Moses Editor for Seakeeping analysis.

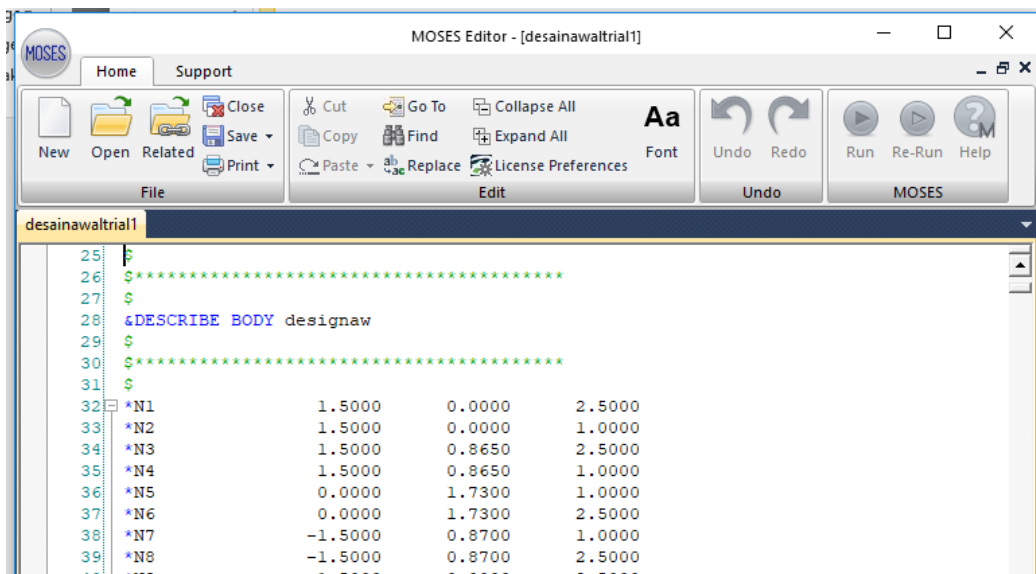


Figure 3. 6 File.DAT for coding in Moses Editor.

Once the solver is finished, the results as seen in Figure 3.7 below can be extracted and analysed by opening File.ans in the folder which was used to save the simulation files. There will be Log, Out, and Ppo text files. These files are going to be used for mooring simulation in Orcaflex.

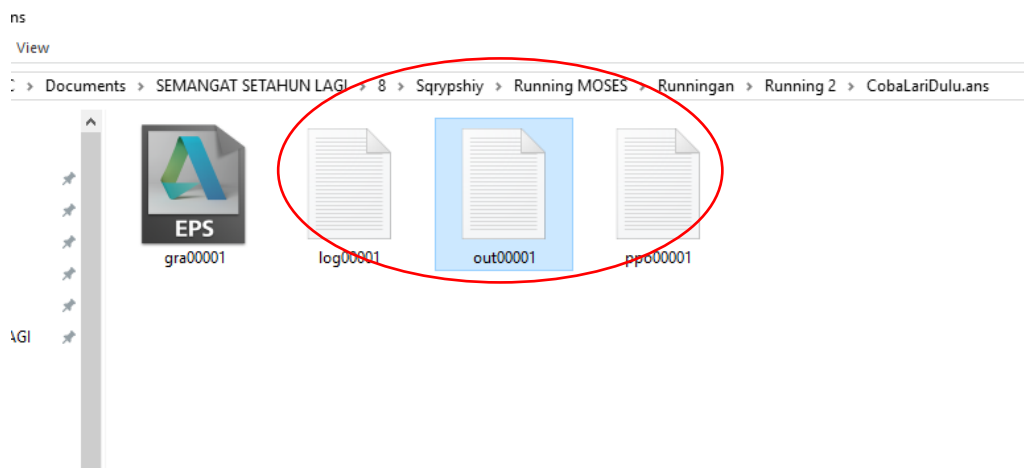


Figure 3. 7 Results of seakeeping simulation in Moses Editor.

“This page is intentionally left blank”



## Chapter 4 Data Analysis

### 4.1 Data of Ponton for 3D Numerical Modelling

The numerical modelling of the ponton starts by drawing in AutoCAD to figure out the 2 Dimension structural drawing of the ponton platform. Then the modelling is continued by doing 3D numerical modelling in Solidworks and Maxsurf.

#### 4.1.1 The Main Dimension of Ponton

The principal dimension of the ponton platform and the floaters derived from 2D drawings in AutoCAD is as shown in the Table 4.2 below.

Table 4.2. Principal Dimension of the unit.

Dimension (meters)	Ponton	Floater
Radius	1.73	0.75
Length	3.5	2.36
Draft (T)	0.837	-
Height (H)	2.50	0.15

### 4.2 3D Numerical Modelling of Ponton

The numerical 3D modelling are done in Solidworks and Maxsurf. There are three variation of design, design Variation 1 is the initial design, design Variation 2 is the ponton designed with reduced floater arms, variation 3 is the design of ponton without floaters.

#### 4.2.1 Design Variation 1

Design Variation 1 of the ponton in Solidworks and Maxsurf are as shown in Figure 4.14 and 4.15 below.

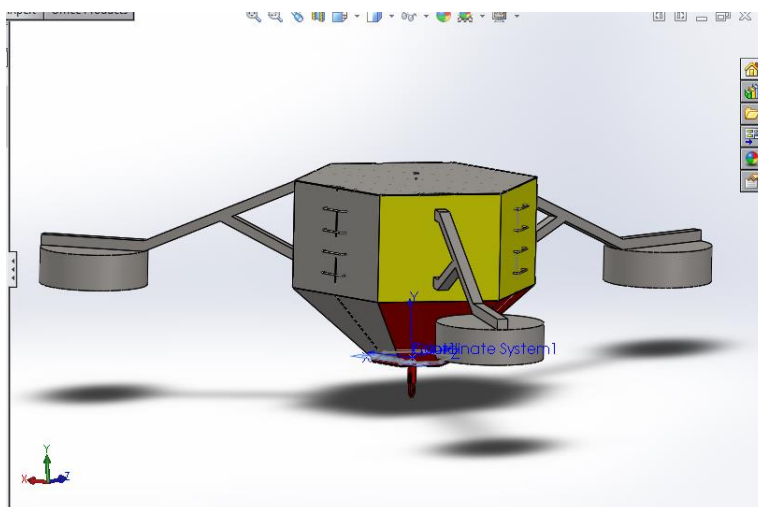


Figure 4.14. Perspective view of Design variation 1 in Solidwork.

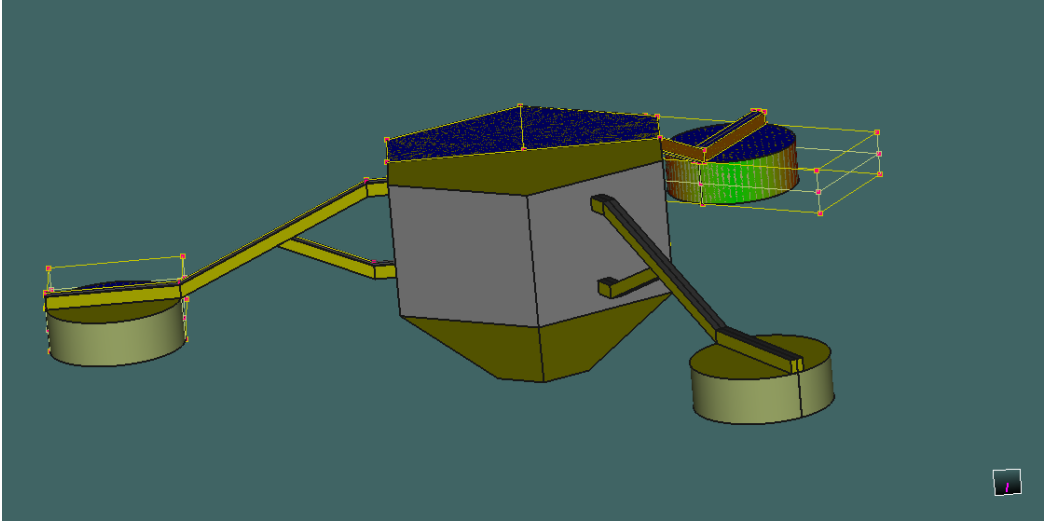


Figure 4.15. Perspective view of Design variation 1 in Maxsurf.

Based on the mass properties of Variation 1 model in Solidworks, the value of center of mass x, y, and z coordinates, radius of gyration, moment of inertia  $I_{xx}$ ,  $I_{yy}$ , and  $I_{zz}$  are as written in Table 4.3 below.

Table 4.3. Calculation from modelling Variation 1 in Solidwork.

Moment of inertia (Ton.m <sup>2</sup> )	x	y	z
	95,246	168,132	95,192
Center of Gravity	0	1.05	0
Radius of Gyration (m)	$I_{xx}$	$I_{yy}$	$I_{zz}$
	3,283	4,362	3,282

#### 4.2.2 Design Variation 2

Design Variation 1 of the ponton in Solidworks and Maxsurf are as shown in the Figure 4.16 and 4.17 below.

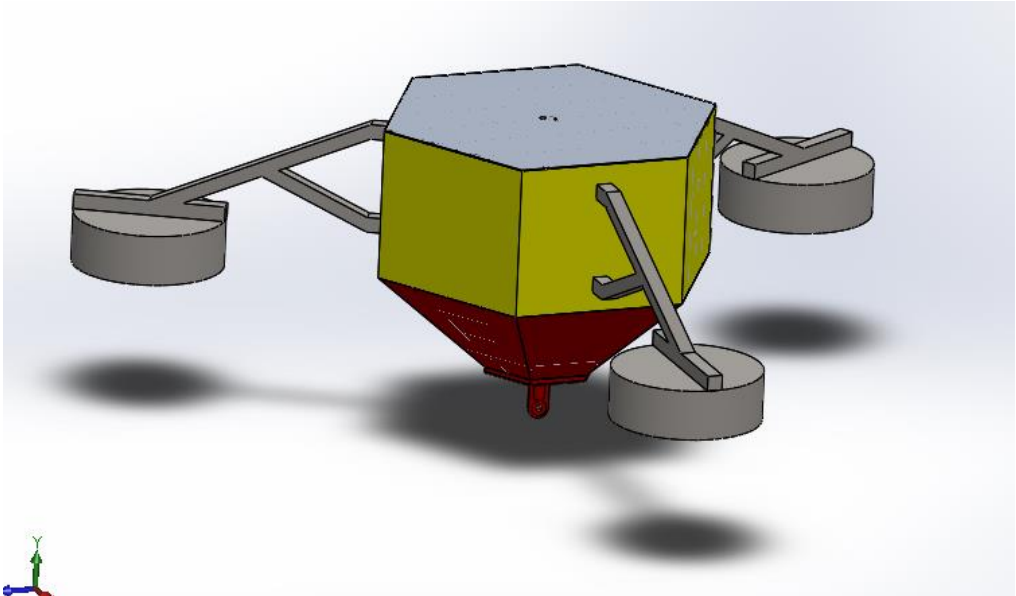


Figure 4.16. Perspective view of Design variation 2 in Solidwork.

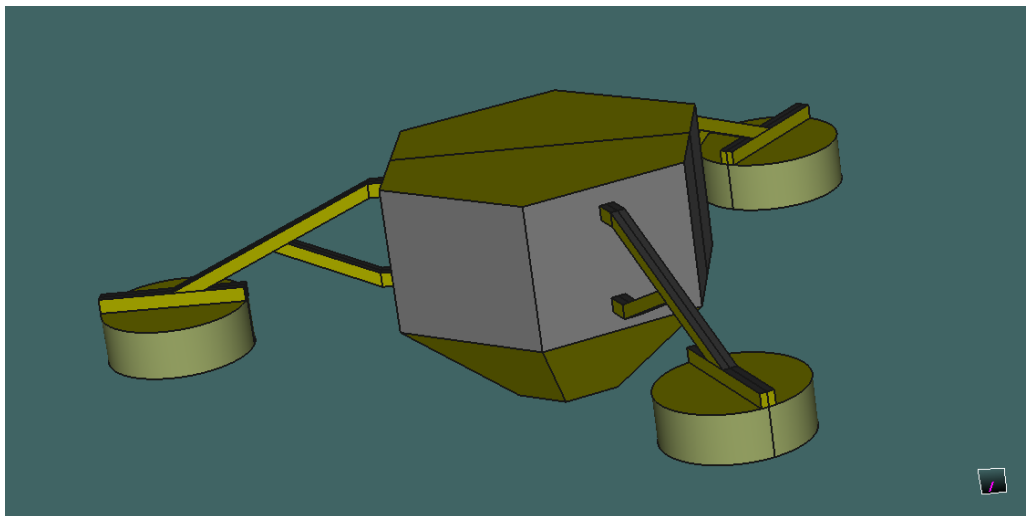


Figure 4.17. Perspective view of Design variation 2 in Maxsurf.

Variation 2 model have floater arms distance of 0,075 meters shorter compared to Variation model 1, otherwise, all the other components of the ponton design stays the same.

Based on the mass properties of Variation 1 model in Solidworks, the value of center of mass x, y, and z coordinates, radius of gyration, moment of inertia  $I_{xx}$ ,  $I_{yy}$ , and  $I_{zz}$  are as written in Table 4.4 below.

Table 4. 4. Calculation from modelling Variation 2 in Solidwork.

<b>Moment of inertia (Ton.m<sup>2</sup>)</b>	<b>x</b>	<b>y</b>	<b>z</b>
	71,369	120,476	71,316
<b>Center of Gravity</b>	0	1.05	0
<b>Radius of Gyration (m)</b>	<b>I<sub>xx</sub></b>	<b>I<sub>yy</sub></b>	<b>I<sub>zz</sub></b>
	2,847	3,699	2,847

### 4.2.3 Design Variation 3

Design Variation 1 of the ponton in Solidworks and Maxsurf are as shown in Figure 4.18 and 4.19 below.

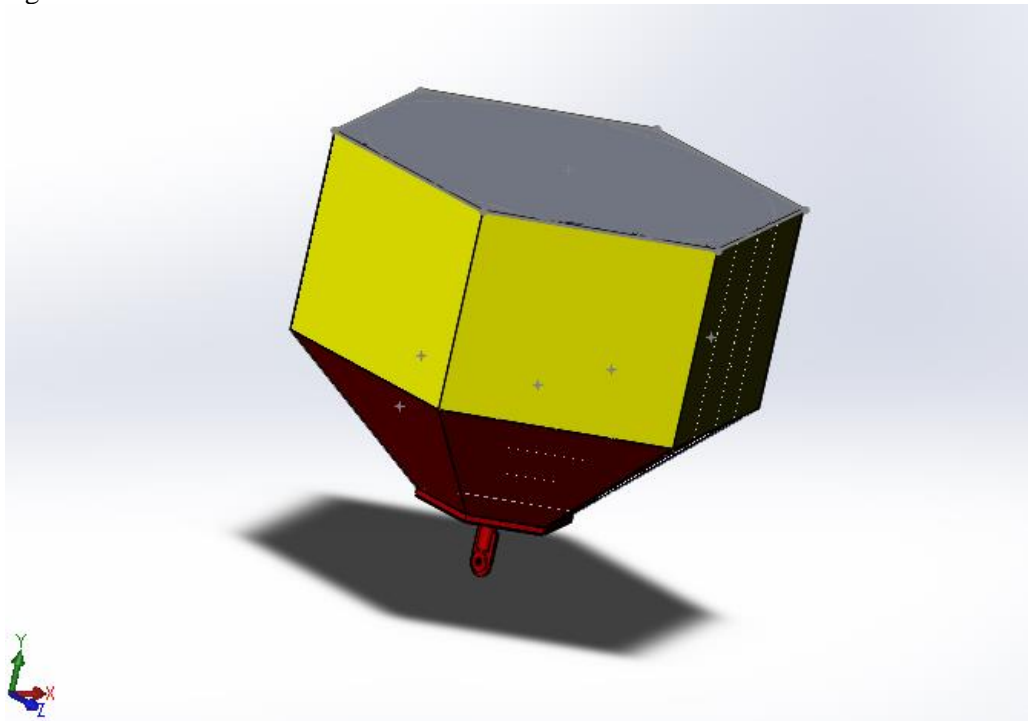


Figure 4.18. Perspective view of Design variation 3 in Solidwork.

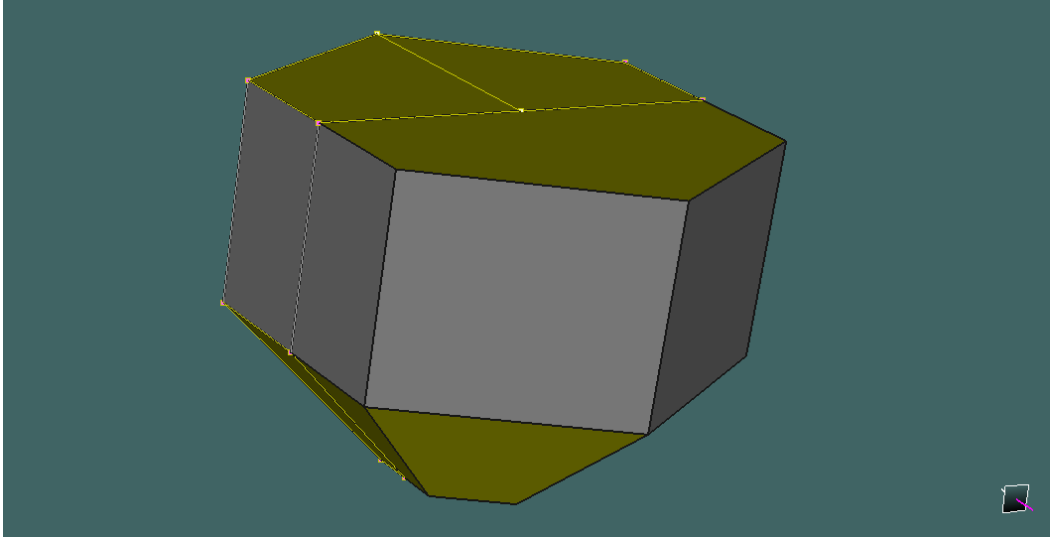


Figure 4.19. Perspective view of Design variation 2 in Maxsurf.

Based on the mass properties of Variation 3 model in Solidworks, the value of center of mass x, y, and z coordinates, radius of gyration, moment of inertia  $I_{xx}$ ,  $I_{yy}$ , and  $I_{zz}$  are as written in Table 4.5 below.

Table 4.5. Calculation from modelling Variation 3 in Solidwork.

<b>Moment of inertia (Ton.m<sup>2</sup>)</b>	<b>x</b>	<b>y</b>	<b>z</b>
	8,917	3,434	8,765
<b>Center of Gravity</b>	0	1.57	0
<b>Radius of Gyration (m)</b>	<b>I<sub>xx</sub></b>	<b>I<sub>yy</sub></b>	<b>I<sub>zz</sub></b>
	2,034	1,262	2,017

### 4.3 Modelling in Moses

The modelling in Moses is done by opening a design file .msd of the 3D model from Maxsurf Modeller Advanced with a fixed hydrostatic data. The model is then proceeded to be set for seakeeping simulation to generate Response Amplitude Operation (RAO) in free floating condition by trimeshing it as seen in Figure 4.20 below, then exporting it into a .DAT file.

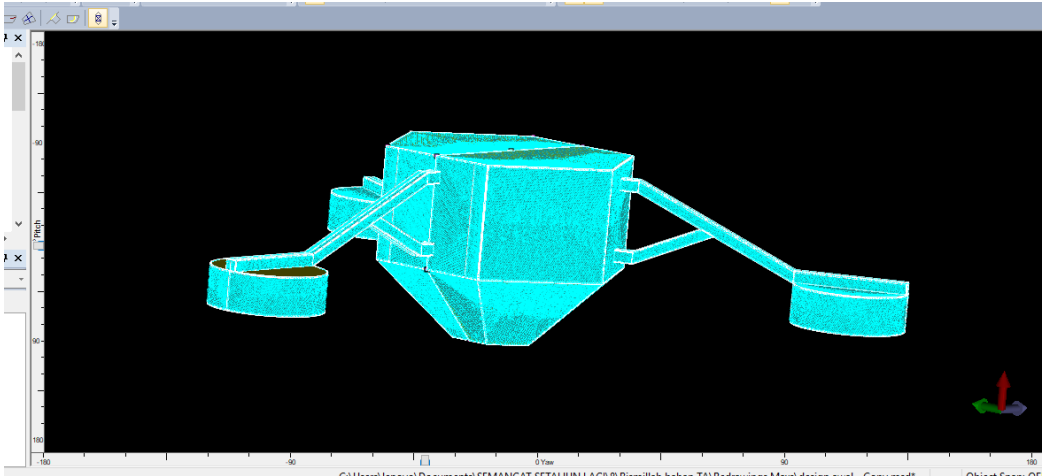


Figure 4.20. Trimesh of variation 1 model in Moses

#### 4.4 Motion Response Analysis

This analysis will produce the motion response of the pontoon in free floating state with irregular waves and loads heading in from  $0^\circ$ ,  $30^\circ$ ,  $60^\circ$ ,  $90^\circ$ , and  $120^\circ$  towards the pontoon as seen in Figure 4.21 below.

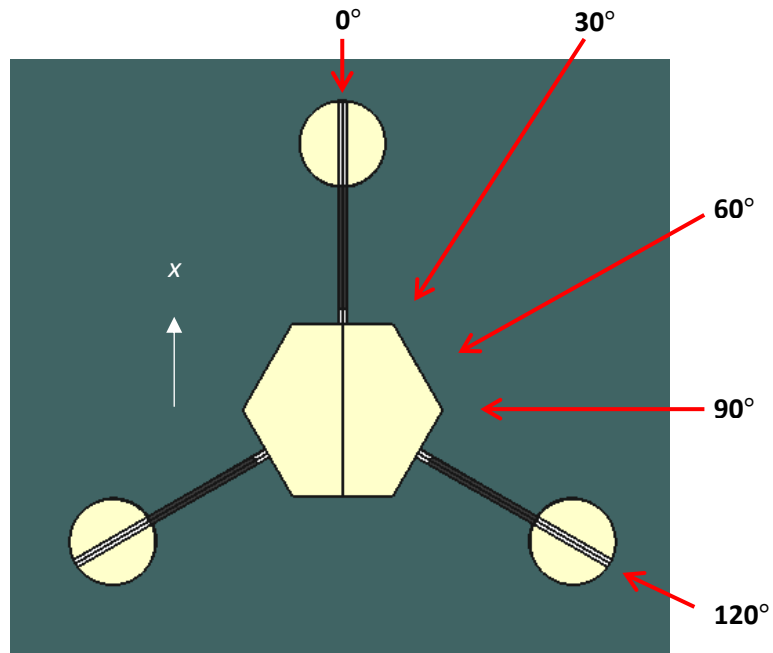


Figure 4.21 Load headings toward the pontoon.

The data input for this analysis are the draft, load heading, radius of gyration, centre of gravity coordinates, wave spectrum, period, current, wind speed, water depth, and the 3D model file in .DAT/.dat format. The motion response in the form of RAO (Response

Amplitude Operator) for six degrees of freedom surge, sway, heave, roll, pitch, and yaw are then generated from running using Moses Editor. In this analysis, the RAO data shows the characteristics of the initially designed ponton motion before mooring system is installed, hence, the free floating state. The RAO data are given in a Wave Frequency (rad/s) versus RAO (m/m) and RAO (deg/m) for both translational and rotational motion consecutively. The analysis of RAO graphs for each variation are as given in the following.

#### 4.4.1 Motion Analysis of Variation 1.

The motion analysis for ponton with floaters are given for surge, sway, heave, roll, pitch and yaw. These analyses are as shown in the following sub chapters.

##### 4.4.1.1 RAO Analysis for Surge Motion

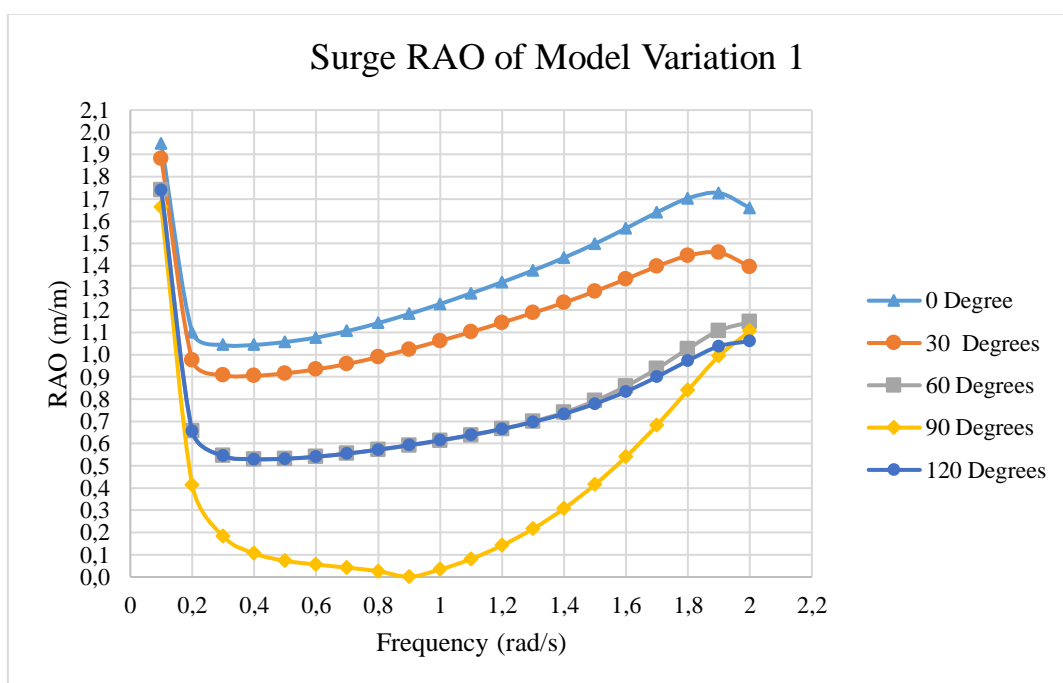


Figure 4.22. Surge RAO of variation 1 in free floating condition.

The data in Figure 4.22 above shows that the Surge RAO value data for all load headings from  $0^\circ$  until  $120^\circ$  have the same pattern, regardless of the different values. Each heading has the highest RAO when the frequency is at the lowest, and then the RAO is declining until it reaches its lowest value at a certain frequency, after that, the RAO is increasing again but it stays below its initial highest value.

The RAO due to load at  $0^\circ$  heading have the highest set of value starting at 1,949 m/m at frequency 0,1 rad/s. The second highest set of value of RAO is due to load at  $30^\circ$  heading starting from 1,882 m/m. The RAO set of value for load heading at  $60^\circ$  and  $90^\circ$

are almost identical starting at 1,740 m/m and 1,664 m/m consecutively, while the lowest set of RAO value is due to load at 90° heading starting from 1,664 m/m. It can be concluded that the highest surge RAO occurs at the lowest frequency and that load coming from 0° heading has the biggest impact on the ponton, this is accordant to the characteristic of surge motion being heavily impacted by wave at bow and stern, which in this analysis is the load heading of 0°.

#### 4.4.1.2 RAO Analysis for Sway Motion

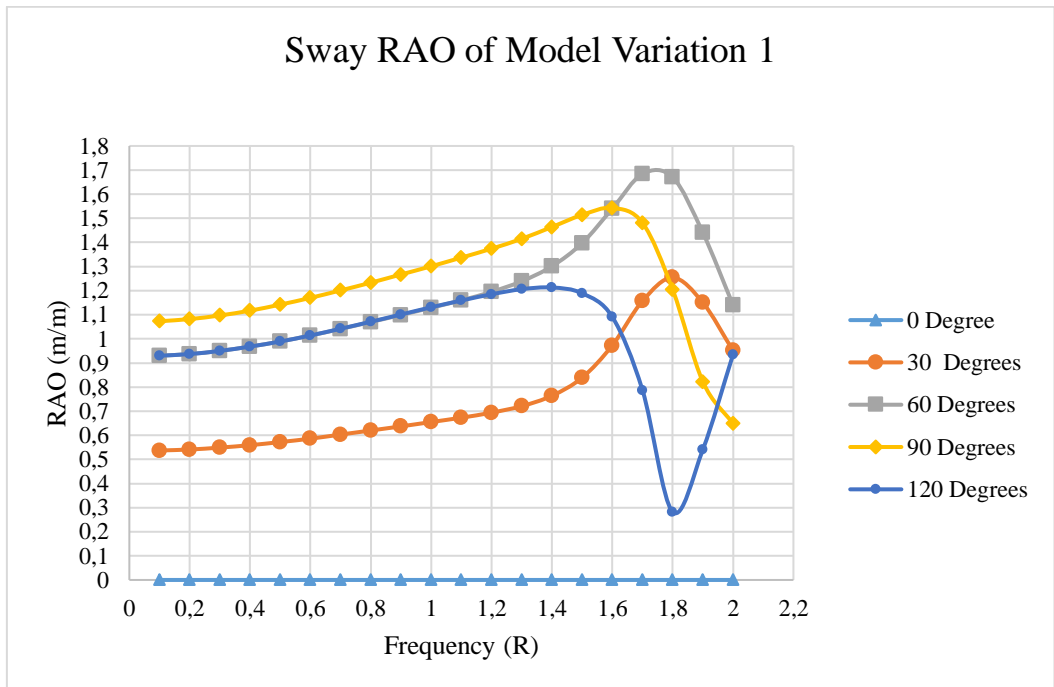


Figure 4.23. Sway RAO of variation 1 in free floating condition.

The data in Figure 4.23 above shows that as the frequency increases, the sway motion RAO values due to all load headings are steadily increasing, except for load at 0° heading that stays at 0 m/m. Although the highest set of sway motion RAO value is due to load from 90° heading starting at 1,073 m/m frequency 0,1 rad/s, the highest RAO is due to load from heading 60° at 1,684 m/m frequency 1,7 rad/s.

Regardless of the random spread of RAO values, it is still accordant to the characteristic of sway motion because sway motion will not occur when load is coming towards the bow or stern, which is proved by the zero values for heading at 0°. Sway motion will most likely be occurring when the load is coming horizontally towards the ponton, which is the highest when load is coming from 90° heading, followed by 120° and 60°, and then the lowest at 30°.



#### 4.4.1.3 RAO Analysis for Heave Motion

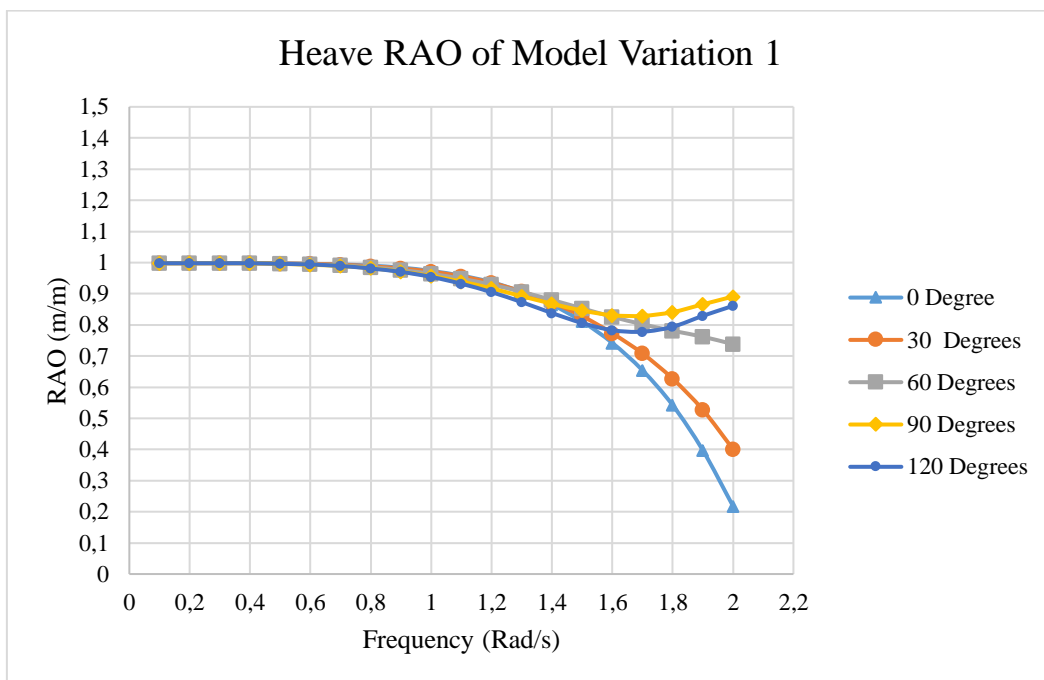


Figure 4.24. Heave RAO of variation 1 in free floating condition.

The data in Figure 4.24 above shows that the heave RAO data have an identical pattern. The graphs are steadily decreasing, although there are a few raises in 90° and 120° headings, the values are expected to also decline towards zero at a certain higher frequency. This is likely due to the symmetrical shape of the ponton hull.

The highest values of heave RAO is reached in every load headings at 0,998 to 0,906 m/m frequency 0,1 to 1,3 rad/s. The heave RAO is highly impacted by load coming from 90° heading because it has the highest average of RAO value, followed by 60°, 120°, 30°, and then the lowest impact at 0° heading.

#### 4.4.1.4 RAO Analysis for Roll Motion

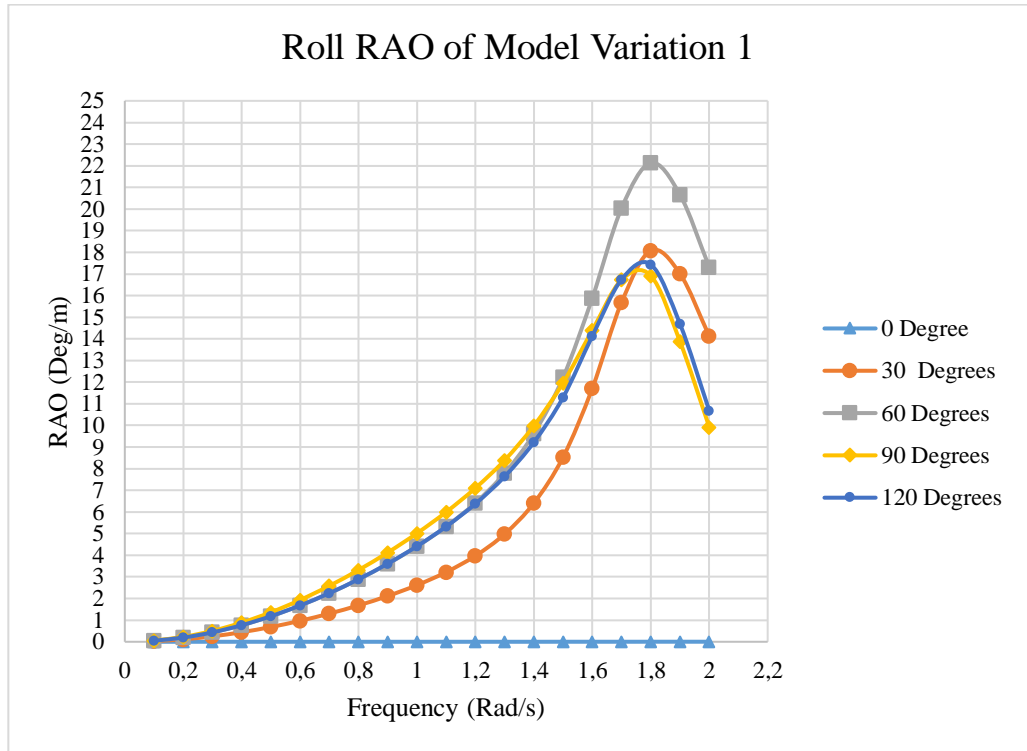


Figure 4.25. Roll RAO of variation 1 in free floating condition.

The data in Figure 4.25 above shows an identical parabolic pattern for every load heading, except for  $0^\circ$  heading, because roll motion is unlikely to be affected by loads coming towards the bow and stern of the ponton, which in this analysis is the  $0^\circ$  heading. This is proofed by the zero RAO values from  $0^\circ$  heading graph.

The highest value of roll RAO is at 22,133 deg/m frequency 1,8 rad/s due to load from  $60^\circ$  heading, followed by 18,081 rad/m frequency 1,8 rad/s from  $30^\circ$  heading, then at 17,437 rad/m frequency 1,8 rad/s from  $120^\circ$  heading, and lastly at 16,920 rad/m frequency 1,8 rad/s from  $90^\circ$  heading. It can be concluded that the ponton roll RAO is more likely to occur as the heading degree increases, loads coming from  $60^\circ$  heading being the most affecting.

### 4.3.1.5 RAO Analysis for Pitch Motion

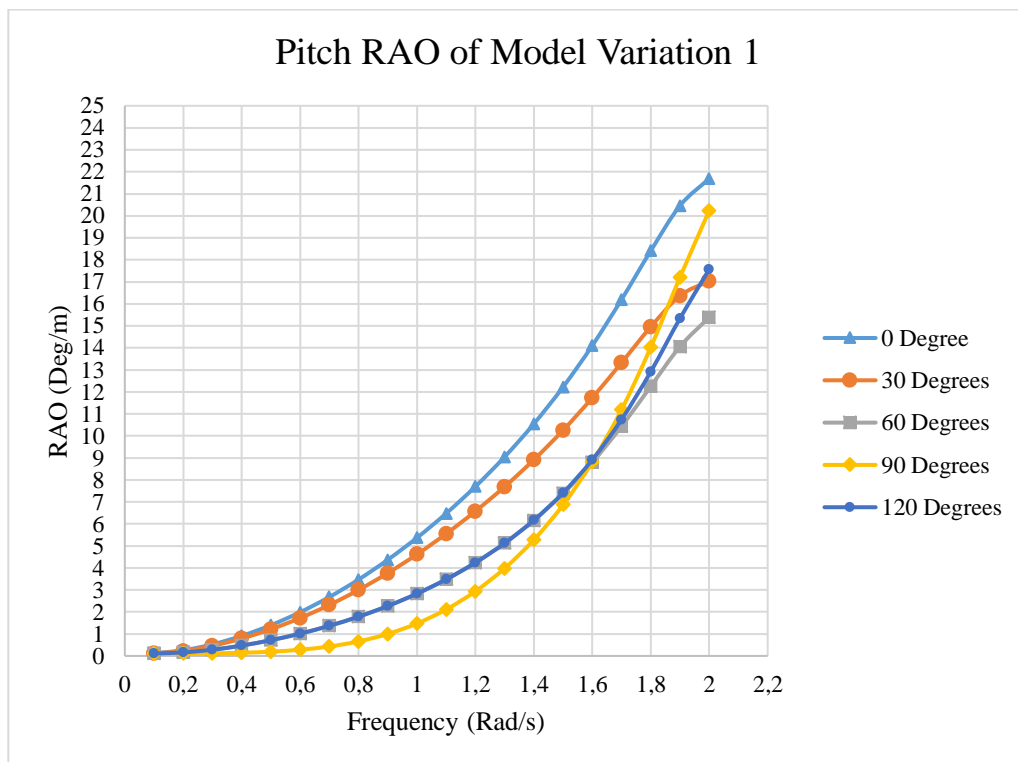


Figure 4.26. Pitch RAO of variation 1 in free floating condition.

The Figure 4.26 above shows that the pitch RAO is likely to occur at all load headings. The highest values of pitch RAO are all occurring at frequency 2 rad/s, the highest of all being at 21,695 deg/m from load heading 0°, then the second highest at 20,240 deg/m from load heading 90°, followed by RAO at 17,569 deg/m from load heading 120°, then at 17,041 deg/m from load heading 30°, and the least highest being at 15,394 deg/m from load heading 60°.

This set of data shows that the pitch RAO for the ponton is heavily affected by loads coming from 0° heading. This is accordant to the characteristic of pitch motion, because pitch is the rotational motion on the z axis of the floating body, which makes it vulnerable to loads coming towards the bow and stern of the floating body, which in this analysis is supposed to be the 0° heading.

#### 4.4.1.5 RAO Analysis for Yaw Motion

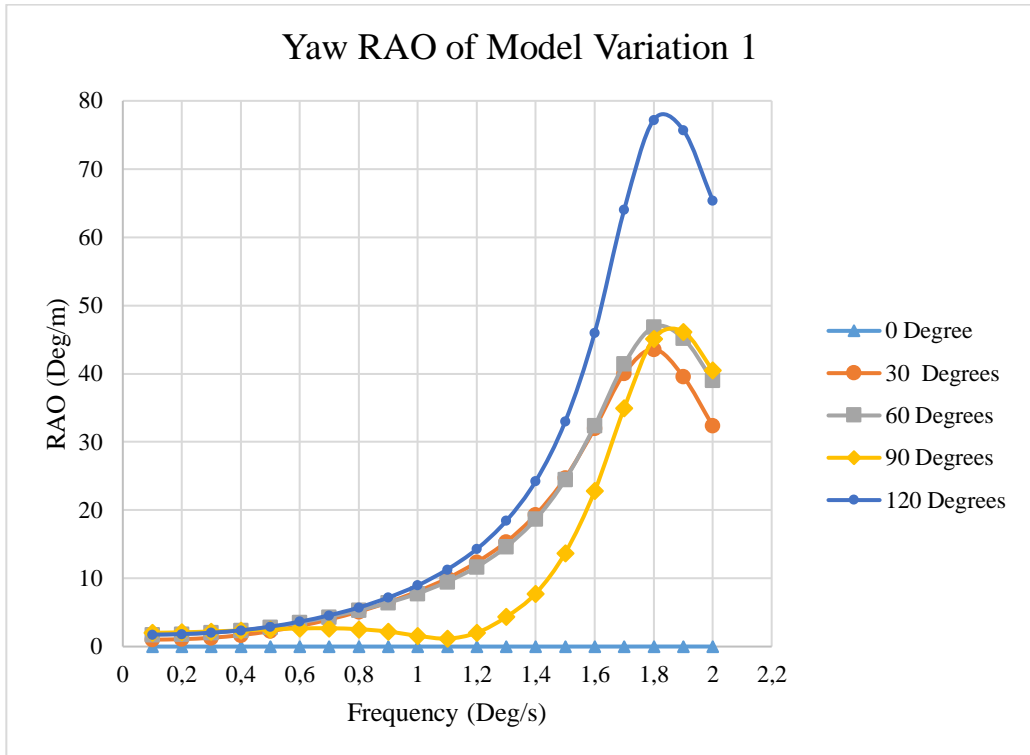


Figure 4.27. Yaw RAO of variation 1 in free floating condition.

Figure 4.27 above shows that yaw RAO is obviously most affected by loads coming from 120° heading. The yaw RAO value data set for heading 120° is remarkably higher if compared to the other headings. Meanwhile, the difference in yaw RAO value data set for heading 0° is also very drastic because all of the values are very close to zero.

The highest yaw RAO is at 77,212 deg/m frequency 1,8 deg/m due to loads from 120° heading, the second highest is at 46,854 deg/m frequency 1,8 deg/s due to load coming from 60° heading, followed by 46,178 deg/m frequency 1,9 deg/s due to load coming from 90° heading, and the least highest at 43,594 deg/m frequency 1,8 deg/s due to load coming from 30° heading. It can be concluded that the yaw RAO of the ponton is highly affected by loads coming from 120° heading and that the load from 0° heading do not have a significant effect on the ponton yaw RAO.

## Motion Response Analysis of Variation 2

The motion analysis for ponton without floaters are given for surge, sway, heave, roll, pitch and yaw. These analyses are as shown in the following sub chapters.

### 4.4.1.6 RAO Analysis for Surge Motion

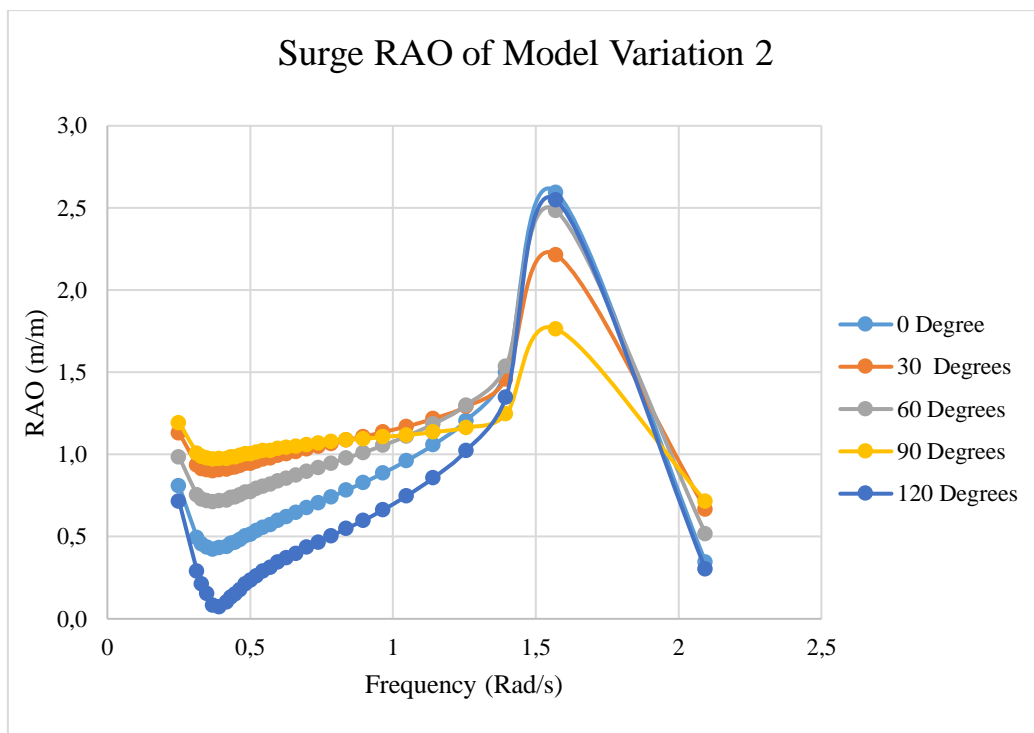


Figure 4.28. Surge RAO of variation 2 in free floating condition.

The data in Figure 4.28 above shows that the Surge RAO value data for all load headings from  $0^\circ$  until  $120^\circ$  have the same pattern. Each heading has the highest RAO when the frequency is at around 1,57 Rad/s, and then the RAO keeps declining.

The highest initial RAO value is 1,194 m/m frequency 1,25 Rad/s due to load heading from  $90^\circ$ , followed by  $30^\circ$ ,  $60^\circ$ ,  $0^\circ$ , and  $120^\circ$ . Highest surge RAOs occurs at frequency 1,57 Rad/s with the highest RAO is 2,596 m/m due to load from heading  $0^\circ$ . it can be concluded that load coming from  $0^\circ$  heading has the biggest impact on the ponton, this is accordant to the characteristic of surge motion being heavily impacted by wave at bow and stern, which in this analysis is the load heading of  $0^\circ$ .

#### 4.4.1.7 RAO Analysis for Sway Motion

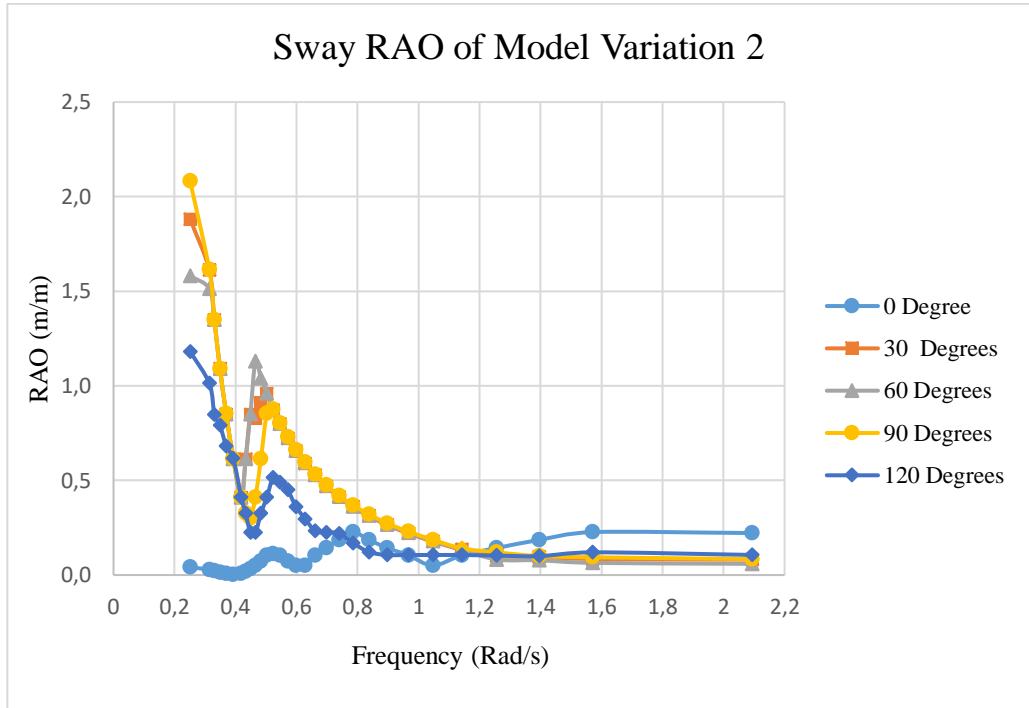


Figure 4.29. Sway RAO of variation 2 in free floating condition.

The data in Figure 4.29 above shows that as the frequency increases, the sway motion RAO values in all load headings are steadily declining. All RAO start to decline around frequency 0,4 Rad/s after the peak, and then it stays stable. The highest value of sway motion RAO is due to load from 90° heading starting at 2 m/m frequency 0,25 rad/s, followed by RAO in load heading 30°, 60°, 120°, and 0° at 1,88 m/m, 1,58 m/m, 1,18 m/m, and 0,04 m/m consecutively.

Based on the analysis, it is still accordant to the characteristic. Sway motion will most likely be occurring when the load is coming horizontally towards the ponton, which is the highest when load is coming from 90° heading, followed by 120° and 60°, and then the lowest at 30°. Sway motion will not likely to occur when load is coming towards the bow or stern, which is proved by values at 0° that are close to zero.

#### 4.4.1.8 RAO Analysis for Heave Motion

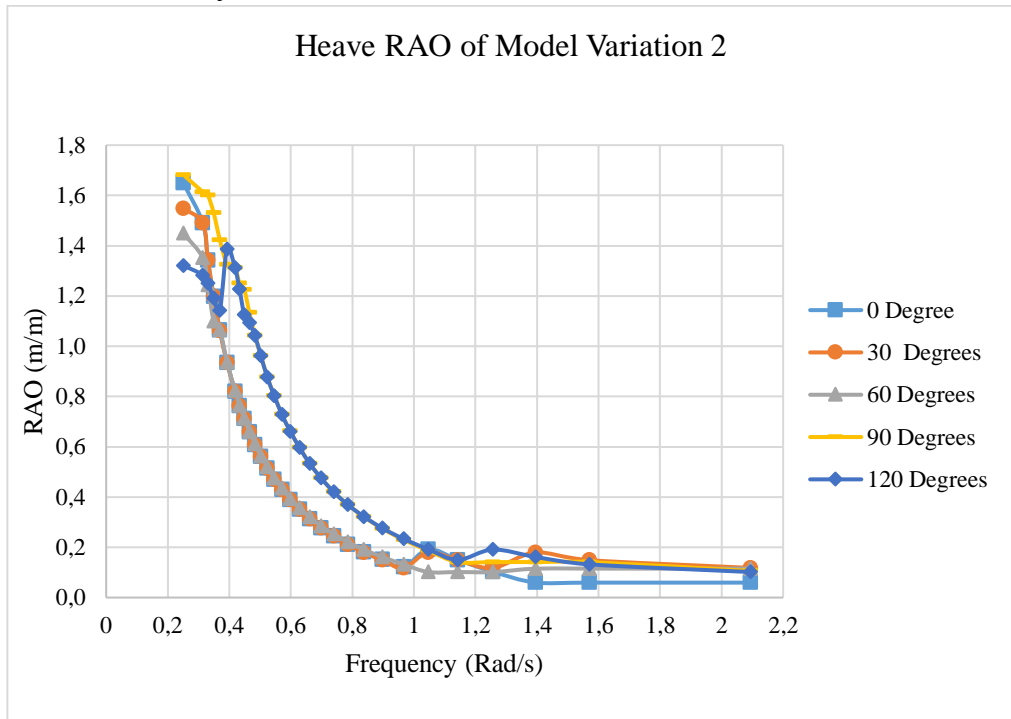


Figure 4.30. Heave RAO of variation 2 in free floating condition.

The data in Figure 4.30 above shows that the heave RAO data have an identical pattern. The graphs are steadily decreasing, although there are a few raises, the values are expected to also decline towards zero at a certain higher frequency. This is likely due to the symmetrical shape of the ponton hull that makes it easier for the ponton to stabilize.

The highest values of heave RAO are reached in load heading 90° at 1,6 m/m frequency 0,24 rad/s. The heave RAO is highly impacted by load coming from 90° heading, followed by 120°, 30°, 0°, and then 60°. The values of heave RAOs for Variation 2 are higher compared to Variation 1 is likely caused by its lower mass.

#### 4.4.1.9 RAO Analysis for Pitch Motion

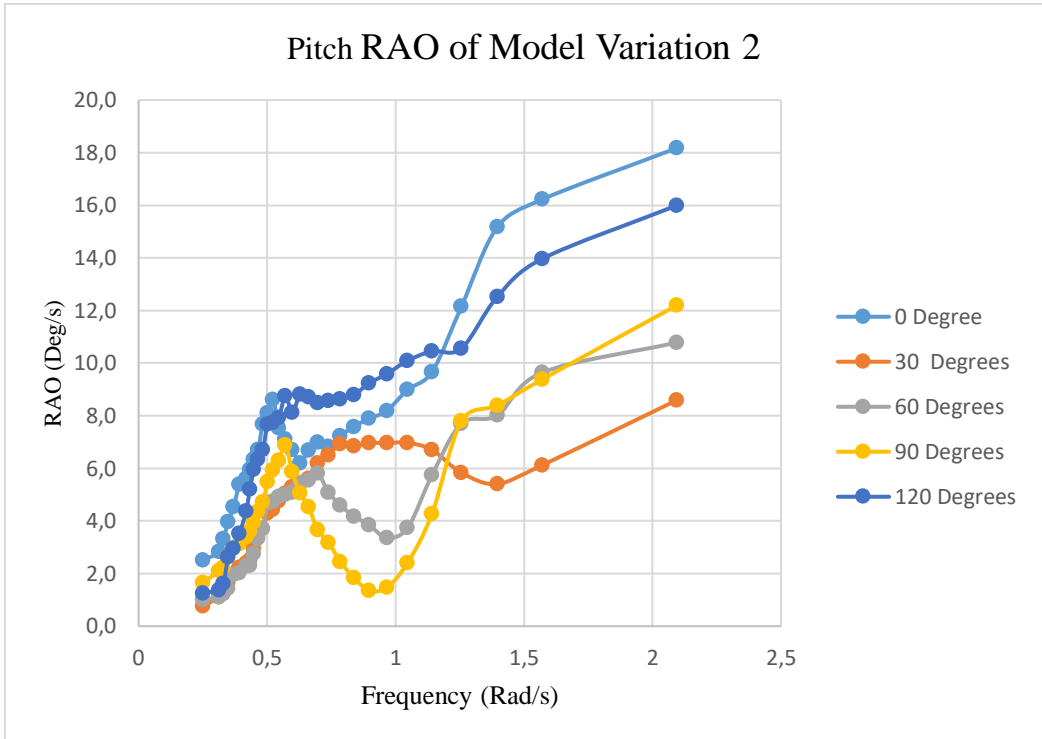


Figure 4.31. Pitch RAO of variation 2 in free floating condition.

Figure 4.31 above shows that pitch RAO keeps on inclining as the frequency increases. The highest pitch RAO occurred is at 18,17 deg/m from load heading 0°, then the second highest at 16 deg/m from load heading 120°, followed by RAO at 12,1 deg/m from load heading 90°, then at 10,04 deg/m from load heading 60°, and the least highest being at 8,5 deg/m from load heading 30°.

This set of data shows that the pitch RAO for the ponton is heavily affected by loads coming from 0° heading. This is accordant to the characteristic of pitch motion, because pitch is the rotational motion on the z axis of the floating body, which makes it vulnerable to loads coming towards the bow and stern of the floating body.



#### 4.4.1.10 RAO Analysis for Roll Motion

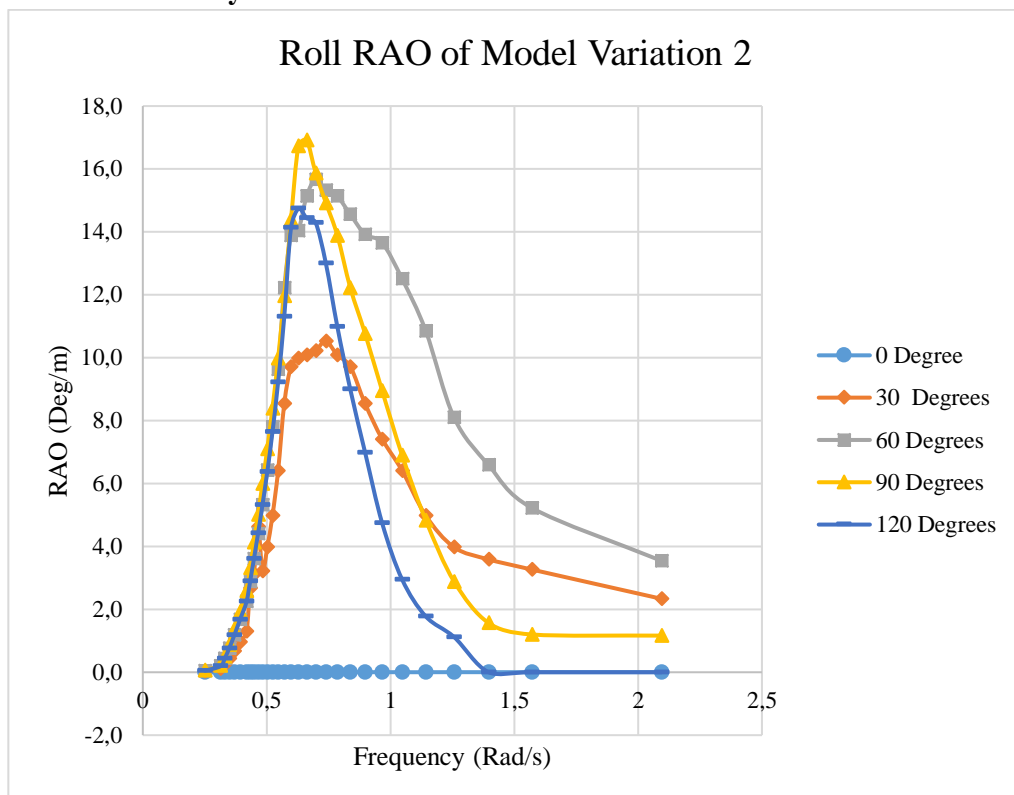


Figure 4.32. Roll RAO of variation 2 in free floating condition.

The data in Figure 4.32 above shows an identical parabolic pattern for every load heading, except for 0° heading, because roll motion is unlikely to be affected by loads coming towards the bow and stern of the ponton, which in this analysis is the 0° heading. This is proofed by the zero RAO values from 0° heading graph.

The highest value of roll RAO is at 16,9 deg/m frequency 0,66 rad/s due to load from 90° heading, followed by 14,92 rad/m frequency 0,7 rad/s from heading 60°, then at 14,4 rad/m frequency 0,66 rad/s from 120° heading, and lastly at 10,9 rad/m frequency 0,78 rad/s from 30° heading, load coming from 90° heading being the most affecting.

#### 4.4.1.11 RAO Analysis for Yaw Motion

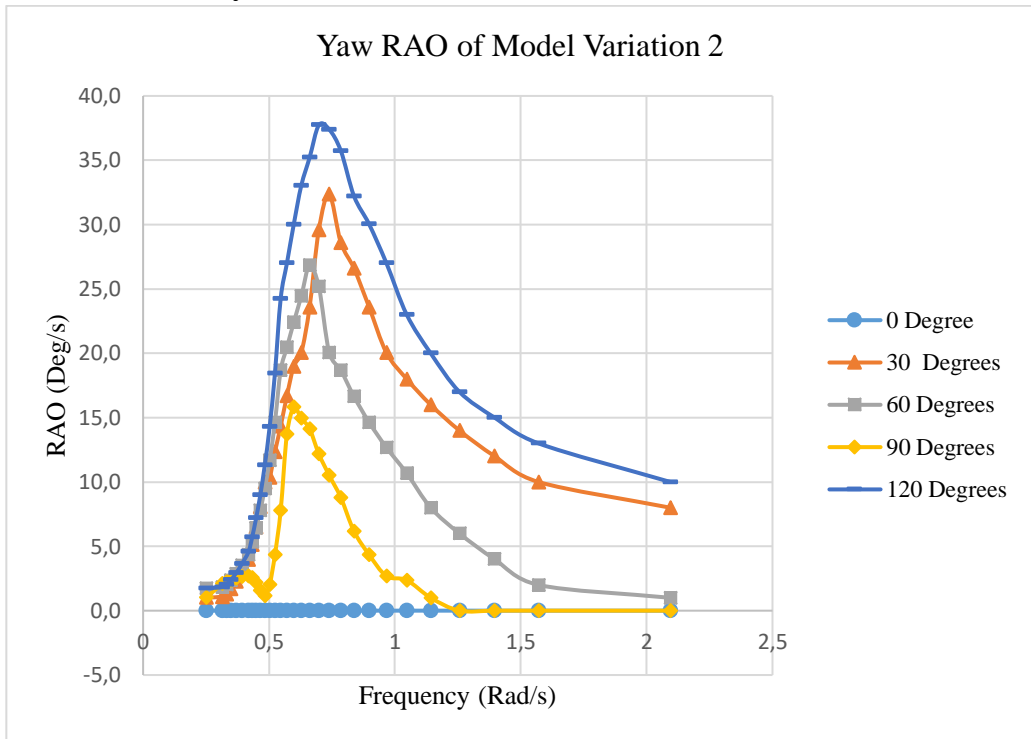


Figure 4.33. Yaw RAO of variation 2 in free floating condition.

The data in Figure 4.33 above shows that yaw RAO is mostly affected by loads coming from 120° heading. The yaw RAO value data set for heading 120° is the highest compared to the other headings. Meanwhile, the difference in yaw RAO value data set for heading 0° is also very drastic because all of the values are very close to zero.

The highest yaw RAO is at 37,2 deg/m frequency 0,7 deg/m due to loads from 120° heading, the second highest is at 32,3 deg/m frequency 0,74 deg/s due to load coming from 30° heading, followed by 26,8 deg/m frequency 0,7 deg/s due to load coming from 60° heading, and the lowest at 14,9 deg/m frequency 0,6 deg/s due to load coming from 30° heading. It can be concluded that the yaw RAO of the ponton is highly affected by loads coming from 90° heading and that the load from 0° heading do not have a significant effect on the yaw RAO.

#### 4.4.2 Motion Response Analysis of Model Variation 3

The motion analysis for ponton with shortened floater arms are given for surge, sway, heave, roll, pitch and yaw. These analyses are as shown in the following sub chapters.

##### 4.4.2.1 RAO Analysis for Surge Motion

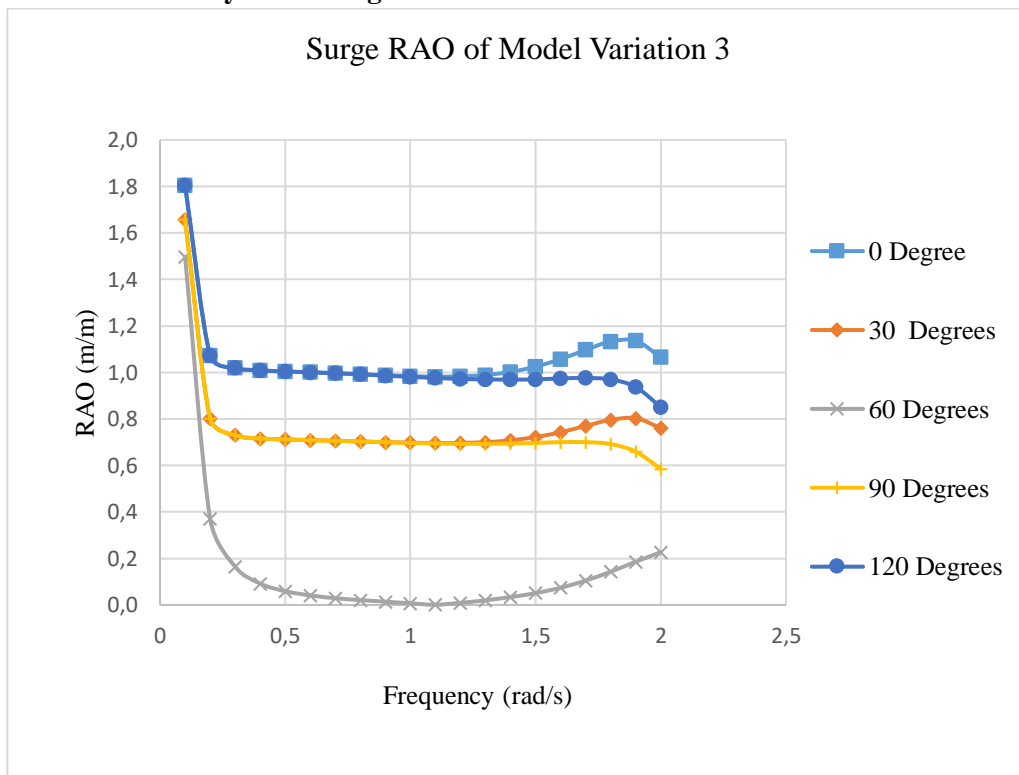


Figure 4.34. Surge motion RAO of model variation 3 in free floating condition.

The data in Figure 4.34 above shows that the Surge RAO value data for all load headings from  $0^\circ$  until  $120^\circ$  have an identical pattern. Each heading has the highest RAO when the frequency is at around  $1.85 \text{ Rad/s}$ , and then the RAO is declining except for RAO due to load from  $60^\circ$  heading.

The highest RAO value is  $1.8 \text{ m/m}$  frequency  $1.85 \text{ Rad/s}$  due to load heading from  $0^\circ$ , followed by  $120^\circ$ ,  $30^\circ$ ,  $90^\circ$ , and  $60^\circ$ . It can be concluded that load coming from  $0^\circ$  heading has the biggest impact on the ponton, this is accordant to the characteristic of surge motion being heavily impacted by wave at bow and stern, which in this analysis is the load heading of  $0^\circ$ .

#### 4.4.2.2 RAO Analysis for Sway Motion

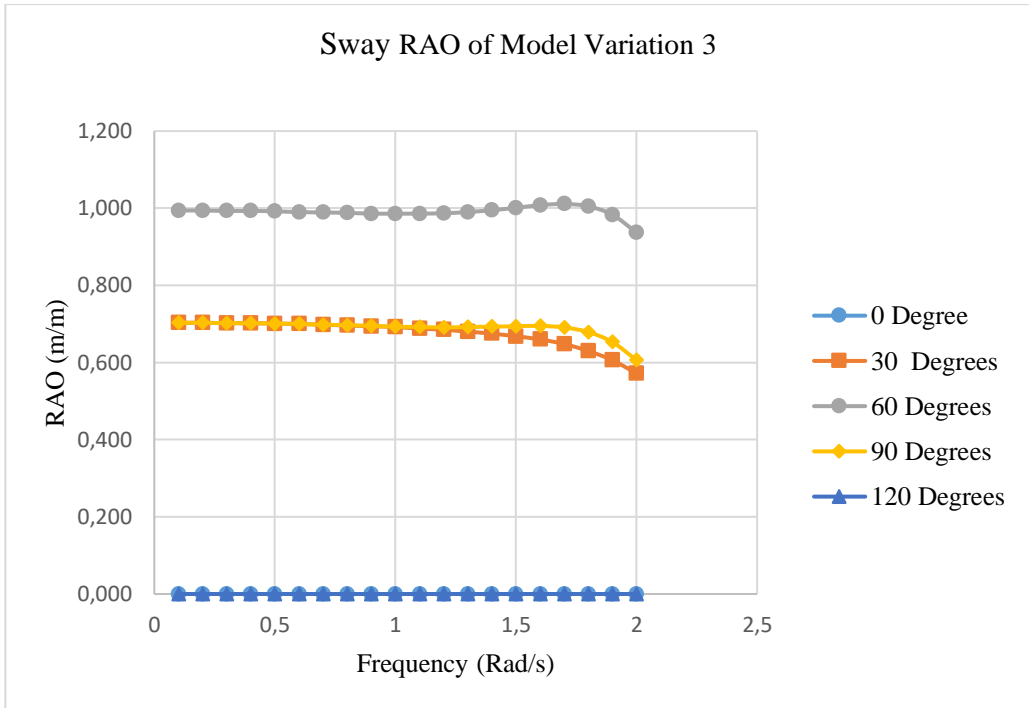


Figure 4.35. Sway RAO of variation 3 in free floating condition.

The data in Figure 4.35 above shows that as the frequency increases, the sway motion RAO values due to all load headings are steadily decreasing, except for load at 120° heading that stays at 0 m/m. The highest set of sway motion RAO value is due to load from 60° heading starting at 0,99 m/m frequency 0,1 rad/s, the highest RAO is due to load from heading 60° at 1,8 m/m frequency 1,005 rad/s.

Regardless of the random spread of RAO values as shown in Figure 52 above, it is still accordant to the characteristic of sway motion because sway motion will not occur when load is coming towards the bow or stern, which is proved by the zero values for heading at 0°. Sway motion will most likely be occurring when the load is coming horizontally towards the ponton, which is the highest when load is coming from 60° heading, followed by 90° and 30°, and then the lowest at 120° and 0°.

#### 4.4.2.3 RAO Analysis for Heave Motion

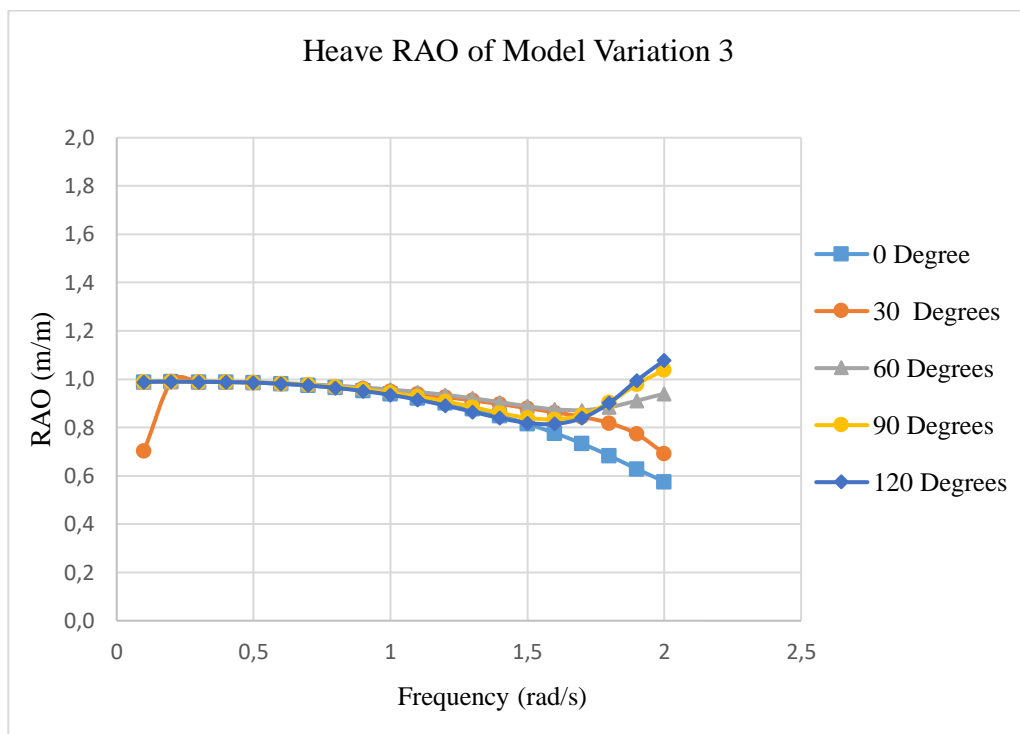


Figure 4.36. Heave RAO of variation 3 in free floating condition.

The data in Figure 4.36 above shows that the heave RAO data have an identical pattern. The graphs are steadily decreasing. This is likely due to the symmetrical shape of the ponton hull that makes it easier for the ponton to stabilize. However, the values began to incline and decline at the same time after frequency 1,6 Rad/s.

The highest values of heave RAO are reached during load heading  $0^\circ$  at 1,07 m/m frequency 24 rad/s. The heave RAO is highly impacted by load coming from  $120^\circ$  heading, followed by  $90^\circ$ ,  $60^\circ$ ,  $30^\circ$ , and then  $0^\circ$ . The values of heave RAOs for Variation 3 are higher compared to Variation 1 and 2 is likely due to lower mass since it does not have any floaters and floater arms.

#### 4.4.2.4 RAO Analysis for Pitch Motion

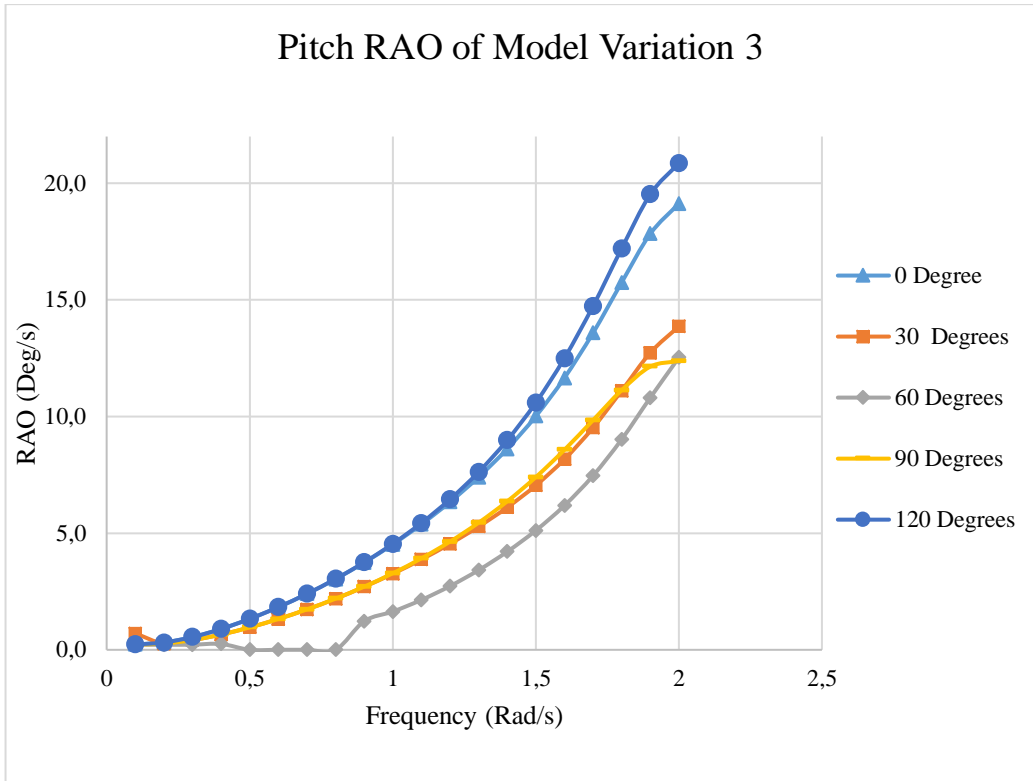


Figure 4.37. Pitch RAO of variation 3 in free floating condition.

Figure 4.37 above shows that pitch RAO keeps on inclining as the frequency increases. The highest pitch RAO occurred is at 20,86 deg/m from load heading 120°, then the second highest at 19,13 deg/m from load heading 0°, followed by RAO at 13,8 deg/m from load heading 30°, then at 12 deg/m from load heading 90°, and the least highest being at 12,3 deg/m from load heading 60°.

This set of data shows that the pitch RAO for the ponton is heavily affected by loads coming from 120° and 0° heading. This is accordant to the characteristic of pitch motion, because pitch is the rotational motion on the z axis of the floating body, which makes it vulnerable to loads coming towards the bow and stern of the floating body.

#### 4.4.2.5 RAO Analysis for Roll Motion

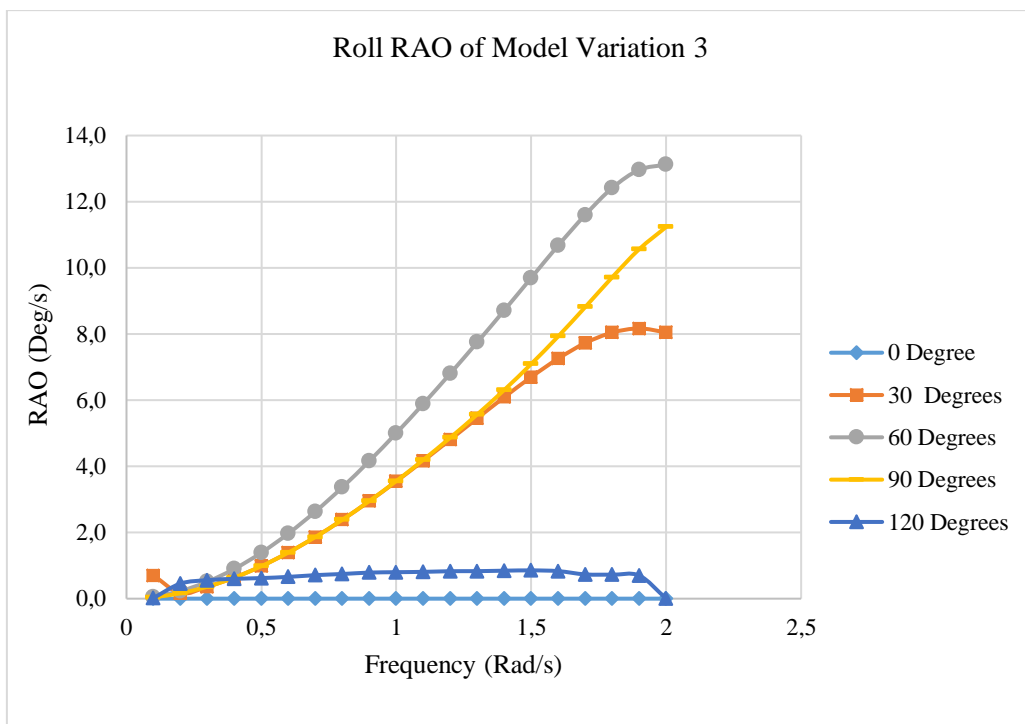


Figure 4.38. Roll RAO of variation 3 in free floating condition.

The data in Figure 4.38 above shows an identical exponential pattern for every load heading, except for  $0^\circ$  heading because it is unlikely going to be affected by loads coming towards the bow and stern of the ponton, which in this analysis is the  $0^\circ$  heading, since it is a horizontally rotational motion. This is proofed by the zero RAO values from load coming from  $0^\circ$  heading in the figure.

The highest value of roll RAO is at 13,1 deg/m frequency 2 rad/s due to load from  $60^\circ$  heading, followed by 11,2 rad/m frequency 2 rad/s from heading  $90^\circ$ , then at 8,04 rad/m frequency 2 rad/s from  $30^\circ$  heading, and lastly at 1,9 rad/m frequency 1,9 rad/s from  $120^\circ$  heading, load coming from  $60^\circ$  heading is the most effecting load to model Variation 1.

#### 4.4.2.6 RAO Analysis for Yaw Motion

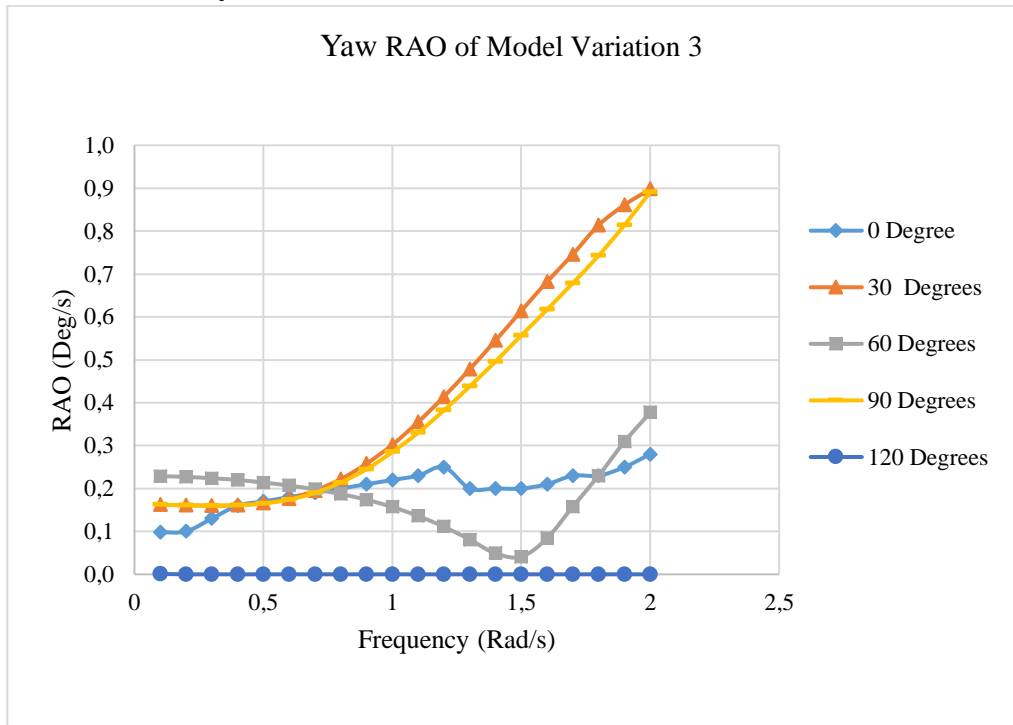


Figure 4.39. Sway RAO of variation 3 in free floating condition.

The data in Figure 4.39 above shows that yaw RAO for this model variation is mostly affected by loads coming from 30° heading. The yaw RAO value data set for heading 30° is the highest compared to the other headings. Meanwhile, the difference in yaw RAO value data set for heading 0° is also very drastic because all of the values are very close to zero.

The highest yaw RAO is at 0,891 deg/m frequency 2 deg/m due to loads from 30° heading, the second highest is also at 0,81 deg/m frequency 2 deg/s due to load coming from 90° heading, followed by 0,37 deg/m frequency 2 deg/s due to load coming from 60° heading, and the lowest at 0,2 deg/m also at frequency 2 deg/s due to load coming from 0° heading. It can be concluded that the yaw RAO of the ponton is highly affected by loads coming from 30° heading and that the load from 120° heading do not have a significant effect on the yaw RAO.



## 4.5 Mooring System Analysis

Mooring system analysis requires two objects, the ponton (vessel) and the mooring line as shown in Figure 4.40 and 4.41 below. The ponton is redrawn while the mooring line is selected and placed according to a single point mooring configuration should be. The mooring line is attached at the bottom of the ponton at point coordinate  $(x,y,z) = (0,0,0)$ . The depth of water is 22,9 meters with length of mooring line 29,4 meters.

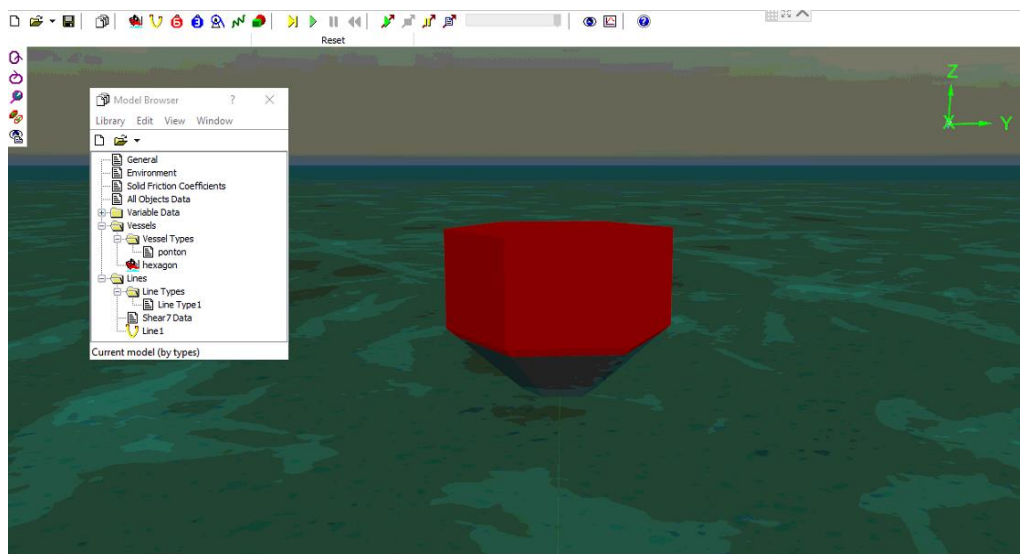


Figure 4.40. 3D view of mooring simulation.

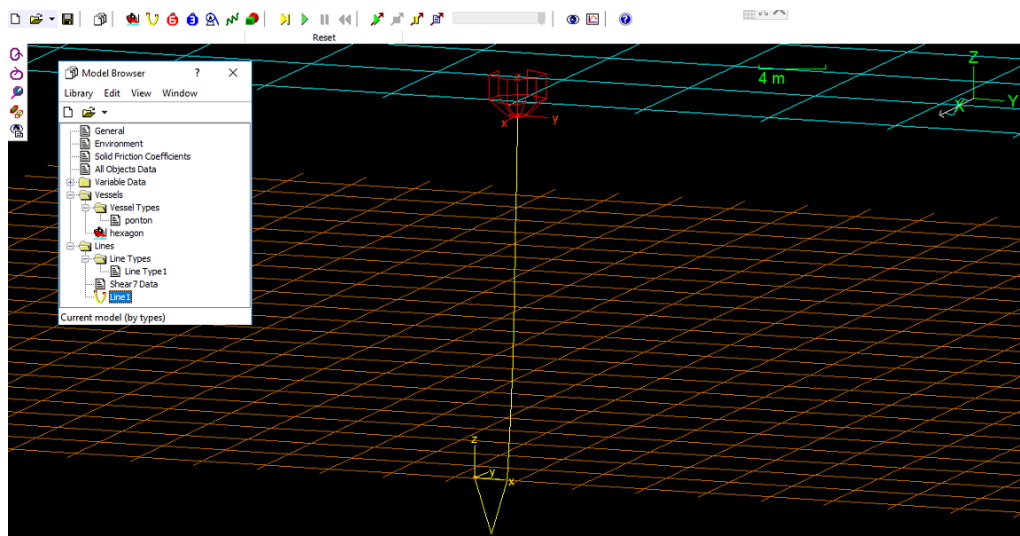


Figure 4.41. Single Point Mooring system perspective view.

#### 4.5.1 Analysis of Ponton Excursion

Excursion of the ponton in x-axes and y-axes is derived from the mooring simulation. The simulation is conducted for 10.800 seconds (operation time) for all load heading  $0^\circ$ ,  $30^\circ$ ,  $60^\circ$ ,  $90^\circ$ ,  $120^\circ$ . the result of the simulation is as shown in Table 4.6 below.

Table 4.6 Excursion Analysis of Ponton with mooring system.

Heading (Degree)	Maximum Excursion Along Axes (meters)	
	x	y
0	2,9	5,1
30	1	2,5
60	1	2,52
90	2,67	2,75
120	1,5	2,5

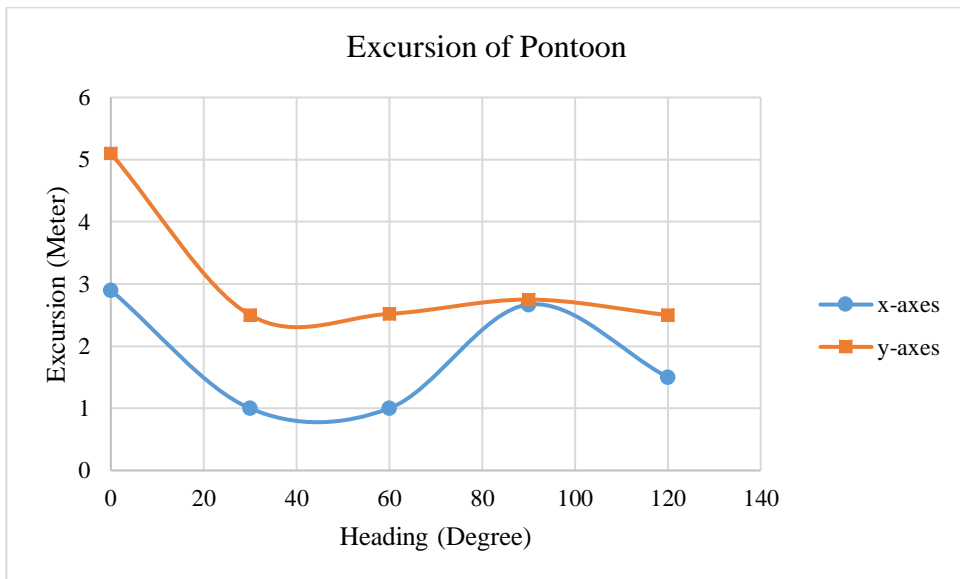


Figure 4.42. Excursion along X and Y axis of Ponton with mooring system.

Based on data in Figure 4.42 above, the comparison of maximum excursion of the ponton after mooring system is installed on X and Y-axis in Figure 4.60 is analysed. The furthest excursion occurred when load is coming from  $0^\circ$  heading at 5,1 meters along X-axis. The shortest excursion occurred when load is coming from  $120^\circ$  heading at 1,5 meters along Y-axis.

### 4.5.2 Analysis of Ponton Motion

The ponton motion analysis of the ponton in x-axes and y-axes derived from the mooring simulation. The simulation is conducted for 10800 seconds (operation time) for all load heading  $0^\circ$ ,  $30^\circ$ ,  $60^\circ$ ,  $90^\circ$ ,  $120^\circ$ . the result of the simulation is as shown in Table 4.7 below.

Table 4.7. Motion Analysis of Ponton with mooring system.

Heading (Degree)	Maximum Rotation along Axes (Degree)	
	x	y
0	18,15	17,53
30	27,9	21,6
60	51,3	21,7
90	62,5	33,7
120	34,6	15,5

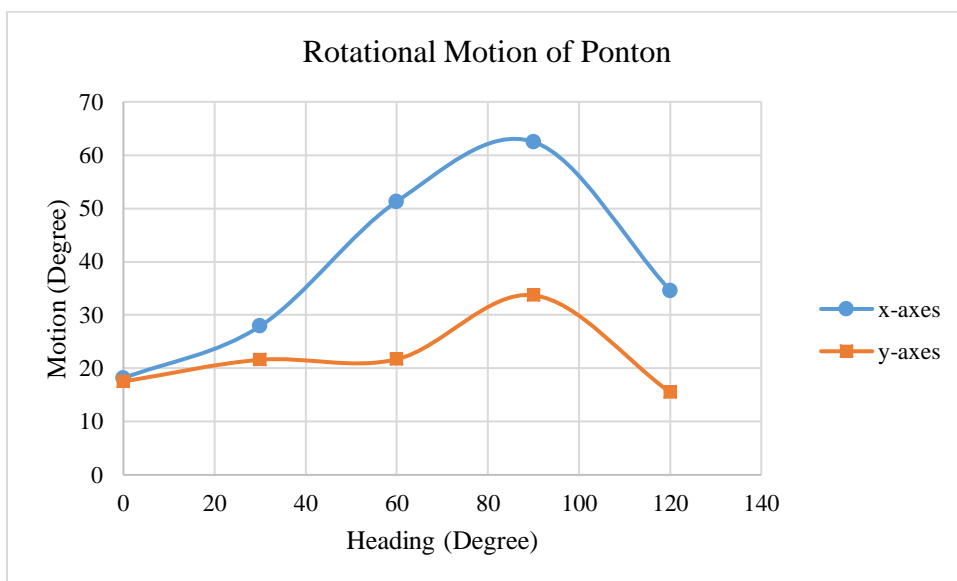


Figure 4. 43. Rotational motion along X and Y axis of Ponton with mooring system.

Figure 4.43 above shows that the highest degree of motion occurred at  $62,5^\circ$  along the x-axis when load is coming from  $90^\circ$  heading, this means that the ponton is experiencing rolling. The lowest degree of motion occurred at  $15,5^\circ$  along y-axis when load is coming from  $120^\circ$  heading, which means that the ponton experienced pitching.

### 4.5.3 Analysis of Mooring Line Tension

This simulation used single point mooring system. The material of mooring line is Nylon rope with a diameter of 56 mm, mass of 196 kg/100 m, and a Maximum Breaking Load of 478,4 kN. Data of mooring line tension from the simulation is as seen in Table 4.8 below.

Table 4.8 Data of Mooring Line Effective Tension at End A and B

Load Heading (Degrees)	Mooring Line Tension (kN)	
	End A	End B
0	34,6	34,25
30	278,45	278,35
60	125,76	125,95
90	95,43	95,78
120	166,12	166,14

Based on the Table 4.8 above, the maximum effective tension on mooring line is 278,45 kN when load is coming from 30° heading towards the ponton while the smallest is 34,25 kN when load is coming from 0° heading towards the ponton.

### 4.5.4 Safety Factor Calculation

The calculation of safety factor is based on the maximum breaking load and the maximum effective tension of the mooring line. The equation is as shown below.

$$\text{Safety Factor} = \frac{\text{maximum breaking load}}{\text{maximum tension}}$$

Based on the equation above, the value of safety factor is 1,71. This value is acceptable for the minimum requirement from API RP 1SK.

## **Chapter 5**

### **Conclusions and Suggestion**

#### **5.1 Conclusion**

There are a number of conclusions based on the analysis in chapter 4. The conclusions are as written below:

1. Model Variation 1 of the wave energy conversion system is the most effective design compared to Variation 2 and 3. The addition of floaters to the hexagonal ponton with a longer arm tend to have a higher value of both translational and rotational motion. Highest RAOs reached during seakeeping simulation for surge, sway, heave, roll, pitch and yaw is 0,998 m/m in heading 90°; 1,684 m/m in heading 60°; 0,998m/m in heading 90°; 22,13 deg/m in heading 60°; 21,65 deg/m in heading 0°; and 77,2 deg/m in heading 120° consecutively.
2. Single point mooring system is suitable for this design because after moored, the ponton is still able to have rotational and translational motion along x and y-axis. Based on the analysis of mooring simulation results, the furthest excursion occurred when load is coming from 0° heading at 5,1 meters along X-axis while the shortest excursion occurred when load is coming from 120° heading at 1,5 meters along Y-axis. Rolling motion reached 62,5° along the x-axis when load is coming from 90° heading while pitching reached 15,5° along y-axis when load is coming from 120° heading.

#### **5.2 Suggestion**

1. The variation of floater arm lengths may be added to be able to increase the accuracy in analysing the behaviours of the system.
2. The 3D numerical modelling needs to be done meticulously, avoid any overlapping surface and make sure that every edge of the model is closed before conducting simulation on Moses.

“This page is intentionally left blank

## References

- Wardhana, Ede Mehta. (2013). *Analisa dan Penempatan Mooring pada Ponton Pembangkit Listrik Tenaga Gelombang Laut - Sistem Bandulan*. Department of Marine Engineering, ITS: Surabaya.
- Robert E. Harris, BSc, PhD, CEng, MIMarEST. *Mooring systems for wave energy converters: A review of design issues and choices*. Edinburgh; A Brief Introduction to Important Vessel Mooring Techniques. Marine Insight, UK.
- Mukhtasor, dkk. *Performance Modelling of a Wave Eenergy Converter: Pembangkit Listrik Tenaga Gelombang Laut Sistem Bandulan ("PLTGL-SB")*. Surabaya; Indonesia.
- Dr Dmtry Sadovnikov, Piotr Sujkowski, Dr Yuriy Drobyshevski. *Maintaining Integrity of FPSO Mooring System*. INTECSEA. Perth; Western Australia.
- API, "Design and Analysis of Stationkeeping System for Floating Structure," American Petroleum Institute (API), New York, 2005.
- Dharma. Wisnu Setia. (2017). *Analisis Penggantian Mooring Struktur Terapung*. Ocean Engineering, ITS: Bandung.
- Fitria. Favi Ainin. (2018). *Studi Pengaruh Penambahan Clumb Buoy Pada System Mooring Platform PLTAL Laut Dalam*. *International Journal of Marine Engineering Innovation and Research*, no. Renewable Energy. Department of Marine Engineering, ITS: Surabaya.
- Munib. Ahmadi. (2019). *Analisis Numerik Respon Gerak pada Lambung Cylindrical Platform PLTAL Laut Dalam*. Department of Marine Engineering, ITS: Surabaya.
- Suwandi. Arief Rachman. (2018). *Studi Kekuatan Konstruksi pada Sambungan Mooring di Pembangkit Listrik Tenaga Arus Laut (PLT Arus Laut Platform Katamaran)*. Department of Marine Engineering, ITS: Surabaya.
- Charizzaka. Ahmad. (2016). *Analisis Pengikatan dan Gerakan Pada Dok Apung Akibat Gaya Luar dengan Variasi Desain Pengikatan di Perairan Dangkal Terbuka*. Department of Ocean Engineering, ITS: Surabaya.
- Santos. L. Castro. (2013). *Mooring for Floatng Offshore Renewable Energy Platforms Classification*. Department of Naval and Oceanic Engineering, Universsity of Coruna: Spain.
- Mukhtasor, dkk. (2016). *Performance Modeling of A Wave Energy Converter: Pembangkit Listrik Tenaga Gelombang Laut Sistem Bandulan ("PLTGL-SB")*. Department of Marine Engineering, ITS: Surabaya.

- Alam, Mohammad Reza (2014). *Wave Energy*. Technology Avenue
- Mandland, Stig (2012). *Dynamic Analysis for The Installation of Offshore Wind Turbine Foundations*. Faculty of Science and Technology, Universiti of Stavanger.
- Pradhana, Ardhyan Wisnu (2015). *Analisa Kekuatan Struktur Global Single Point Mooring Akibat Beban Gelombang Ekstrim*. Jurusan Teknik Kelautan, ITS: Surabaya.
- Djarmiko, Eko B (2012). *Perilaku dan Operabilitas Bangunan Laut di Atas Gelombang Acak*. ITS Press: Surabaya.
- Kusuma, Rindu Fajar (2018). *Simulasi Respon Gerak Ponton Trimaran Pada Pembangkit Listrik Tenaga Gelombang Laut*. Department of Marine Engineering, ITS: Surabaya.



## **Attachment**

### a. Moses Log File

WELCOME TO MOSES Version 07.10.01.11  
=====

This Program is licensed for the exclusive use of  
  
Bentley Select Licensee

Copying of this program or use by anyone other than an employee of the above firm without written consent of Bentley Systems is strictly prohibited.

Default License Suite: MOSES Automatic Elevation  
=====

```
>&dimen -REMEMBER -DIMEN meters m-tons
>&device -oecho no -primary device -auxin desainawaltrial1.DAT
>&TITLE MENCOBALagi
>INMODEL
      Time To perform Inmodel                : CP=      0.63
>&INSTATE desainawaltrial1 -CONDITION 1.0
>&picture iso
>&picture bow
>&picture side
>&picture top
>&weight -compute 0.17 3.86 5.86 4.83
>&equi -iter 100
      +++ C U R R E N T   S Y S T E M   C O N F I G U R A T I O N +++
      =====
```

Process is DEFAULT: Units Are Degrees, Meters, and M-Tons Unless Specified

Body	X	Y	Z	RX	RY	RZ
DESIGNAW Location	0.00	0.00	-1.00	0.00	0.00	0.00
N Force	-0.00	-0.00	0.00	0	0	0

Equilibrium Converged in 1 Iterations

>&status B\_W

+++ B U O Y A N C Y   A N D   W E I G H T   F O R   D E S I G N A W +++  
=====

Process is DEFAULT: Units Are Degrees, Meters, and M-Tons Unless Specified  
Results Are Reported In Body System

Draft =      1.00 Roll Angle =      0.00 Pitch Angle =      0.00

Wet Radii Of Gyration About CG

K-X =      3.86 K-Y =      5.86 K-Z =      4.83

GMT =   -15.81 GML =   -5.52

Name	Weight	/-- Center of Gravity ---/			Sounding	% Full
		---X---	---Y---	---Z---		
----- Part DESIGNAW -----						
LOAD_GRO	3.16	-1.63	-0.00	0.17		
=====						
Total	3.16	-1.63	-0.00	0.17		
Buoyancy	3.16	-1.63	-0.00	0.63		

>hstatics

>cform 0 0 0 -draft 1.0

>report

\*\*\* ERROR: REPORT Is Not a Valid Command At This Time

```

=====
>hydrodynamics
>&parameter -m_distance 1
>g_pressure -heading 0 45 90 135 180 -period 62.83185307 31.41592654 \
    20.94395102 15.70796327 12.56637061 10.47197551 8.97597901 7.853981634
    6.981317008 6.283185307 5.711986643 5.235987756 4.833219467 \
    4.487989505 4.188790205 3.926990817 3.695991357 3.490658504 \
    3.306939635 3.141592654

```

Setting Pressure Name for DESIGNAW to DESIGNAW

```

=====
Time to Generate 226 Panels For D           : CP=    0.02
Time For 3D Diff. 226 Panels, Freq. 1      : CP=    4.37
Time For 3D Diff. 226 Panels, Freq. 2      : CP=    1.89
Time For 3D Diff. 226 Panels, Freq. 3      : CP=    1.17
Time For 3D Diff. 226 Panels, Freq. 4      : CP=    0.37
Time For 3D Diff. 226 Panels, Freq. 5      : CP=    0.43
Time For 3D Diff. 226 Panels, Freq. 6      : CP=    0.84
Time For 3D Diff. 226 Panels, Freq. 7      : CP=    0.54
Time For 3D Diff. 226 Panels, Freq. 8      : CP=    0.81
Time For 3D Diff. 226 Panels, Freq. 9      : CP=    0.95
Time For 3D Diff. 226 Panels, Freq. 10     : CP=    0.96
Time For 3D Diff. 226 Panels, Freq. 11     : CP=    0.99
Time For 3D Diff. 226 Panels, Freq. 12     : CP=    0.27
Time For 3D Diff. 226 Panels, Freq. 13     : CP=    1.76
Time For 3D Diff. 226 Panels, Freq. 14     : CP=    6.33
Time For 3D Diff. 226 Panels, Freq. 15     : CP=    4.64
Time For 3D Diff. 226 Panels, Freq. 16     : CP=    0.99
Time For 3D Diff. 226 Panels, Freq. 17     : CP=    1.14
Time For 3D Diff. 226 Panels, Freq. 18     : CP=    0.98
Time For 3D Diff. 226 Panels, Freq. 19     : CP=    1.56
Time For 3D Diff. 226 Panels, Freq. 20     : CP=    1.08

```

Setting Drift Name for DESIGNAW to DESIGNAW

=====

```

Time To Set Up Convolution For DESIGNAW      : CP=    0.16
Time to Sum Pressures For 226 Panels on DESIGNAW: CP=    0.04
>&env sea
>&status force
      +++ F O R C E S   A C T I N G   O N   D E S I G N A W +++
      =====

Process is DEFAULT: Units Are Degrees, Meters, and M-Tons Unless Specified
Results Are Reported In Body System

Type of Force      X          Y          Z          MX          MY          MZ
-----
Weight             0.00      0.00     -3.16          0          -4          0
Buoyancy          -0.00     -0.00      3.16          0           5          0
-----
Total              0.00      0.00     -0.00          0           0          0
>hydr_sum
>V_mdriфт
>report
>end
>end
>freq_response
>rao -speed 0
      Time To Compute RAOs                      : CP=    0.34|
>fr_point 0 0 0 DESIGNAW
      RAOs Moved to X =    0.0 Y =    0.0 Z =    0.0
      =====

```

```

Total                0.00      0.00     -0.00      0      0      0
>hydr_sum
>V_mdrift
>report
>end
>end
>freq_response
>rao -speed 0
      Time To Compute RAOs                : CP=      0.34
>fr_point 0 0 0 DESIGNAW
      RAOs Moved to X =      0.0 Y =      0.0 Z =      0.0
      =====
>
>report
>end
>equ_sum
>matrices -file yes
>end
>&finish

```

```

MOSES   Finished with 2 Errors
=====
      CP Time                36.66
      =====
      Total Units            36.66
      =====

```

b. Moses Out000 File

```

Page 1 License - Bentley Select Licensee Rev 07.10.01.11
*****
* * * * * MOSES * * * * *
* * * * * March 24, 2019 * * * * *
* * * * * * * * * * *
* * * * * MENCOBAlagi * * * * *
* * * * * * * * * * *
*****

+++ A D D E D I N E R T I A C O E F F I C I E N T S F O R D E S I G N A W +++
=====

Results are in Body System
Pressure Name = DESIGNAW

Process is DEFAULT: Units Are Degrees, Meters, and M-Tons Unless Specified

Values Normalized By Mass with Weight = 3.2
-----/----- Added Radii of Gyration ----/
Encounter /--- Added Mass Coefficients -----/ /----- Added Radii of Gyration ----/
Period /-Surge- -Sway - -Heave- -Roll - -Pitch- --Yaw--
Sec.

62.83 0.6067 0.4853 3.9210 5.015 4.683 1.510
31.42 0.6065 0.4847 3.9370 5.020 4.715 1.510
20.94 0.6073 0.4854 3.9621 5.039 4.753 1.512
15.71 0.6086 0.4868 3.9889 5.074 4.793 1.518
12.57 0.6099 0.4880 4.0160 5.118 4.826 1.527
10.47 0.6114 0.4891 4.0440 5.172 4.848 1.537
8.98 0.6128 0.4900 4.0743 5.238 4.856 1.548
7.85 0.6144 0.4909 4.1089 5.320 4.844 1.561
6.98 0.6160 0.4916 4.1504 5.419 4.811 1.576
6.28 0.6178 0.4924 4.2022 5.540 4.751 1.594
5.71 0.6200 0.4934 4.2678 5.685 4.662 1.615
5.24 0.6226 0.4953 4.3510 5.856 4.545 1.640
4.83 0.6259 0.4990 4.4545 6.053 4.401 1.668
4.49 0.6304 0.5062 4.5792 6.274 4.241 1.699
4.19 0.6365 0.5202 4.7228 6.506 4.080 1.732
3.93 0.6450 0.5461 4.8797 6.717 3.939 1.762
    
```

```

*****
*                               *** MOSES ***                               March 24, 2019
*                               -----
*
* MENCOBALagi
*
*****

```

+++ LINEAR RADIATION DAMPING COEFFICIENTS FOR DESIGNAW +++

Results are in Body System

Pressure Name = DESIGNAW

Process is DEFAULT: Units Are Degrees, Meters, and M-Tons Unless Specified

Encounter Period Sec.	Values Normalized By Mass with Weight = 3.2											
	-Surge-	-Sway -	-Heave-	-Roll -	-Pitch-	-Yaw--	-Surge-	-Sway -	-Heave-	-Roll -	-Pitch-	-Yaw--
62.83	0.0000	-0.0000	0.0004	0.004	0.094	-0.005	0.0000	-0.0000	0.0004	0.004	0.094	-0.005
31.42	0.0000	-0.0000	0.0032	0.012	0.267	-0.014	0.0000	-0.0000	0.0032	0.012	0.267	-0.014
20.94	0.0000	-0.0000	0.0105	0.023	0.489	-0.026	0.0000	-0.0000	0.0105	0.023	0.489	-0.026
15.71	0.0000	-0.0001	0.0237	0.044	0.750	-0.039	0.0000	-0.0001	0.0237	0.044	0.750	-0.039
12.57	0.0001	-0.0002	0.0435	0.079	1.044	-0.053	0.0001	-0.0002	0.0435	0.079	1.044	-0.053
10.47	0.0001	-0.0004	0.0699	0.136	1.363	-0.068	0.0001	-0.0004	0.0699	0.136	1.363	-0.068
8.98	0.0001	-0.0009	0.1027	0.225	1.701	-0.080	0.0001	-0.0009	0.1027	0.225	1.701	-0.080
7.85	0.0001	-0.0020	0.1412	0.354	2.052	-0.088	0.0001	-0.0020	0.1412	0.354	2.052	-0.088
6.98	-0.0001	-0.0042	0.1851	0.533	2.407	-0.084	-0.0001	-0.0042	0.1851	0.533	2.407	-0.084
6.28	-0.0006	-0.0081	0.2351	0.776	2.757	-0.044	-0.0006	-0.0081	0.2351	0.776	2.757	-0.044
5.71	-0.0016	-0.0150	0.2938	1.095	3.089	0.108	-0.0016	-0.0150	0.2938	1.095	3.089	0.108
5.24	-0.0034	-0.0264	0.3671	1.509	3.388	0.201	-0.0034	-0.0264	0.3671	1.509	3.388	0.201
4.83	-0.0063	-0.0444	0.4654	2.040	3.637	0.308	-0.0063	-0.0444	0.4654	2.040	3.637	0.308
4.49	-0.0106	-0.0718	0.6046	2.715	3.819	0.437	-0.0106	-0.0718	0.6046	2.715	3.819	0.437
4.19	-0.0164	-0.1117	0.8061	3.569	3.921	0.595	-0.0164	-0.1117	0.8061	3.569	3.921	0.595
3.93	-0.0236	-0.1660	1.0946	4.629	3.938	0.785	-0.0236	-0.1660	1.0946	4.629	3.938	0.785
3.70	-0.0313	-0.2306	1.4967	5.893	3.878	1.005	-0.0313	-0.2306	1.4967	5.893	3.878	1.005



+++ MOTION RESPONSE OPERATORS +++  
=====

Results are in Body System

Of Point On Body DESIGNAW At X = 0.0 Y = 0.0 Z = 0.0

Process is DEFAULT: Units Are Degrees, Meters, and M-Tons Unless Specified

E N C O U N T E R		Surge /		Sway /		Heave /		Roll /		Pitch /		Yaw /	
Frequency	Period	Wave Ampl.	Phase	Wave Ampl.	Phase	Wave Ampl.	Phase	Wave Ampl.	Phase	Wave Ampl.	Phase	Wave Ampl.	Phase
-(Rad/Sec)-	-(Sec)-	Ampl.	Ampl.	Ampl.	Ampl.	Ampl.	Ampl.	Ampl.	Ampl.	Ampl.	Ampl.	Ampl.	Ampl.
0.1000	62.83	1.658	25	0.703	90	0.989	0	0.041	90	0.223	-10	0.162	-90
0.2000	31.42	0.803	62	0.703	90	0.990	0	0.162	90	0.269	-36	0.161	-92
0.3000	20.94	0.730	77	0.702	90	0.989	0	0.362	91	0.416	-58	0.160	-97
0.4000	15.71	0.716	82	0.702	89	0.989	0	0.637	91	0.655	-67	0.161	-103
0.5000	12.57	0.712	85	0.701	89	0.986	0	0.983	92	0.960	-71	0.166	-110
0.6000	10.47	0.709	86	0.700	88	0.982	0	1.394	93	1.321	-71	0.176	-119
0.7000	8.98	0.706	87	0.698	88	0.977	0	1.863	94	1.731	-70	0.195	-128
0.8000	7.85	0.703	88	0.696	87	0.969	-1	2.384	95	2.192	-69	0.222	-136
0.9000	6.98	0.700	88	0.694	87	0.961	-2	2.947	97	2.706	-67	0.258	-142
1.0000	6.28	0.698	88	0.692	86	0.950	-3	3.546	98	3.279	-65	0.302	-147
1.1000	5.71	0.696	89	0.688	85	0.939	-5	4.170	100	3.919	-63	0.355	-151
1.2000	5.24	0.697	89	0.685	84	0.926	-7	4.810	101	4.636	-62	0.414	-154
1.3000	4.83	0.700	89	0.680	83	0.912	-10	5.455	103	5.446	-61	0.478	-156
1.4000	4.49	0.708	90	0.675	80	0.897	-14	6.091	104	6.363	-61	0.545	-157
1.5000	4.19	0.722	90	0.668	81	0.880	-19	6.701	106	7.402	-63	0.614	-157
1.6000	3.93	0.743	89	0.660	80	0.863	-26	7.258	107	8.570	-65	0.682	-158
1.7000	3.70	0.770	87	0.648	78	0.844	-34	7.727	108	9.844	-70	0.746	-158
1.8000	3.49	0.796	83	0.630	76	0.818	-44	8.043	109	11.126	-77	0.814	-157
1.9000	3.31	0.803	77	0.606	74	0.773	-57	8.168	109	12.137	-88	0.861	-156
2.0000	3.14	0.761	68	0.572	71	0.692	-72	8.049	110	12.384	-103	0.898	-154





## c. Damping file ppo000 in Moses

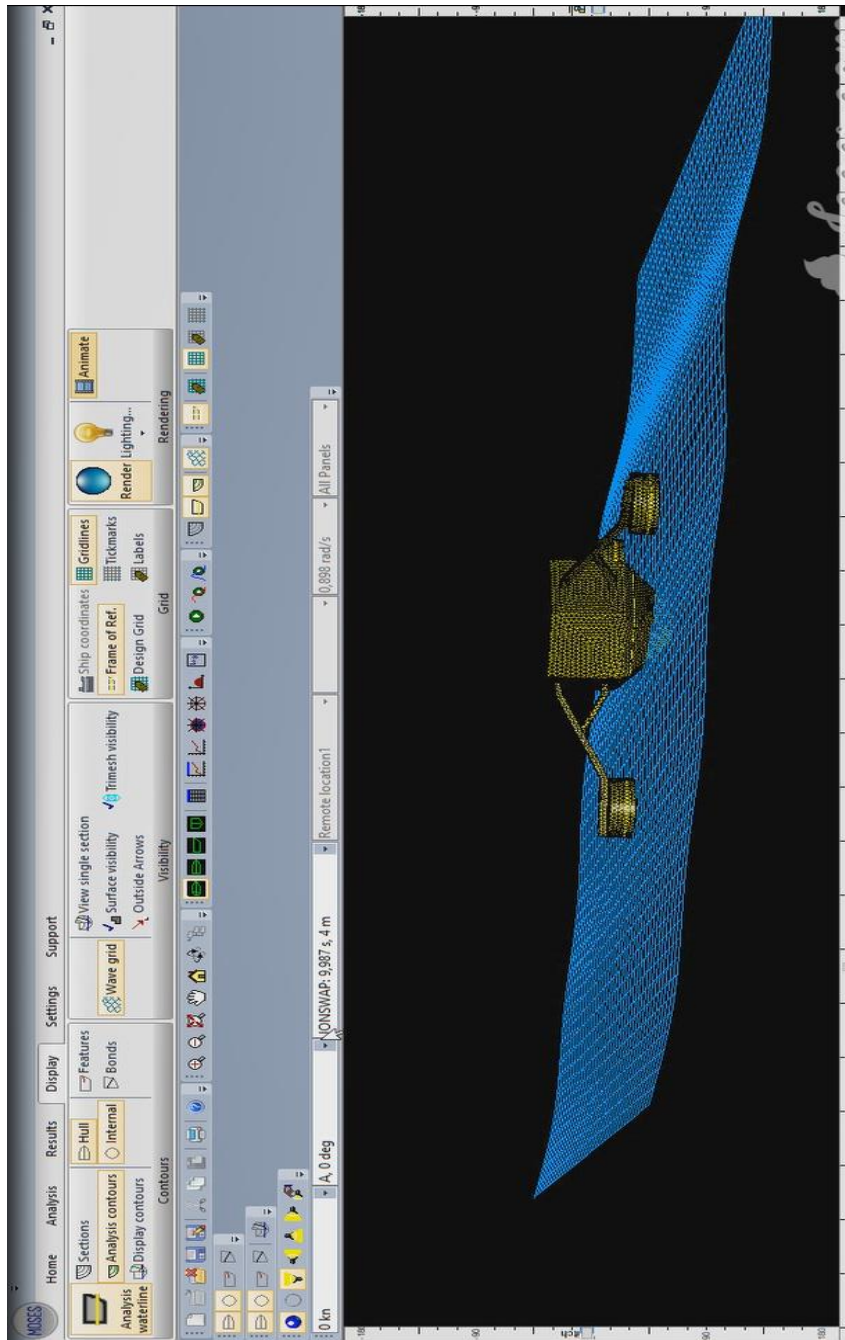
```

$ MATRICES
$ Dimensions are Meters and M-Tons
Frequency 0.1000 Period 62.8319
Added Mass
6.06679E-01 2.60766E-06 -2.67129E-01 3.79856E-05 1.68163E+00 -3.42176E-05
2.45681E-06 4.85295E-01 1.90501E-07 -2.06444E+00 1.83178E-05 3.54110E-01
1.22567E-01 -1.03843E-06 3.92098E+00 9.77963E-06 1.59709E+00 -5.68873E-05
3.79856E-05 -2.06444E+00 9.77963E-06 2.51521E+01 -1.09305E-04 -3.41745E+00
1.68163E+00 1.83178E-05 1.59709E+00 1.47538E-05 2.19317E+01 3.31610E-05
-3.42176E-05 3.54110E-01 -5.68873E-05 -6.39229E+00 3.17050E-04 2.27993E+00
Damping
5.18012E-07 -3.10193E-11 -9.96840E-05 -5.81976E-11 1.62326E-06 4.48039E-10
-4.54436E-12 -1.02602E-06 2.39890E-09 -1.27399E-05 5.62797E-10 -5.37442E-06
-6.64795E-07 -6.57640E-12 4.06420E-04 -4.28232E-08 3.40692E-03 1.01057E-07
-5.81976E-11 -1.27399E-05 -4.28232E-08 4.37980E-05 -1.12393E-07 -8.98266E-06
1.62326E-06 5.62797E-10 3.40692E-03 -3.87406E-10 8.92205E-03 -1.96619E-09
4.48039E-10 -5.37442E-06 1.01057E-07 -1.98599E-05 2.68418E-07 -2.44819E-05
Frequency 0.2000 Period 31.4159
Added Mass
6.06483E-01 2.52493E-06 -2.70220E-01 3.94891E-05 1.68234E+00 -3.62594E-05
2.40838E-06 4.84653E-01 1.09147E-07 -2.06090E+00 1.82413E-05 3.52251E-01
1.23325E-01 -4.94550E-07 3.93705E+00 8.71238E-06 1.70350E+00 -5.43414E-05
3.94891E-05 -2.06090E+00 8.71238E-06 2.51986E+01 -1.33583E-04 -3.42252E+00
1.68234E+00 1.82413E-05 1.70350E+00 -1.20184E-06 2.22271E+01 3.27004E-05
-3.62594E-05 3.52251E-01 -5.43414E-05 -6.40832E+00 3.38288E-04 2.28092E+00
Damping
4.24894E-06 -4.22884E-10 -7.91378E-04 -4.57653E-10 7.75350E-06 3.51948E-09
-6.87196E-11 -8.27706E-06 1.74513E-08 -1.01126E-04 1.36199E-09 -4.31076E-05
-5.75288E-06 -9.26114E-12 3.21066E-03 -3.85577E-07 2.70048E-02 8.29907E-07
-4.57653E-10 -1.01126E-04 -3.85577E-07 1.46696E-04 -1.01404E-06 -7.26314E-05
7.75350E-06 1.36199E-09 2.70048E-02 -1.12785E-08 7.11646E-02 -1.24636E-08
3.51948E-09 -4.31076E-05 8.29907E-07 -1.60441E-04 2.21756E-06 -1.95096E-04
Frequency 0.3000 Period 20.9440

```

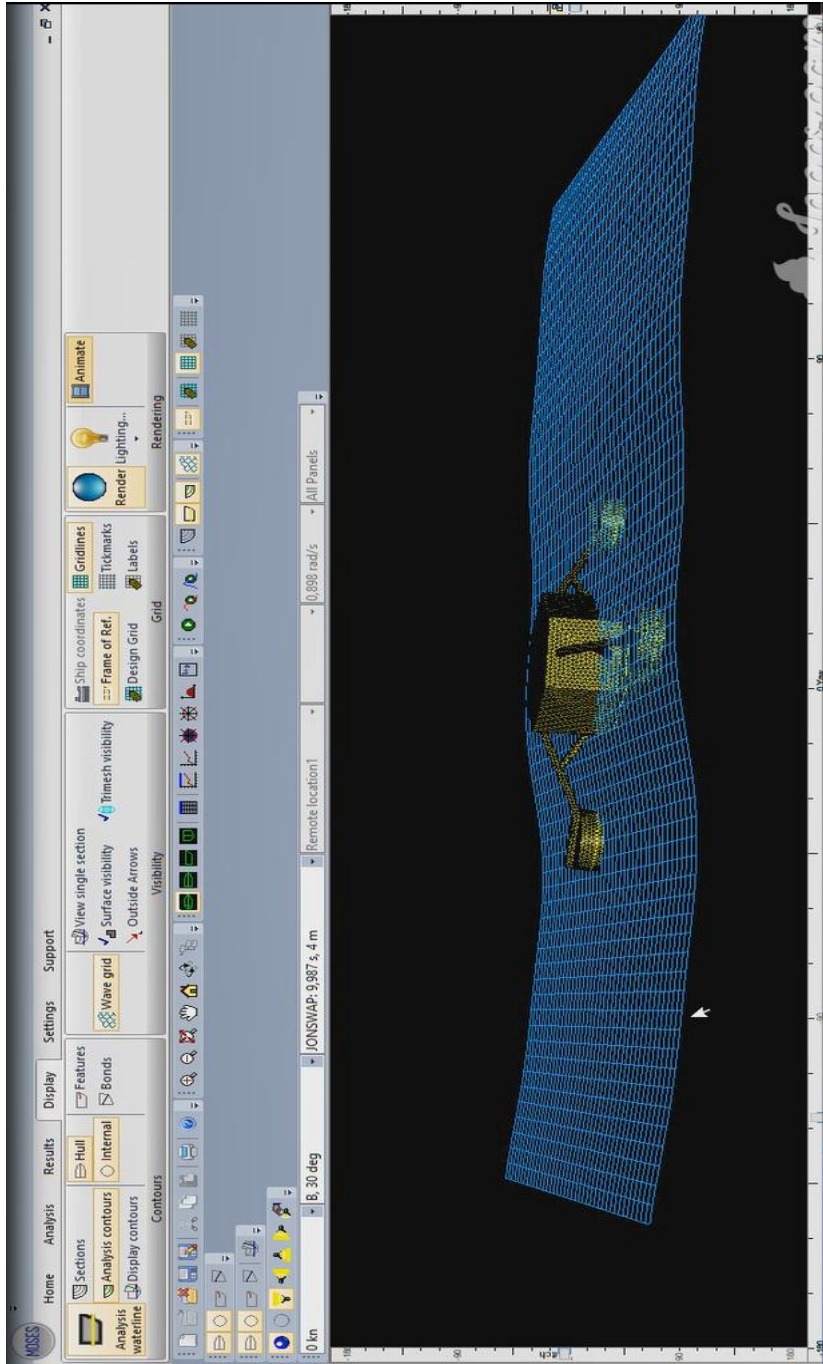
Frequency	0.4000	Period	15.7080
Added Mass			
6.08576E-01	2.67490E-06	-2.77400E-01	4.12263E-05
2.25342E-06	4.86797E-01	2.95215E-07	-2.07016E+00
1.25701E-01	-8.22232E-07	3.98889E+00	9.16076E-06
4.12263E-05	-2.07016E+00	9.16076E-06	2.57416E+01
1.68866E+00	1.96547E-05	1.86295E+00	-7.27344E-06
-3.72070E-05	3.50494E-01	-5.10776E-05	-6.57379E+00
Damping			
3.57912E-05	-1.66287E-09	-6.02470E-03	-1.78224E-09
-9.03651E-10	-7.54065E-05	1.49809E-07	-7.21309E-04
-4.31381E-05	-1.58740E-09	2.36815E-02	-3.14718E-06
-1.78224E-09	-7.21309E-04	-3.14718E-06	1.89752E-03
-1.02058E-04	2.63121E-08	2.08374E-01	-3.03760E-08
1.80236E-08	-3.68268E-04	6.55767E-06	-1.52334E-03
Frequency 0.5000 Period 12.5664			
Added Mass			
6.09944E-01	2.64960E-06	-2.79734E-01	4.26091E-05
2.13800E-06	4.87992E-01	-4.13934E-07	-2.07676E+00
1.27817E-01	-4.00119E-07	4.01602E+00	9.11812E-06
4.26091E-05	-2.07676E+00	9.11812E-06	2.61940E+01
1.69249E+00	1.89961E-05	1.88723E+00	-1.74358E-07
-3.91048E-05	3.49573E-01	-5.18848E-05	-6.70905E+00
Damping			
6.81487E-05	-1.62484E-09	-1.13345E-02	2.49079E-09
-1.27686E-09	-1.79561E-04	2.78777E-07	-1.13402E-03
-4.74157E-05	-5.80260E-09	4.34589E-02	-6.07308E-06
2.49079E-09	-1.13402E-03	-6.07308E-06	6.17264E-03
-4.40358E-04	4.00781E-08	3.95774E-01	2.27278E-08
2.04567E-08	-7.97894E-04	1.27478E-05	-3.71223E-03
6.08576E+00	1.68866E+00	1.96547E+01	3.74352E-05
2.25342E-05	1.96547E-05	2.95215E+00	3.50494E-01
1.25701E-06	1.86295E+00	9.16076E-06	-5.10776E-05
4.12263E-04	-1.52836E-04	-1.52836E-04	-3.47927E+00
1.68866E+00	2.29702E+01	2.29702E+01	3.74352E-05
-3.72070E-04	3.69984E-04	3.69984E-04	2.30443E+00
3.57912E-08	-1.02058E-04	-1.02058E-04	1.80236E-08
-9.03651E-04	2.63121E-08	2.63121E-08	-3.68268E-04
-4.31381E-06	2.08374E-01	2.08374E-01	6.55767E-06
-1.78224E-06	-6.83535E-04	-6.83535E-04	1.89752E-03
-1.02058E-09	5.62977E-01	5.62977E-01	-1.86621E-09
1.80236E-05	-1.51251E-03	-1.51251E-03	1.79725E-05
6.09944E-05	3.91048E-05	3.91048E-05	-3.91048E-05
2.13800E-05	3.49573E-01	3.49573E-01	4.26091E-05
1.27817E-06	-5.18848E-05	-5.18848E-05	1.88723E+00
4.26091E-04	-3.53060E+00	-3.53060E+00	-1.59946E-04
1.69249E-05	4.10866E-05	4.10866E-05	2.32880E+01
-3.91048E-04	2.33119E+00	2.33119E+00	3.88158E-04
6.81487E-04	2.04567E-08	2.04567E-08	-4.40358E-04
-1.27686E-08	-7.97894E-04	-7.97894E-04	4.00781E-08
-4.74157E-06	1.27478E-01	1.27478E-01	3.95774E-01
2.49079E-05	-1.62538E-03	-1.62538E-03	-1.66780E-05
-4.40358E-08	8.79787E-08	8.79787E-08	1.08922E+00
2.04567E-03	-2.83777E-03	-2.83777E-03	3.55832E-05

**d. Seakeeping Simulation in Moses Motion of Model Variation 1**  
1. Heading  $0^\circ$ .

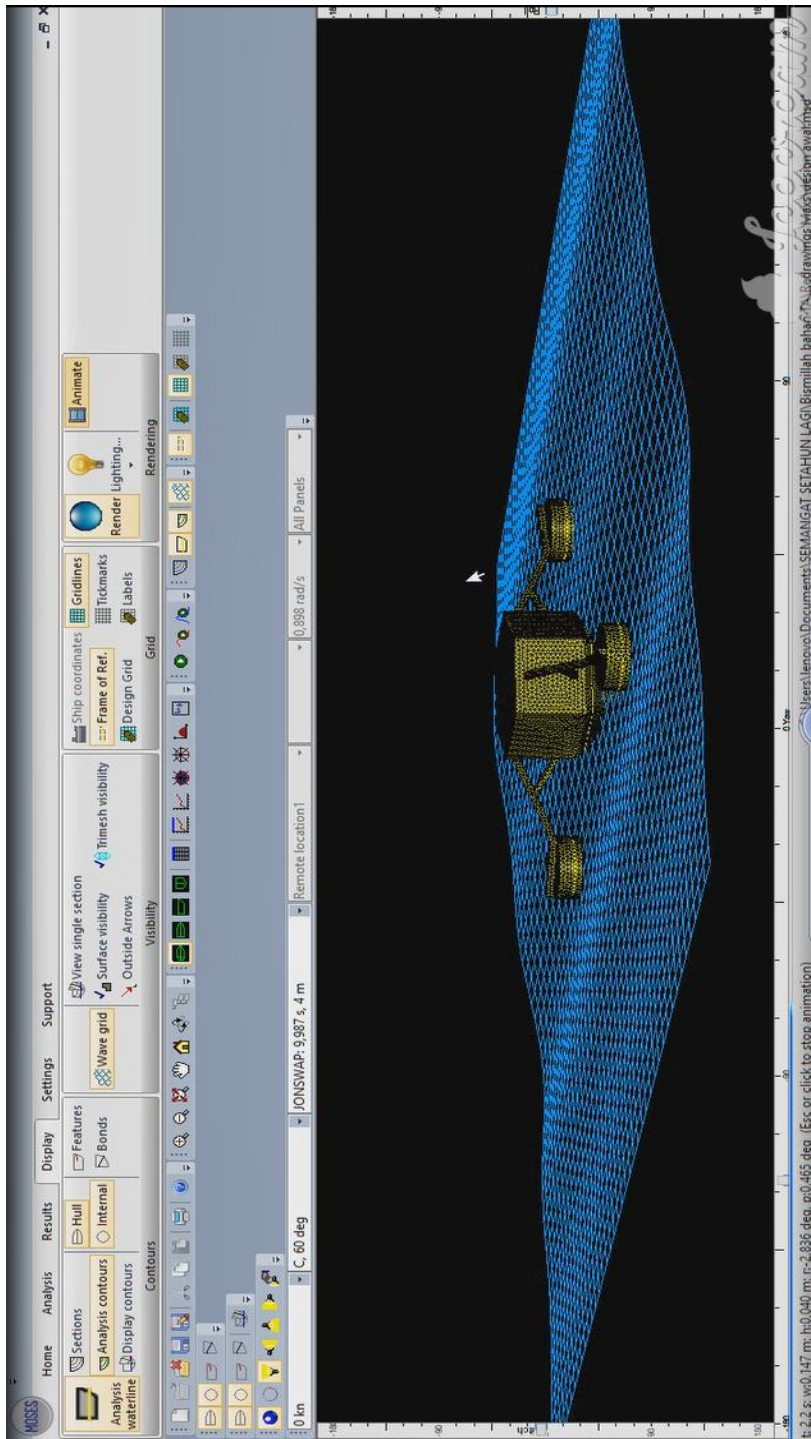




2. Heading 30°.

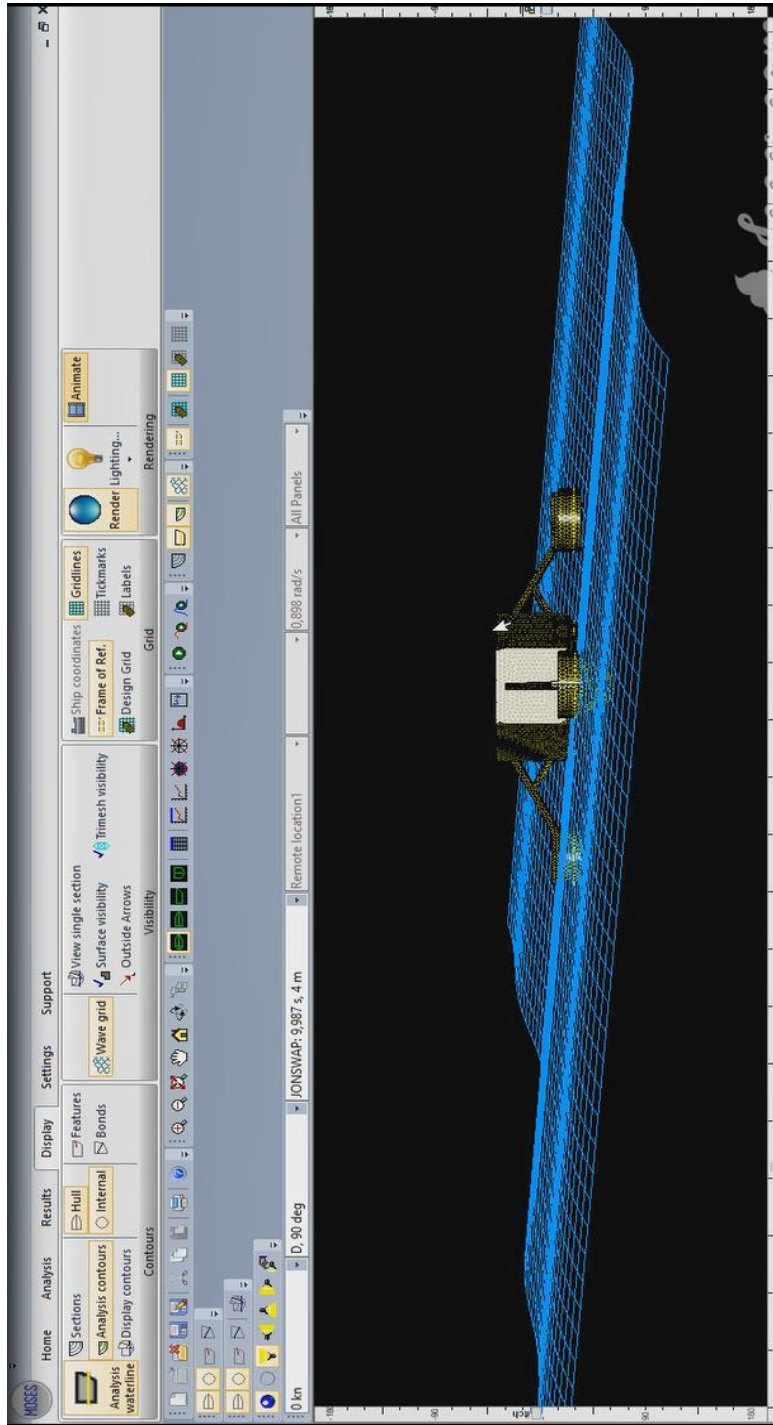


3. Heading 60°.

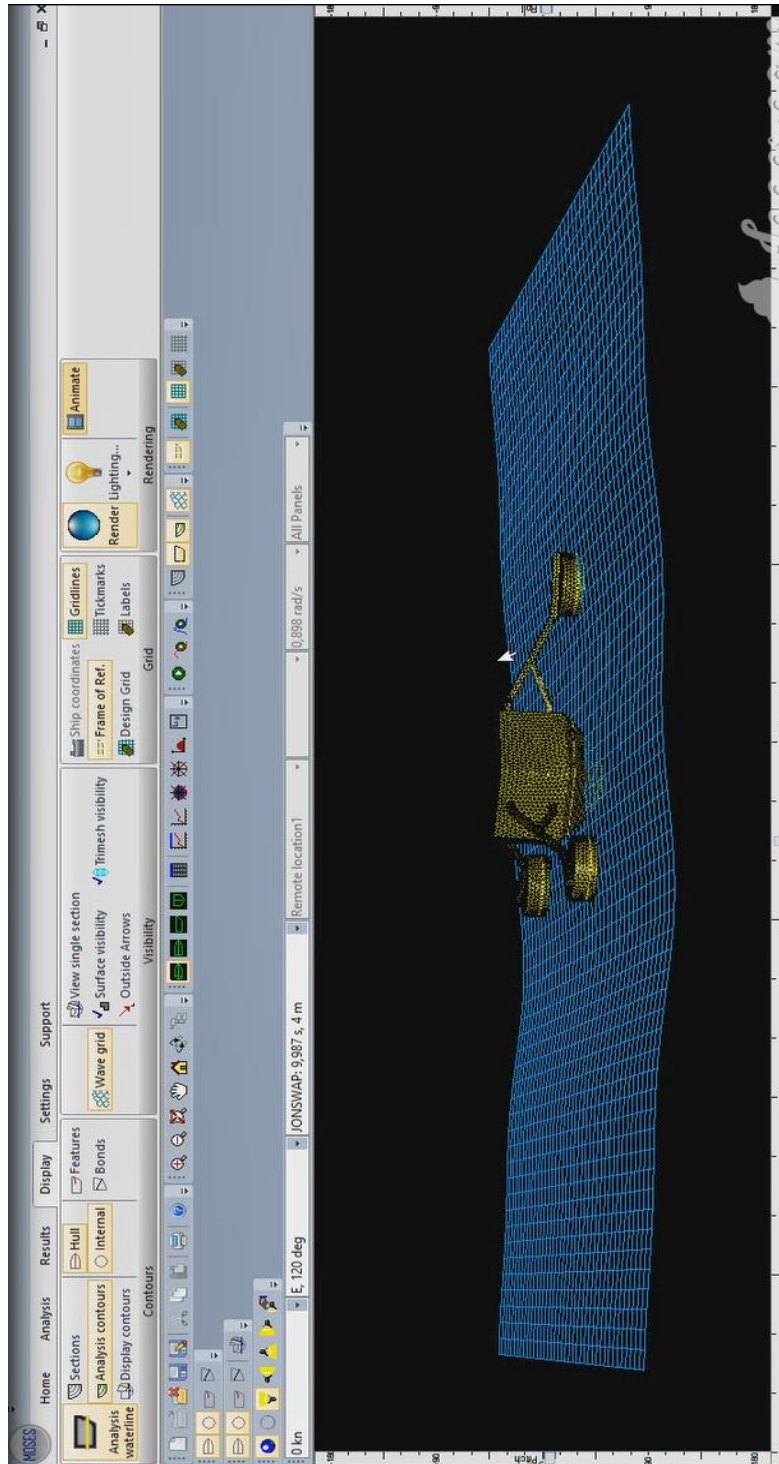


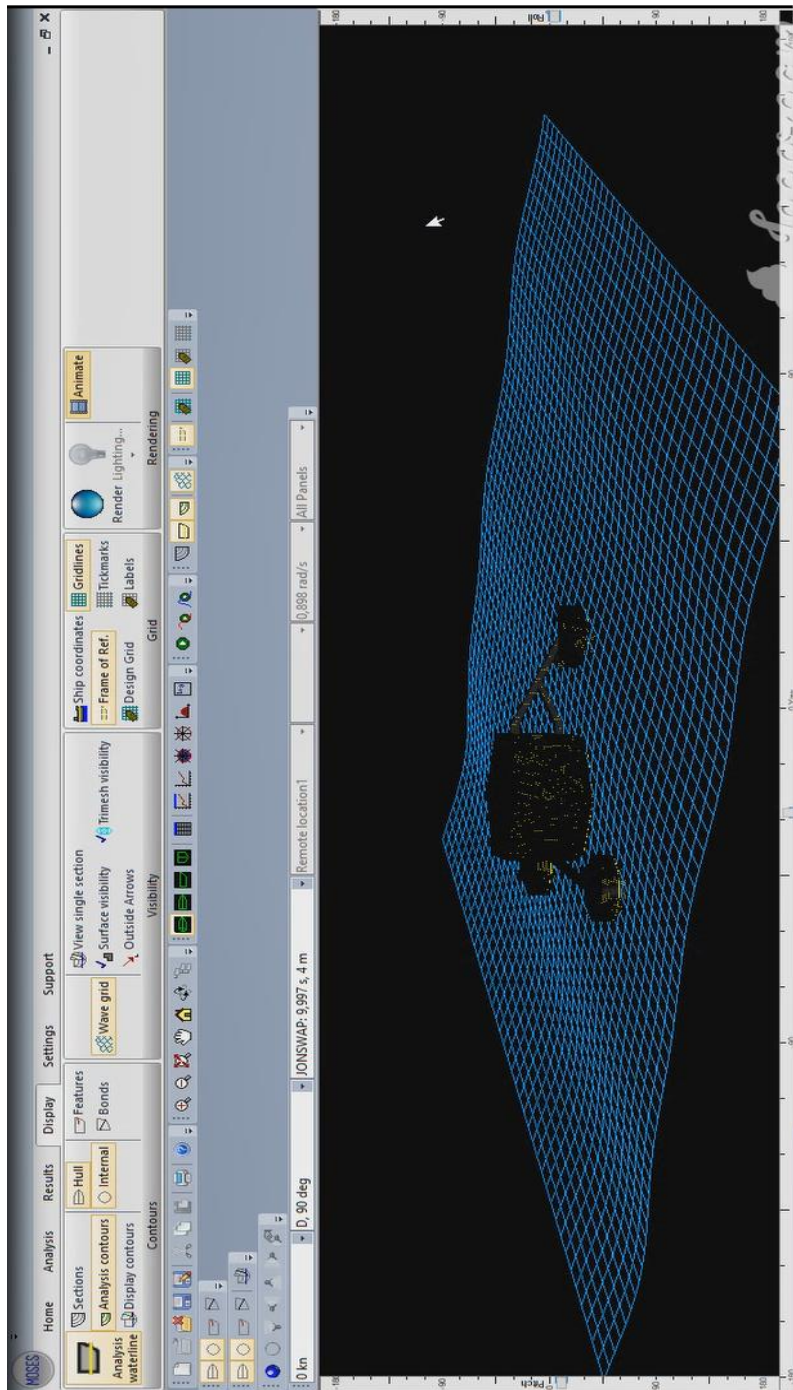


4. Heading 90°.

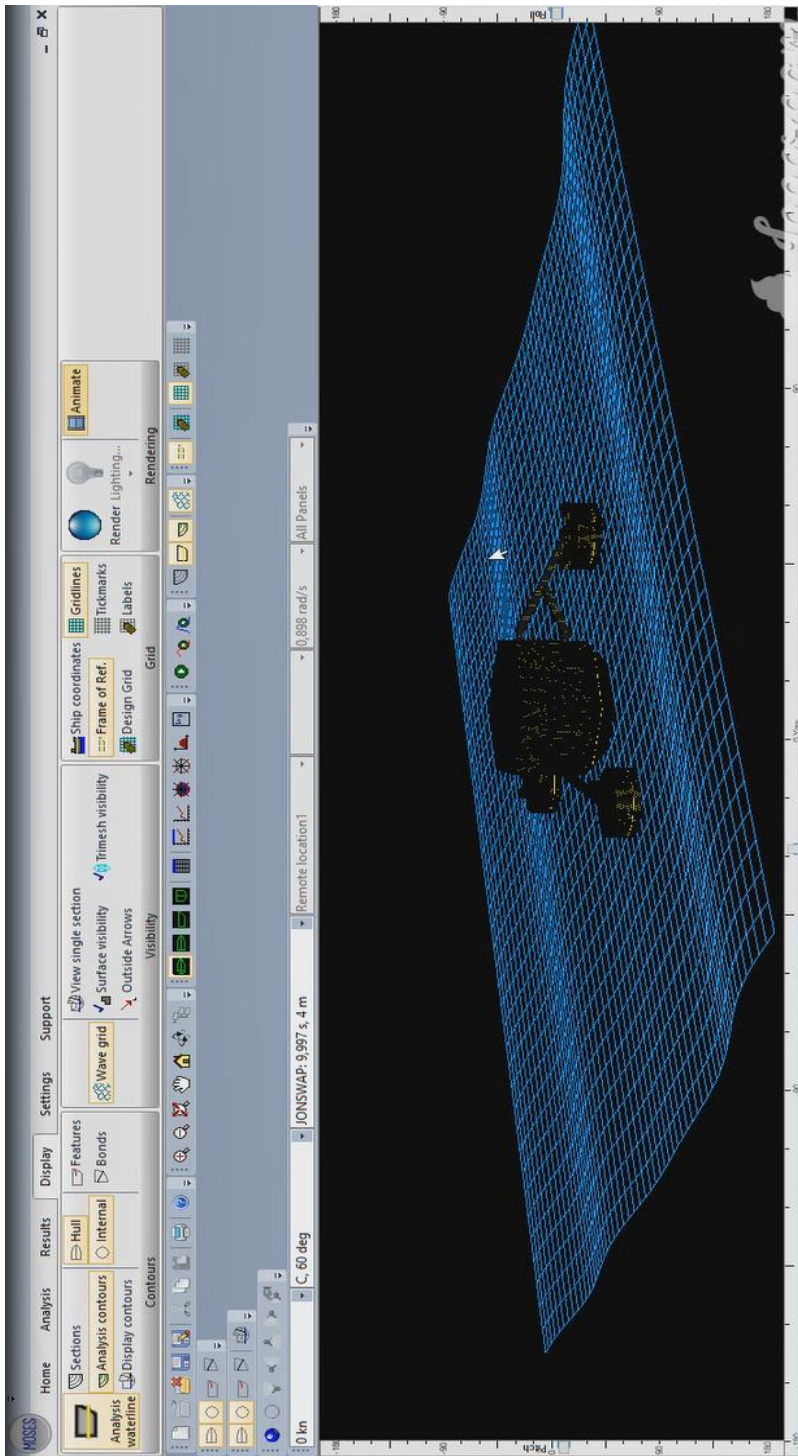


5. Heading 120°.



**e. Seakeeping Simulation in Moses Motion of Model Variation 2**1. Heading  $90^\circ$ .

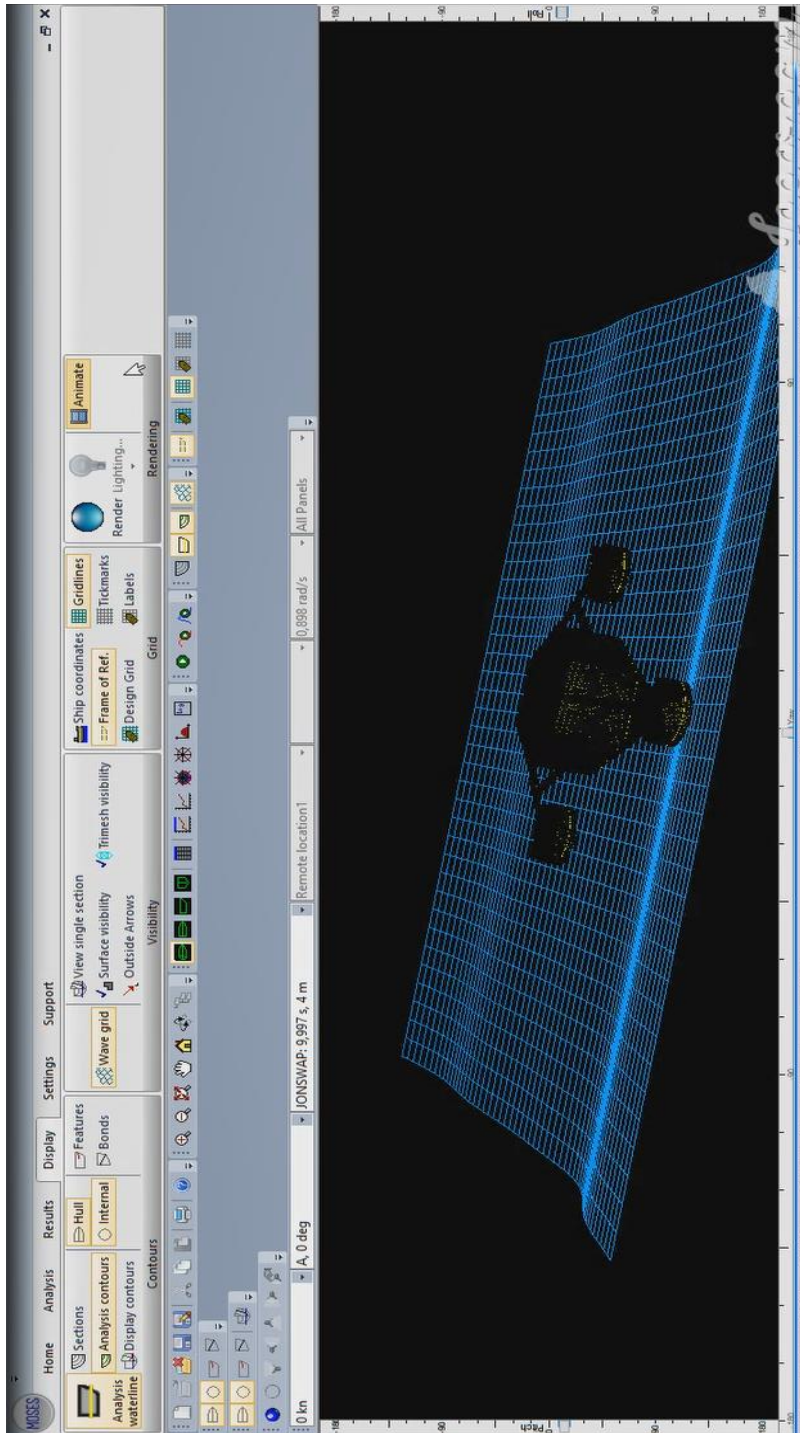
2. Heading 60°.



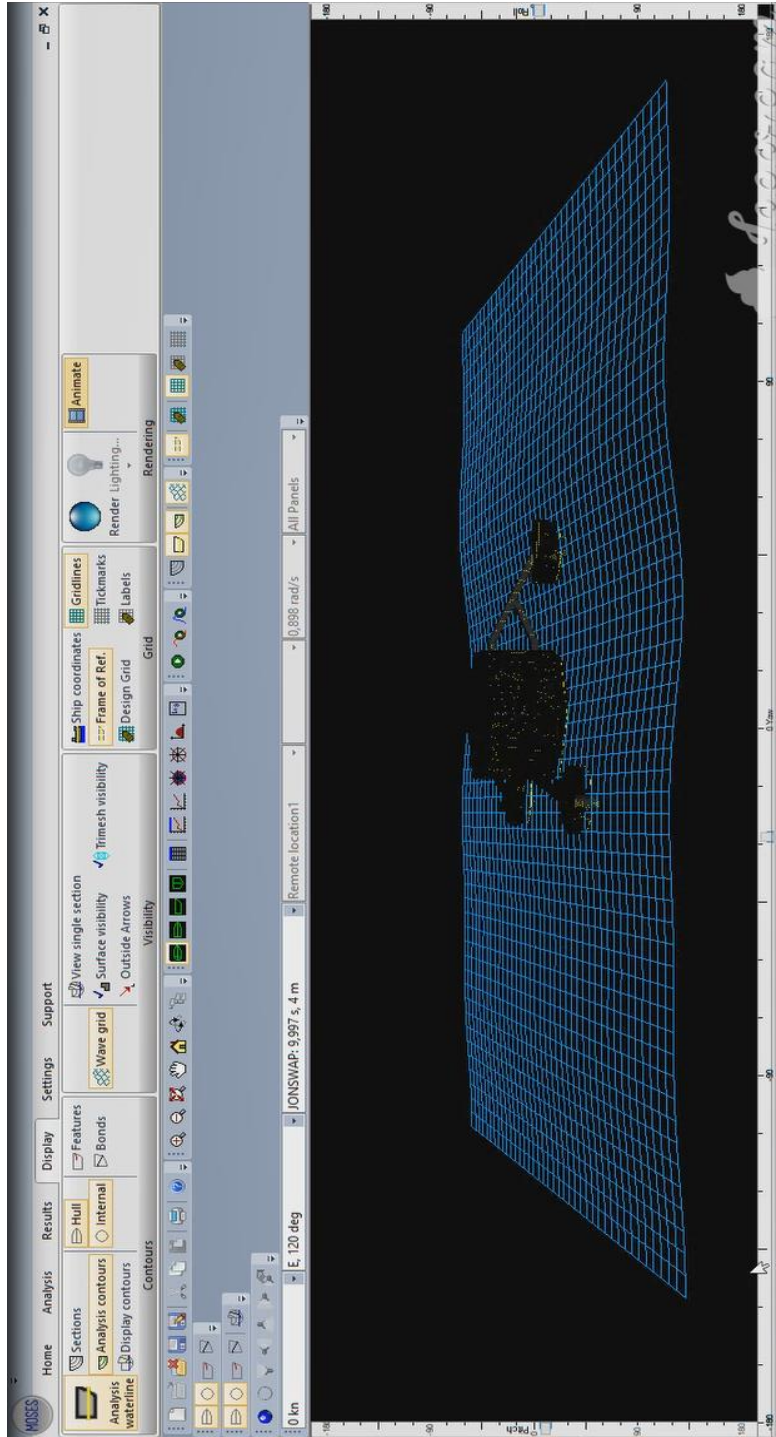


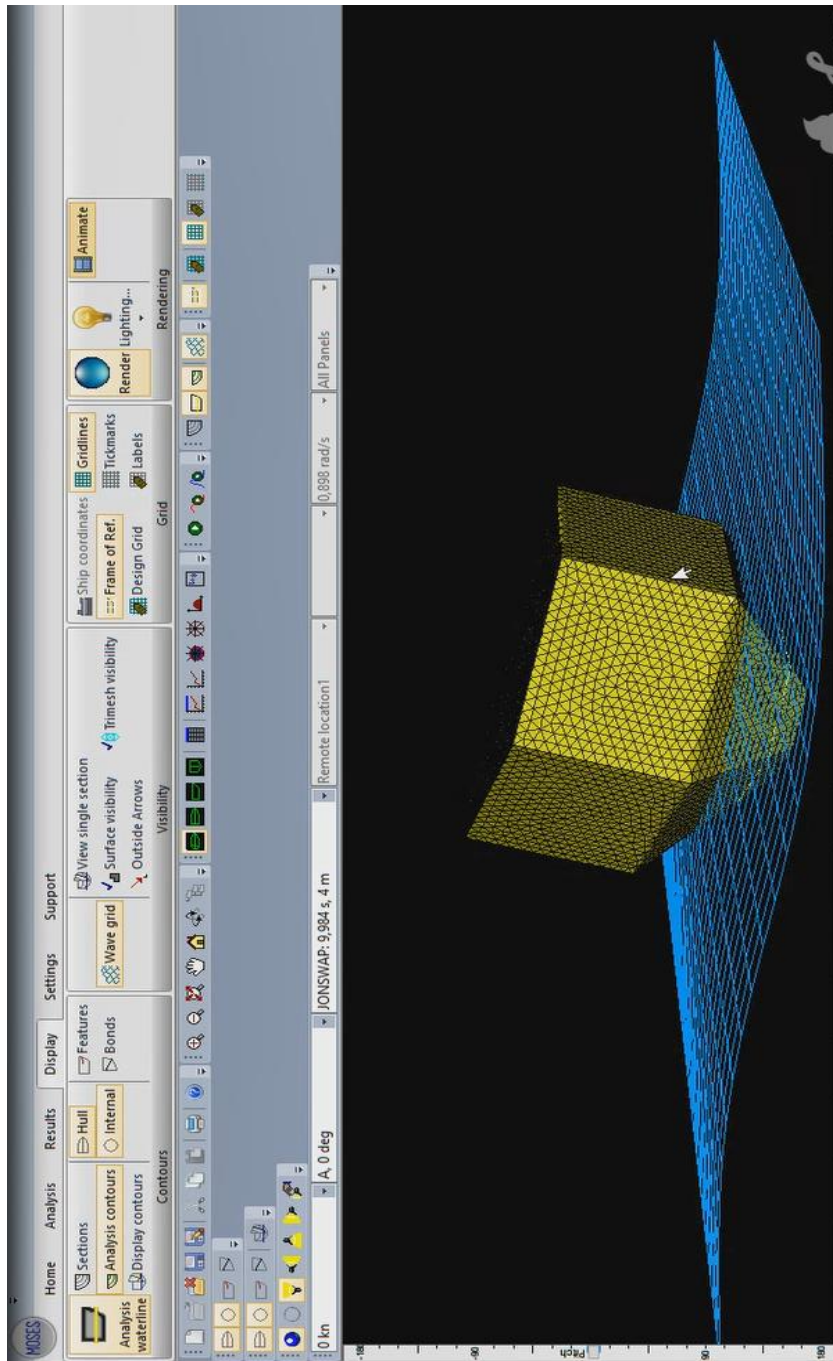


4. Heading 0°.



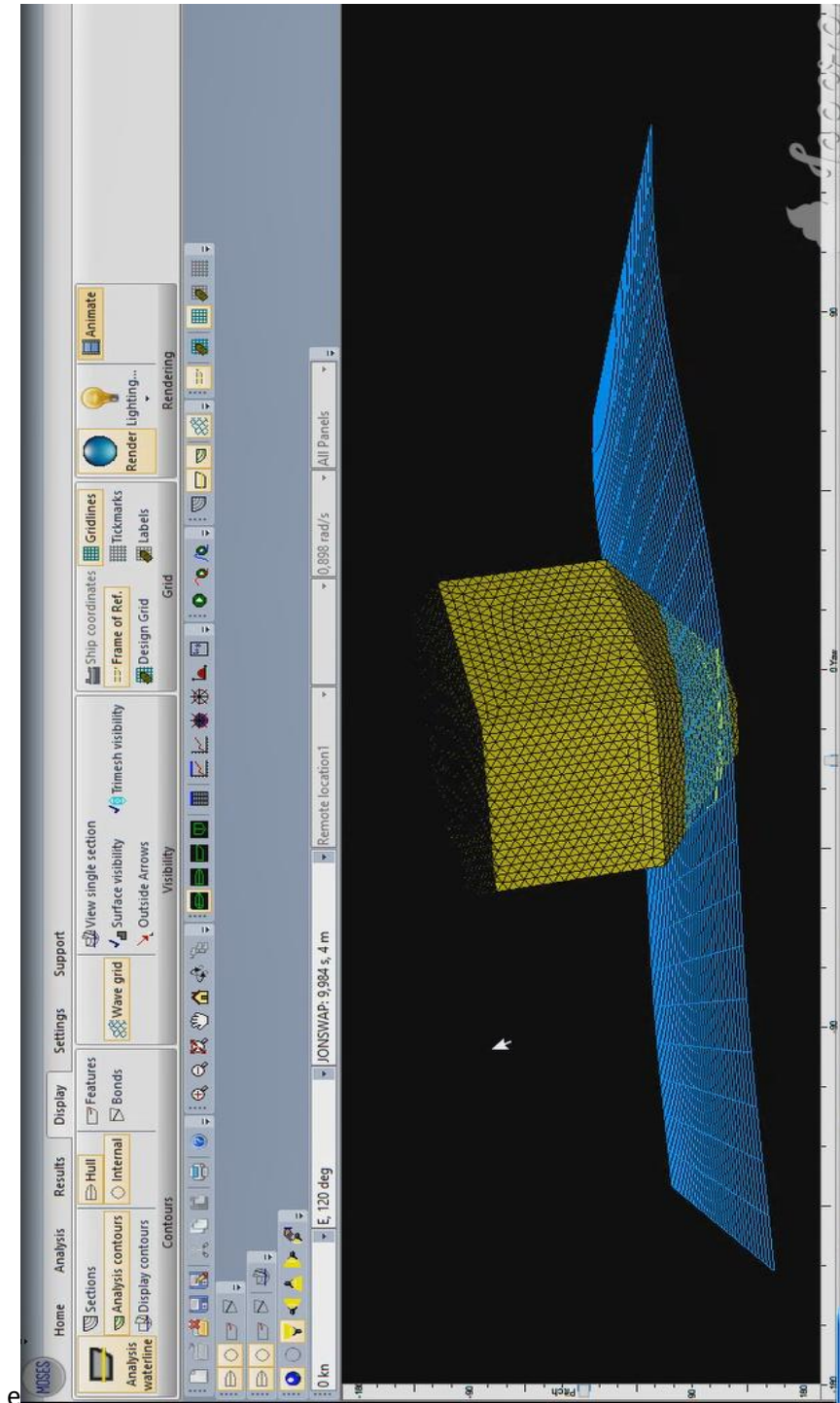
5. Heading 120°.



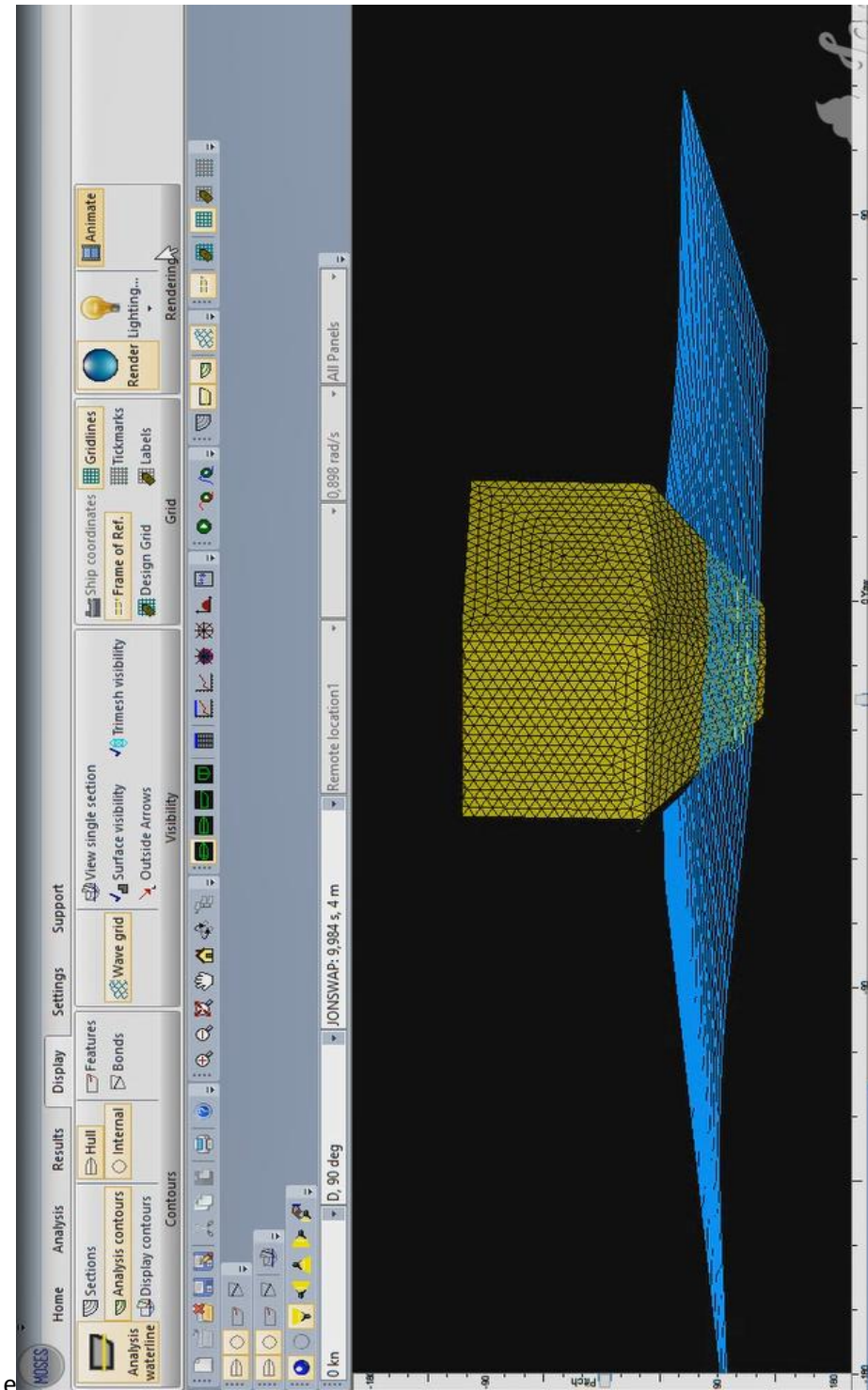
**f. Seakeeping Simulation in Moses Motion of Model Variation 3.**1. Heading  $0^\circ$ .



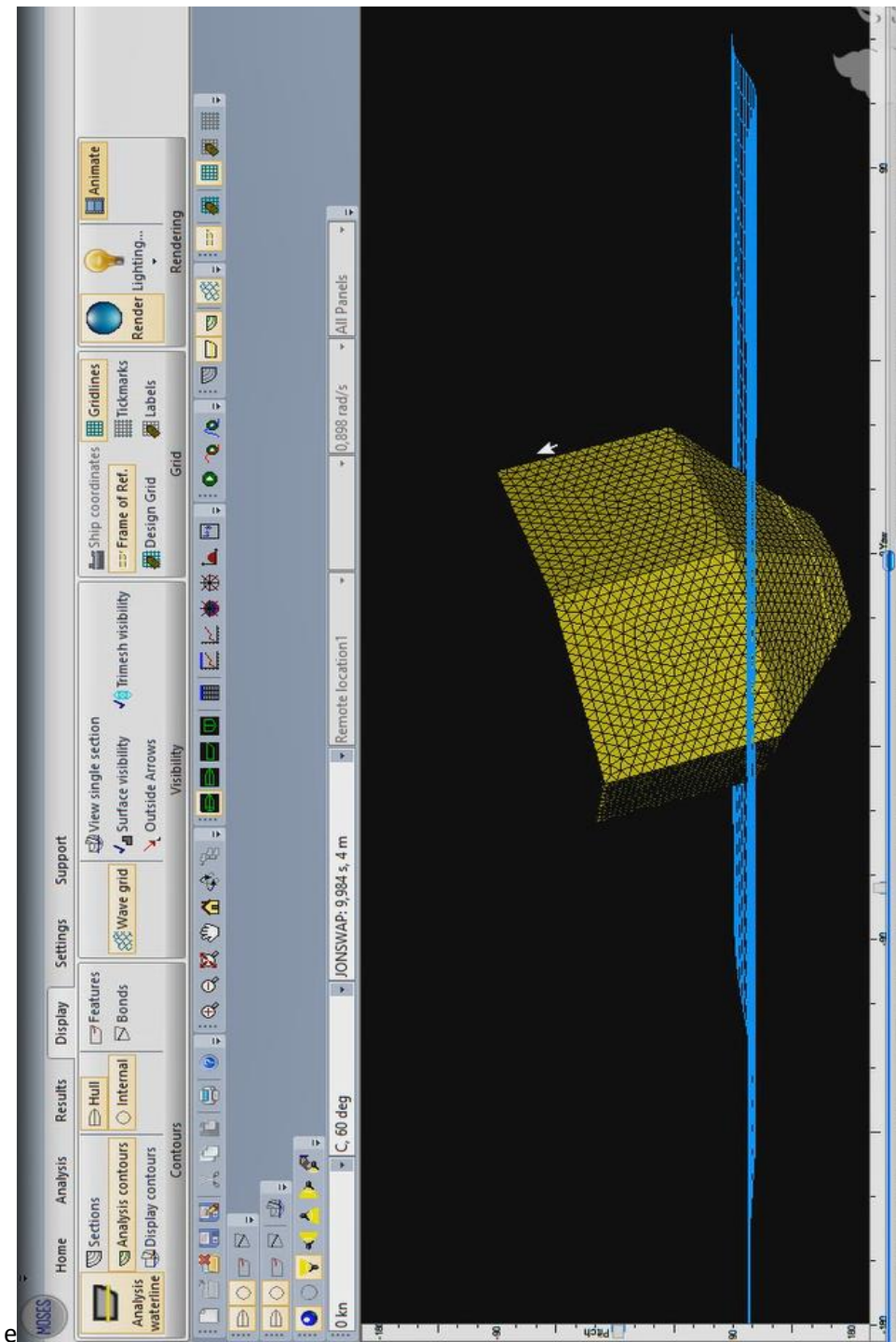
2. Heading 120°.



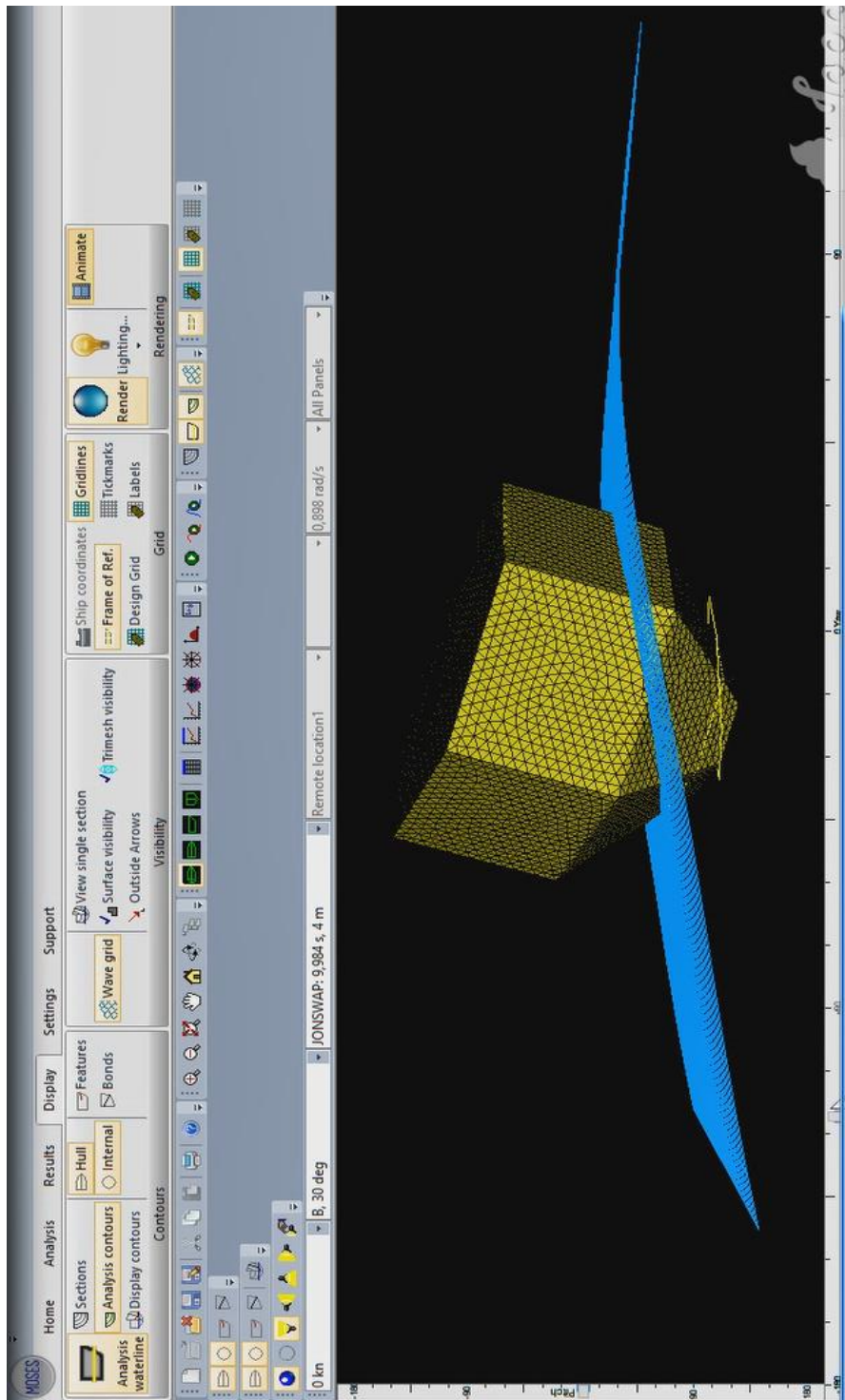
3. Heading 90°.



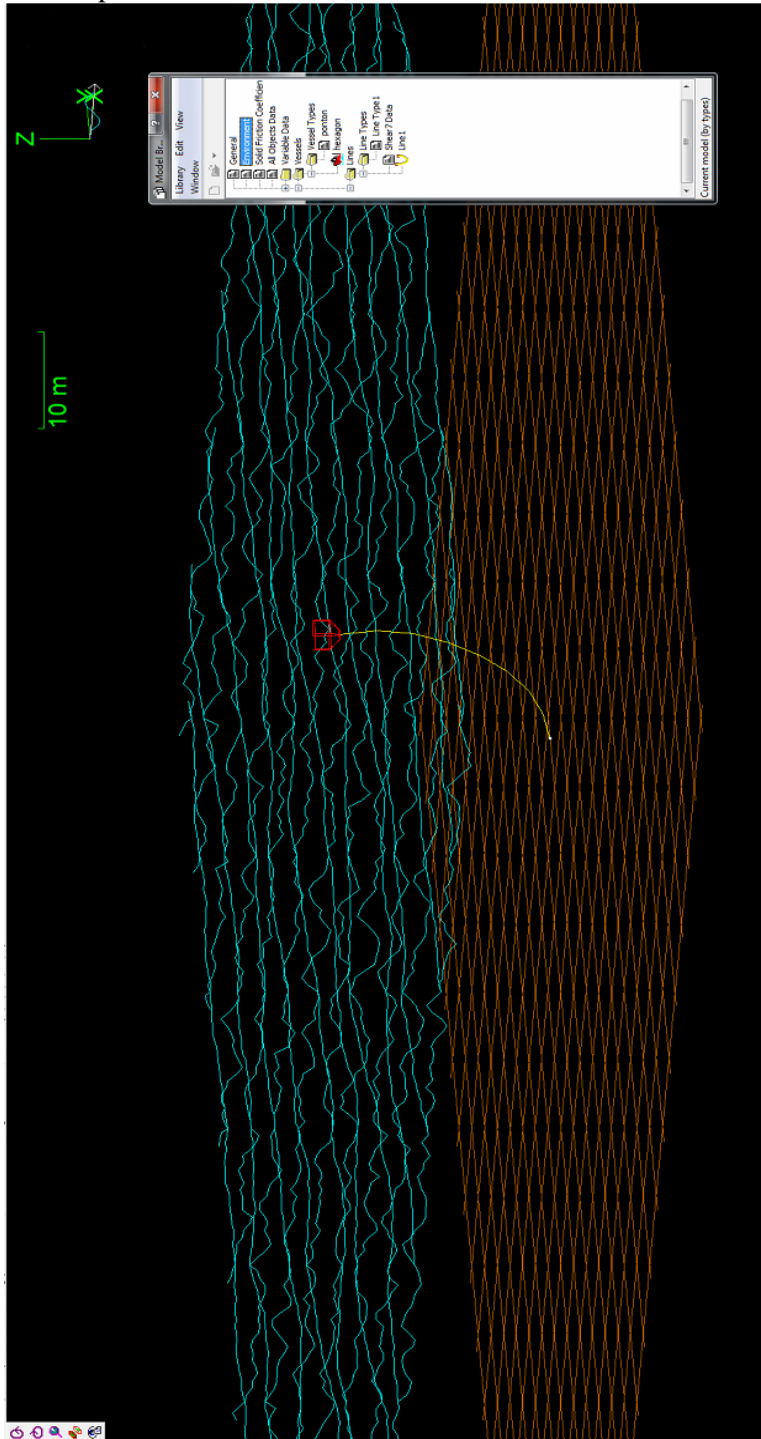
4. Heading 60°.
- 5.



## 6. Heading 30°.

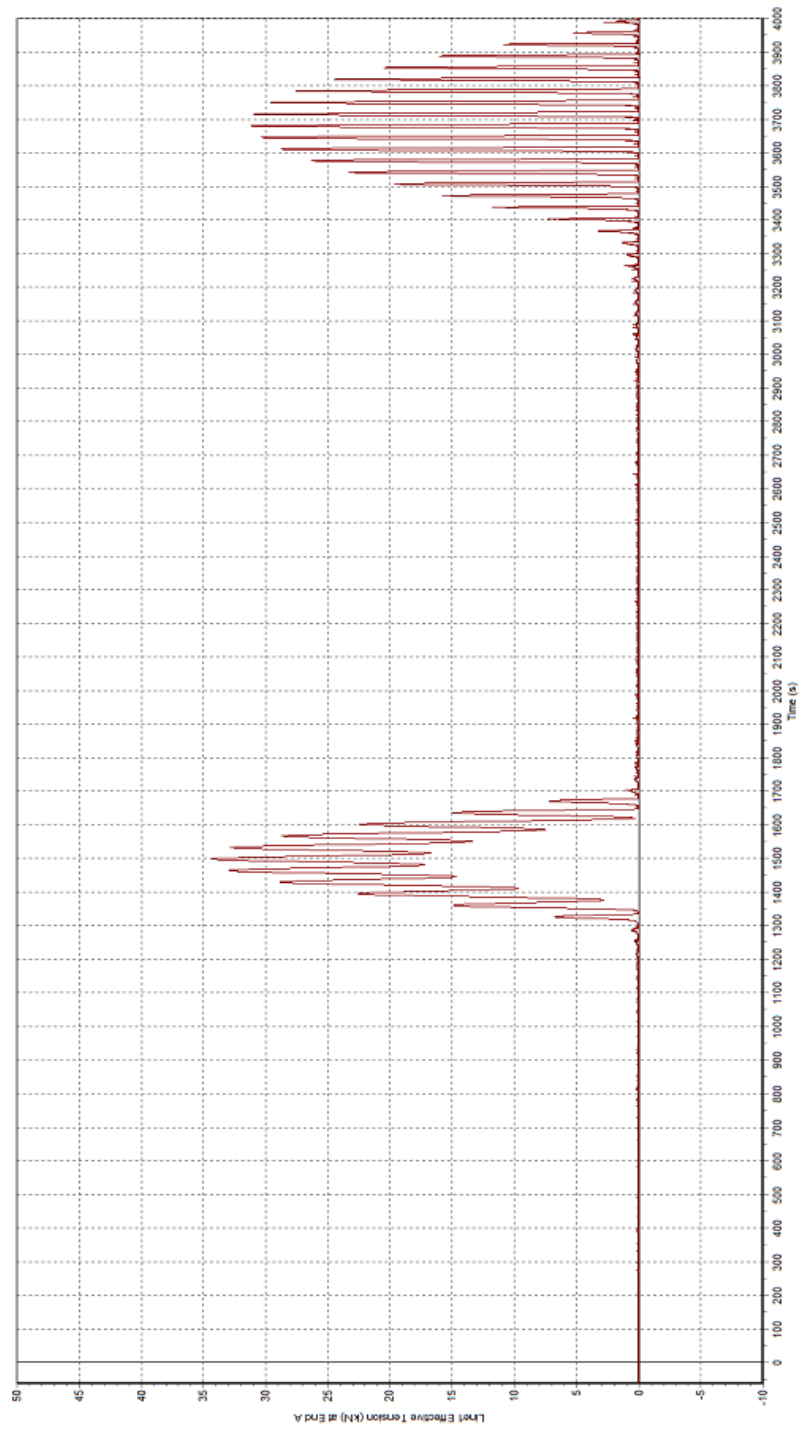


**g. Mooring System Simulation.**  
**1. Heading 0°**  
1.1 Simulation Perspective view

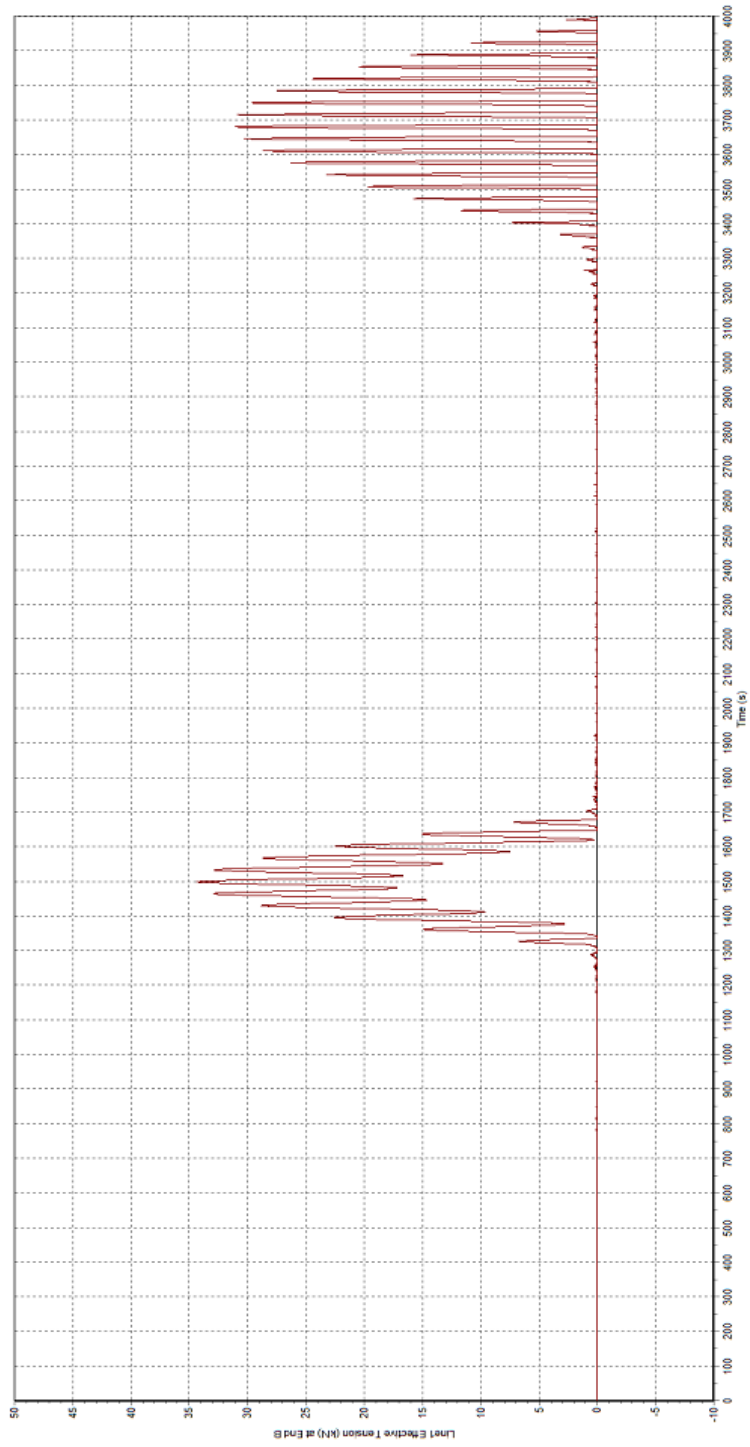




## 1.2 Effective Tension at End A

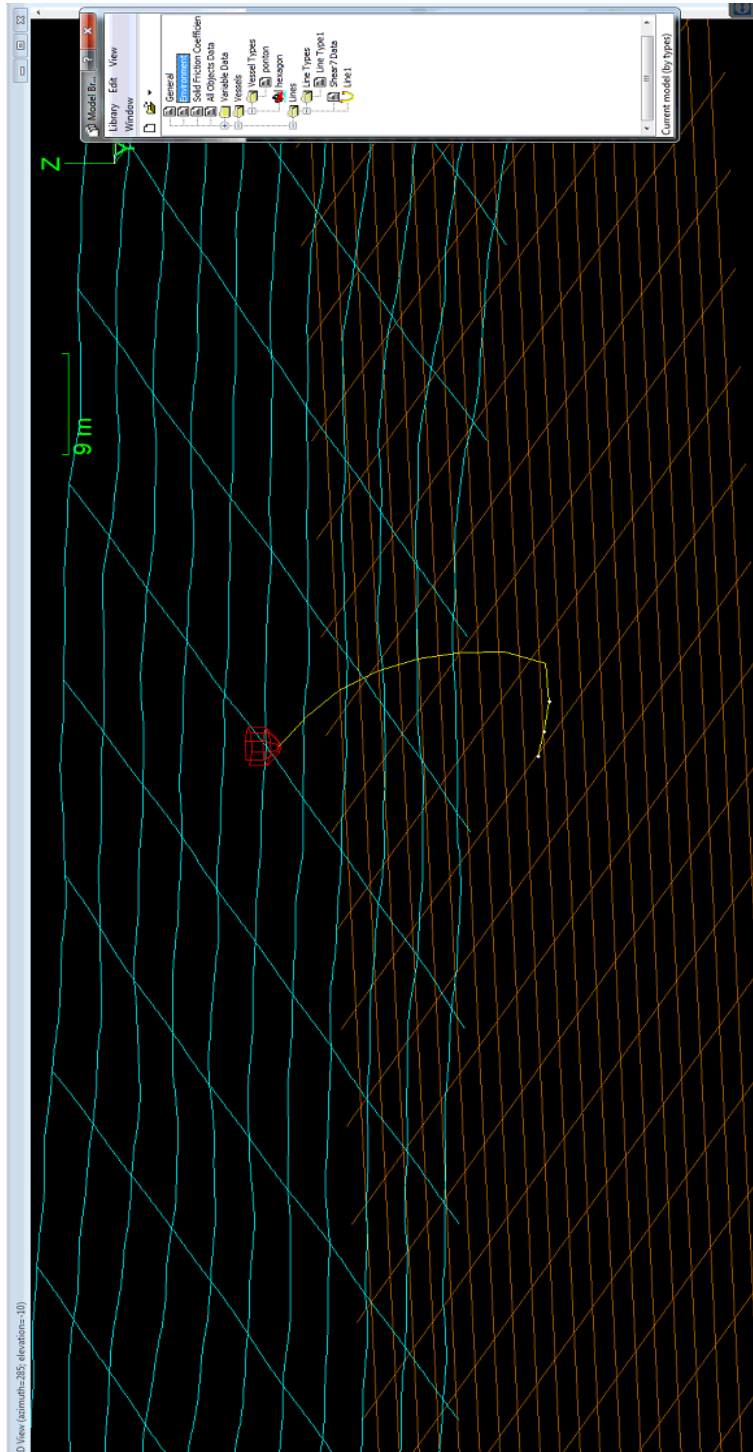


### 1.3 Effective Tension at End B



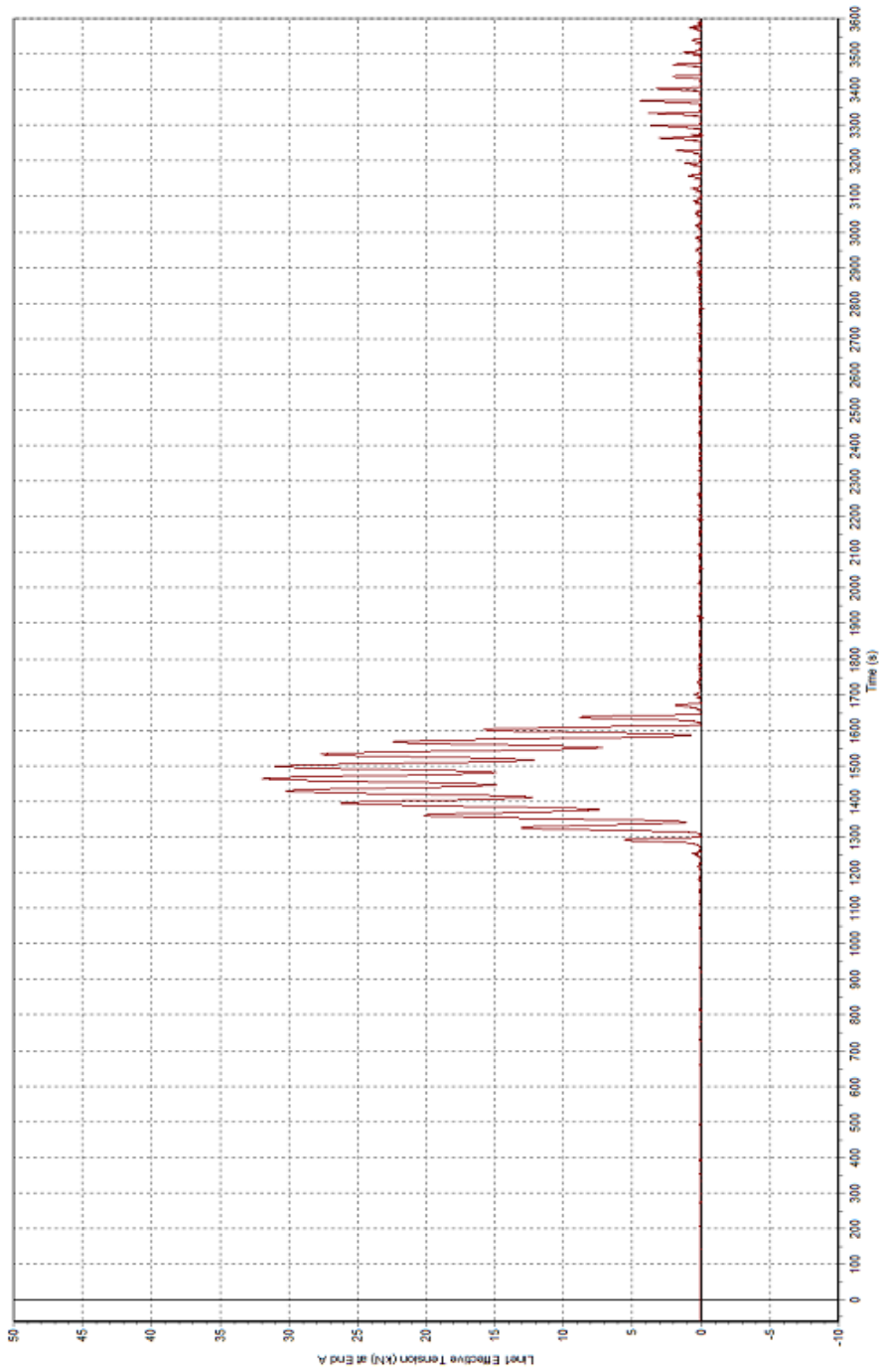
## 2. Heading 30°.

### 2.1 Perspective View of Simulation

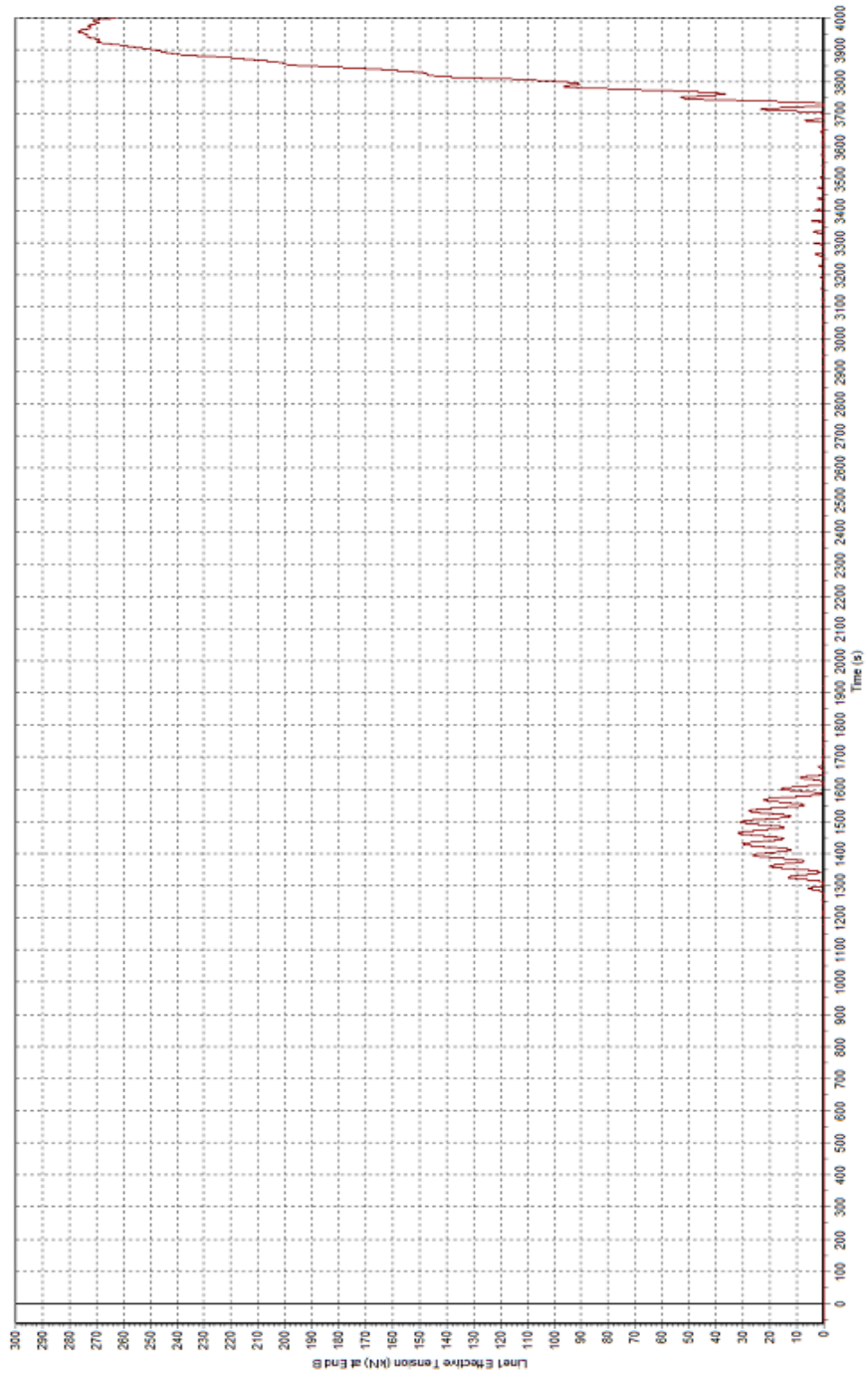




## 2.2 Effective Tension at End A

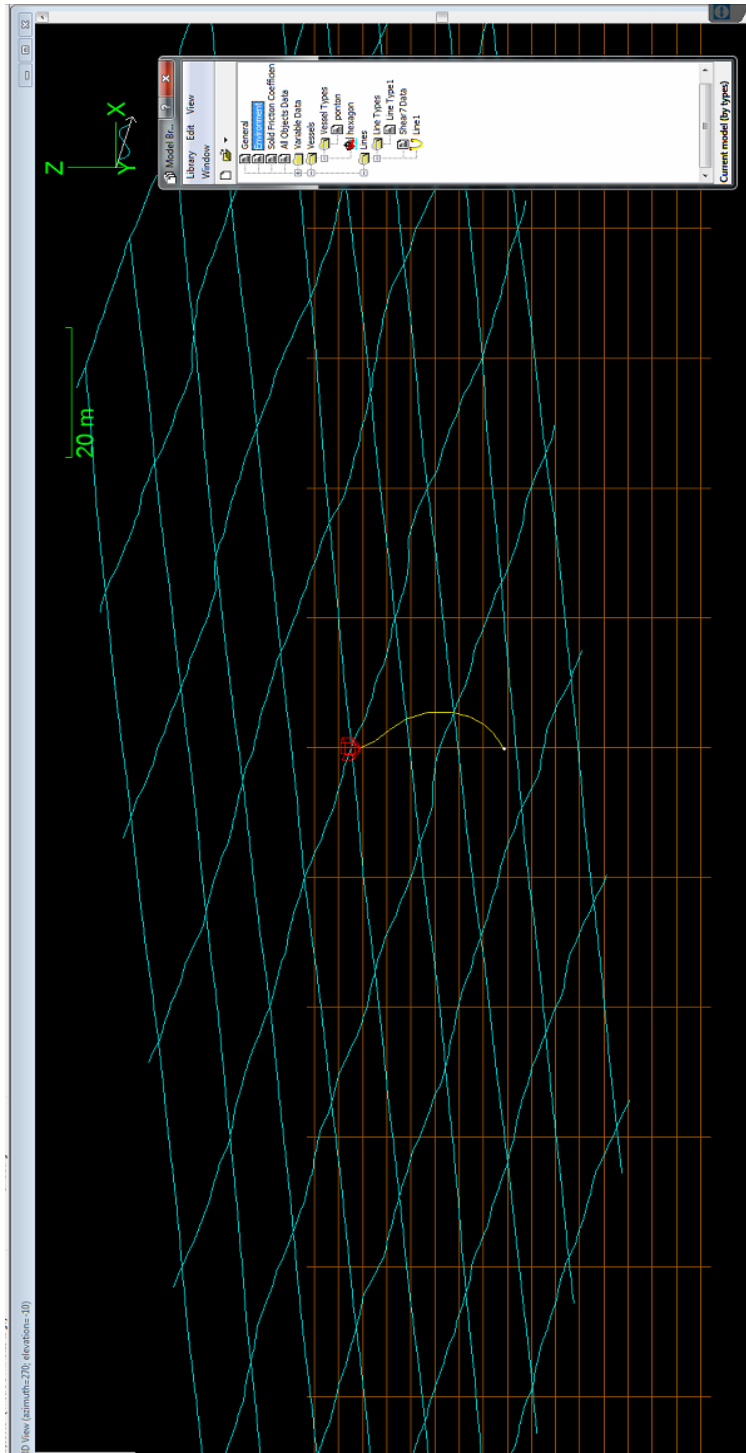


## 2.3 Effective Tension at End B

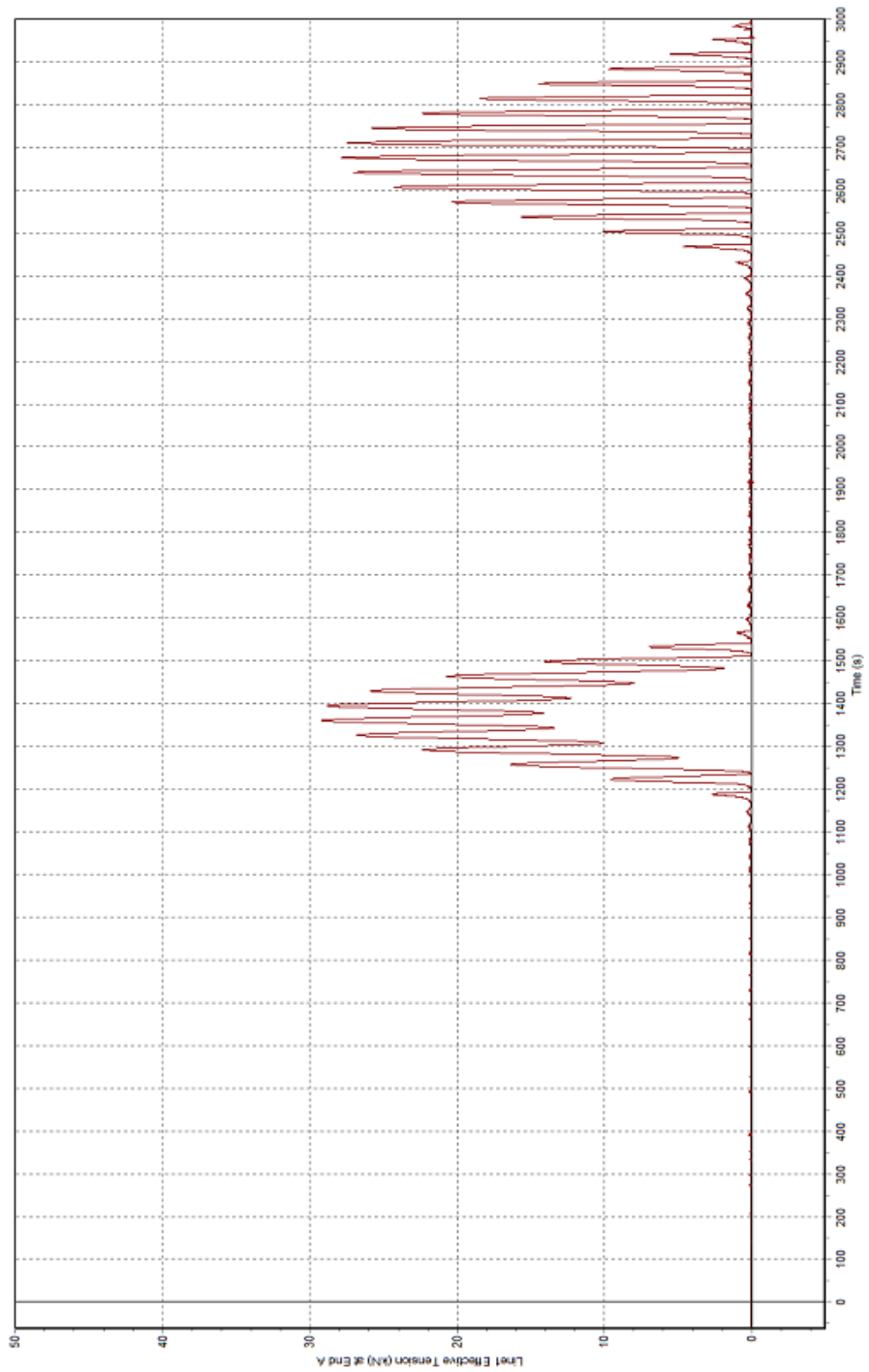


### 3. Heading 60°.

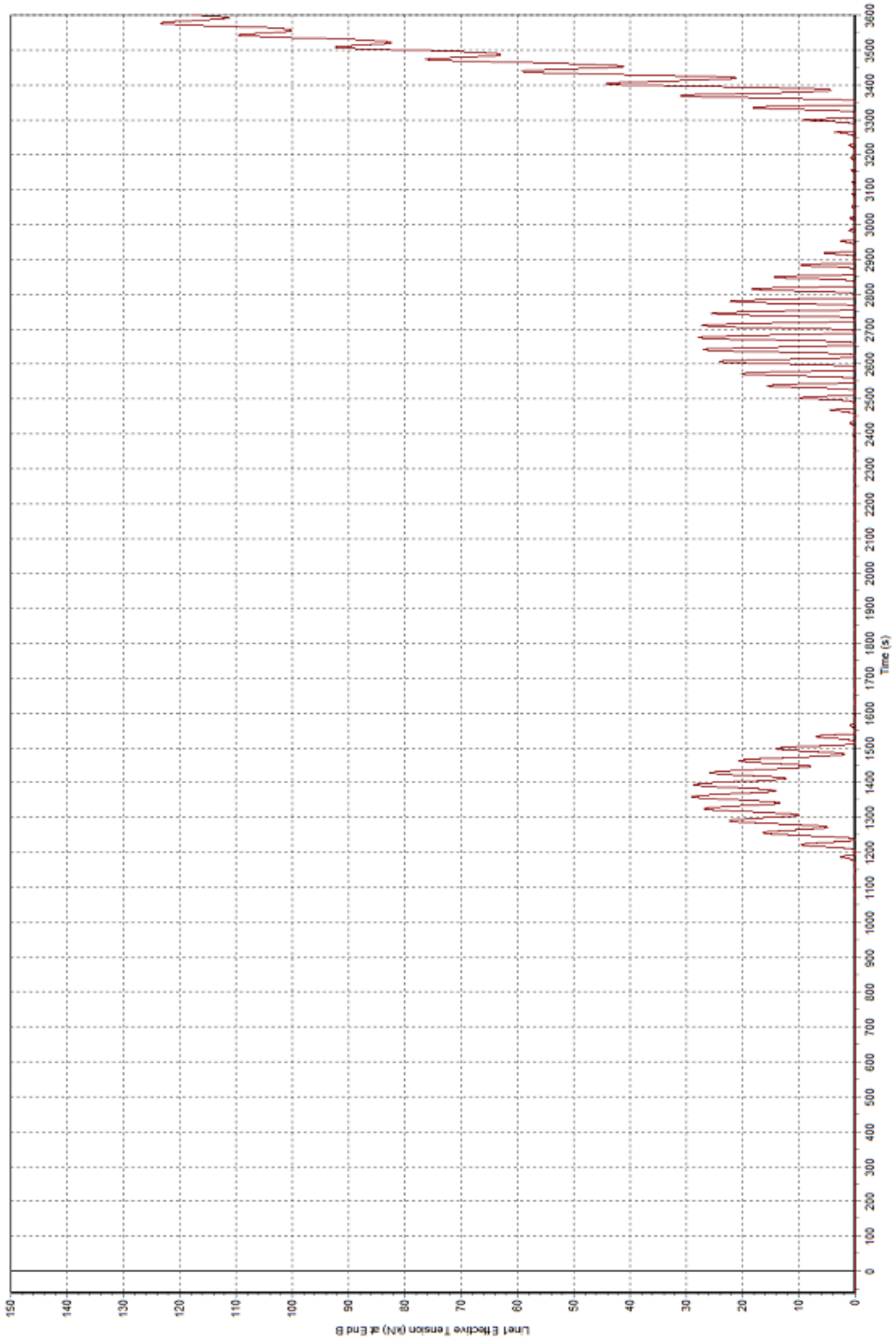
#### 3.1 Perspective View of Simulation



## 3.2 Effective Tension at End A

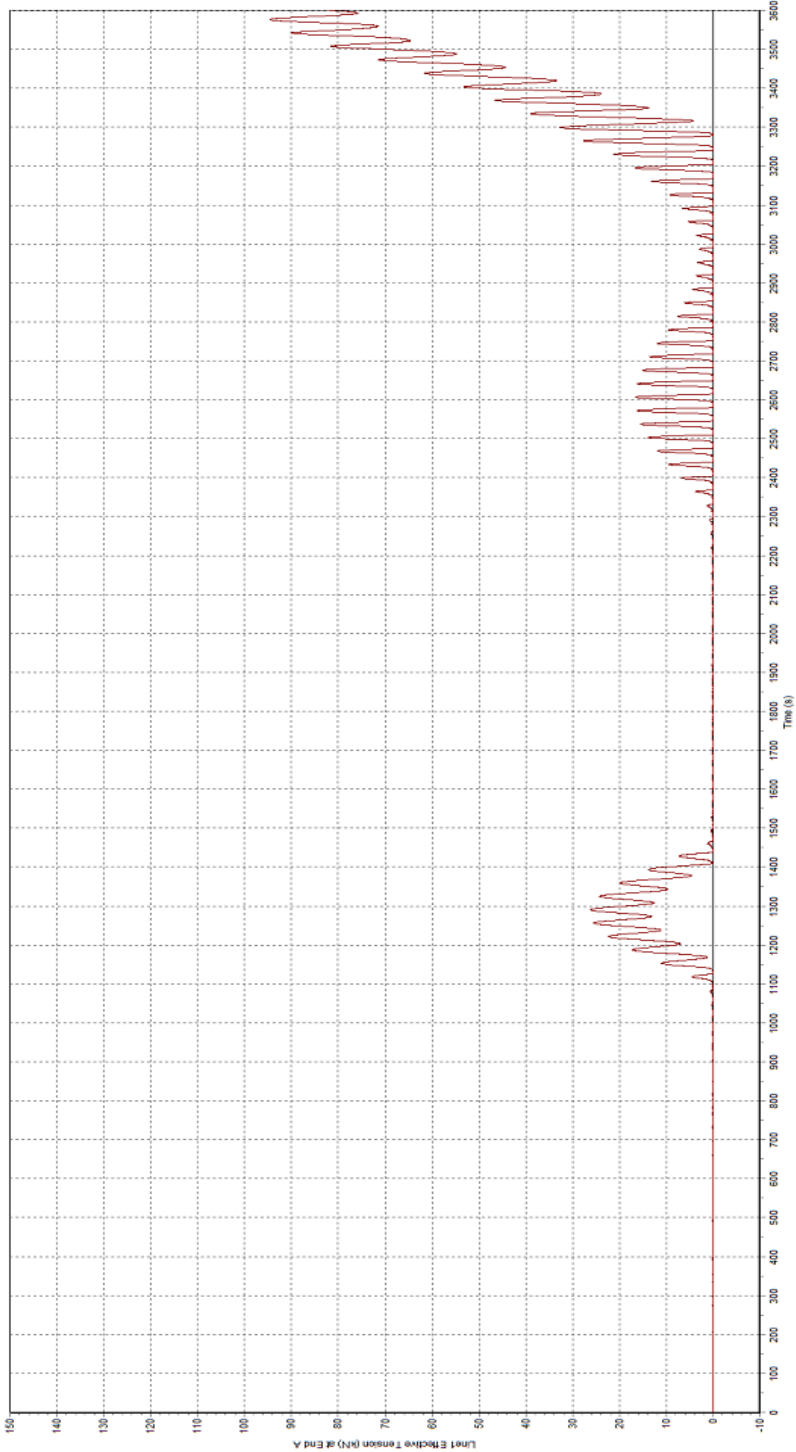


### 3.3 Effective Tension at End B

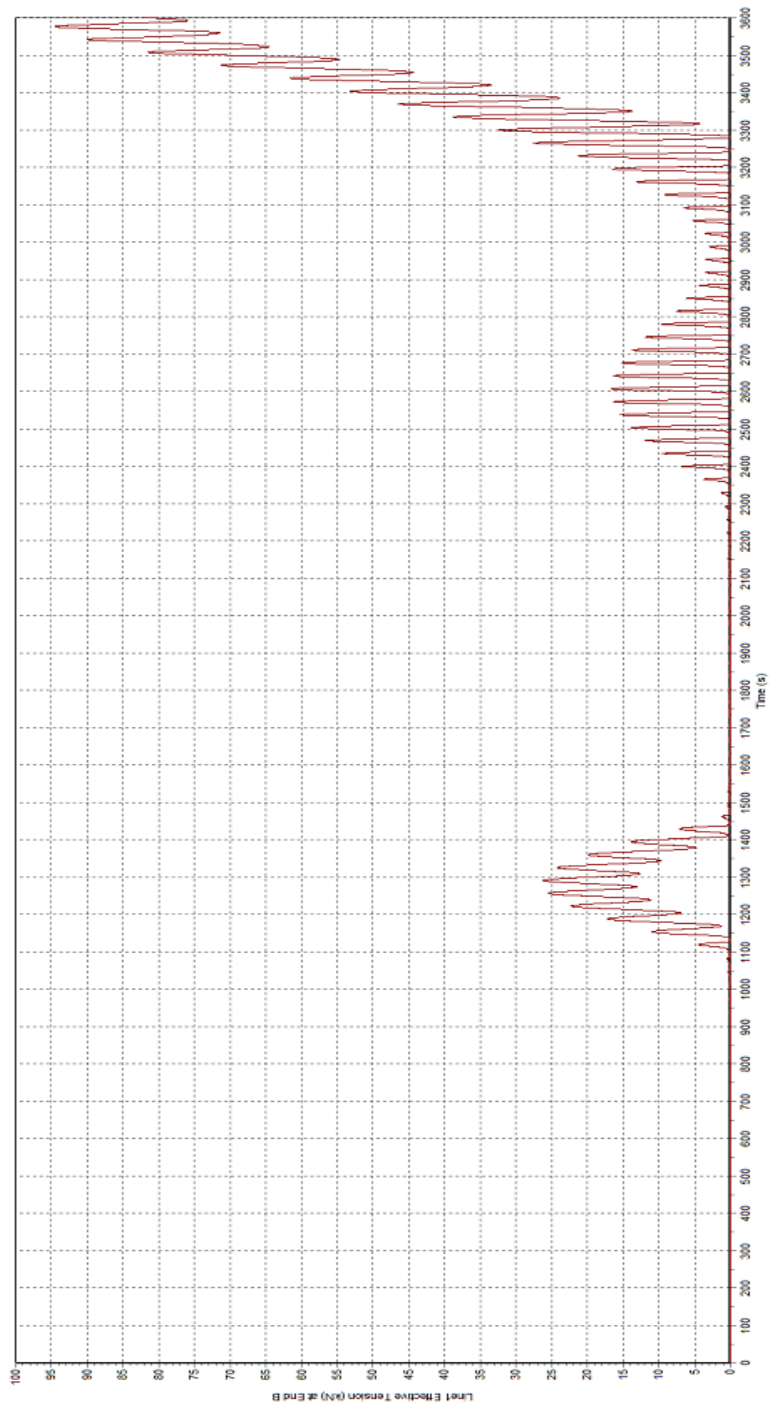




### 4.1 Effective Tension at End A



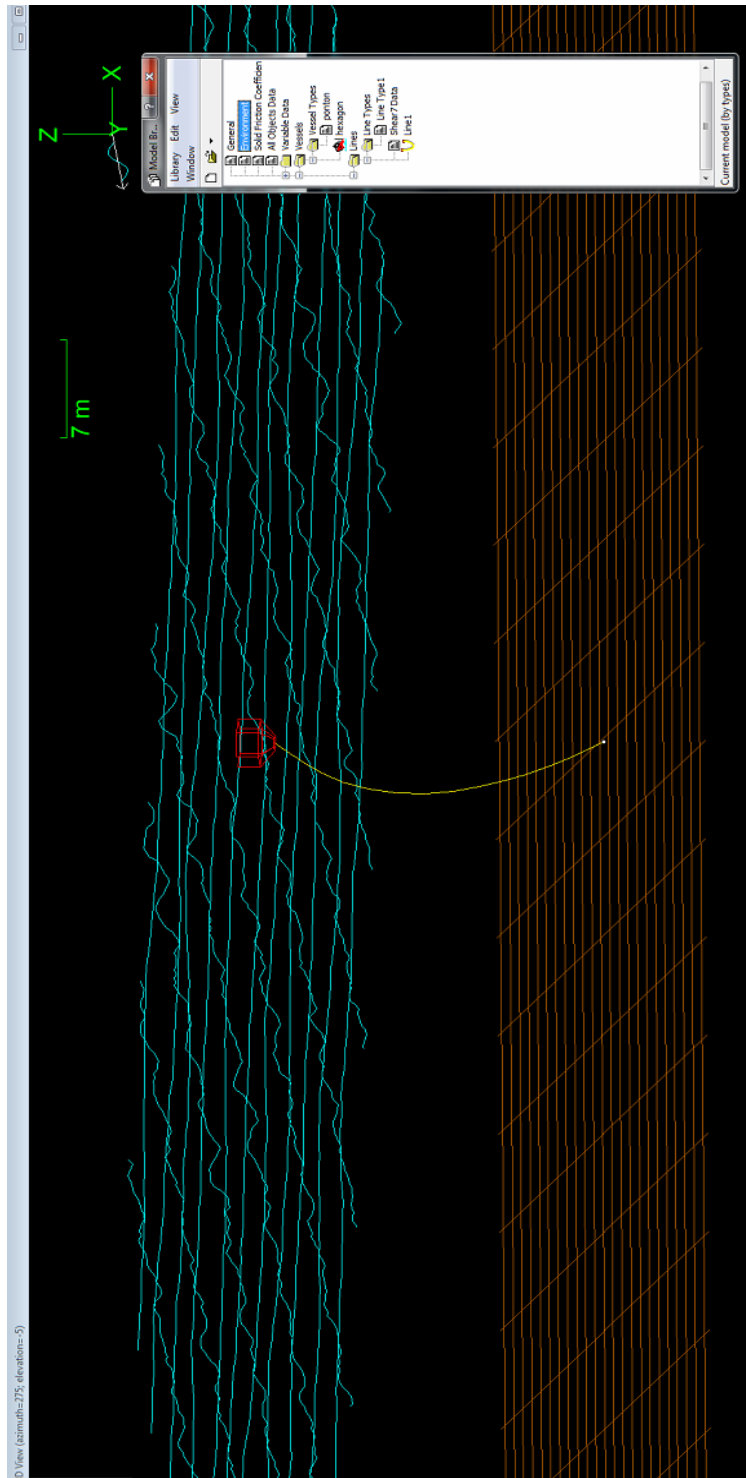
## 4.2 Effective Tension at End B



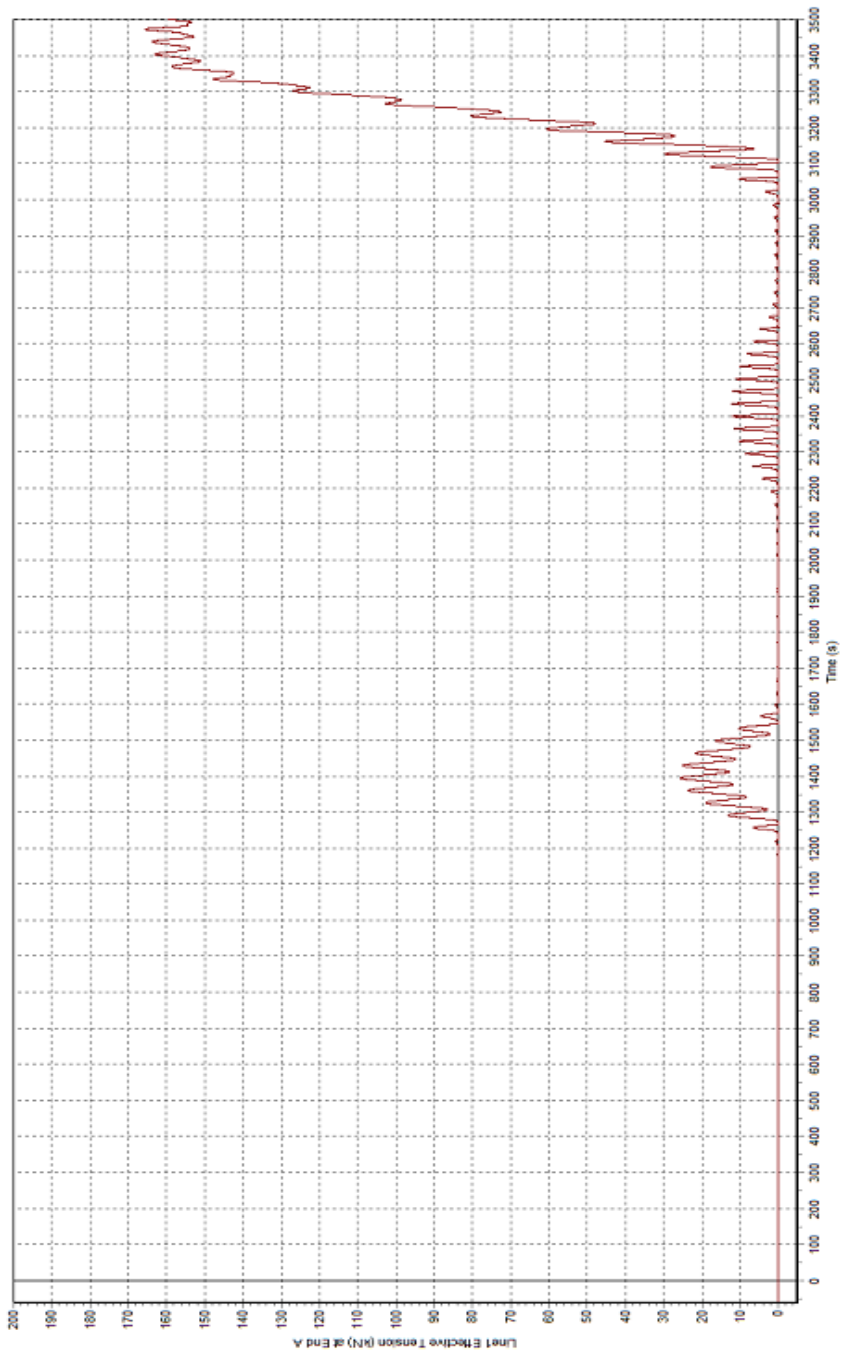


## 5. Heading 120°.

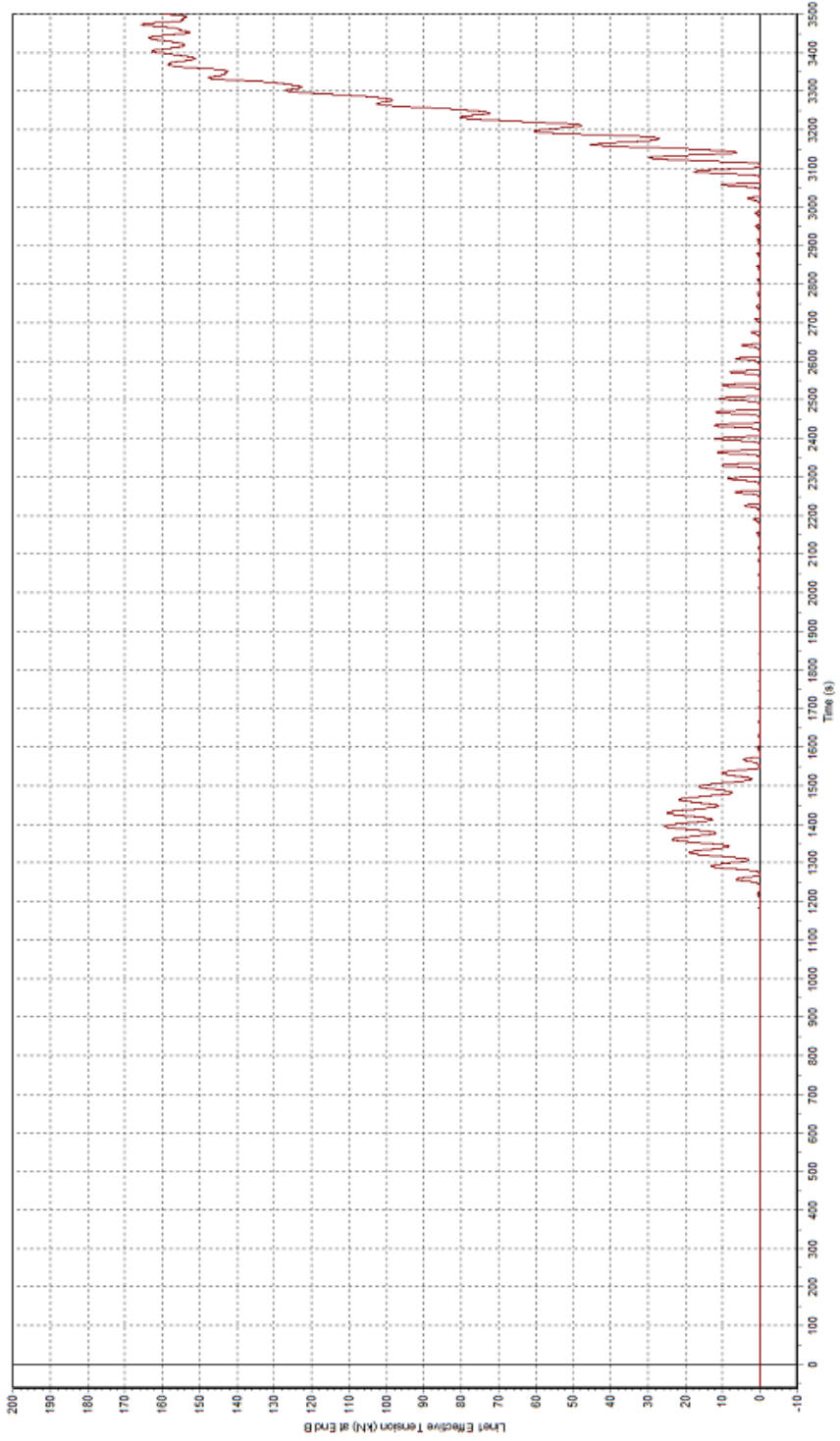
### 5.1 Perspective View of Simulation



## 5.2 Effective Tension at End A



### 5.3 Effective Tension at End B



## h. Mooring Line Specification.

Diameter mm	Circumference in	Weight kg/100mtr	MBL t	MBL kN
8	1	4.0	1.4	13.2
10	1¾	6.3	2.1	20.3
12	1½	9.0	3.0	29.4
14	1¾	12.3	4.1	40.2
16	2	16.0	5.3	51.9
18	2¾	20.3	6.7	65.6
20	2½	25.0	8.3	81.3
22	2¾	30.3	10.0	98.0
24	3	36.0	12.0	117.6
26	3¾	42.3	13.8	135.2
28	3½	49.0	15.8	154.9
30	3¾	56.3	17.8	174.5
32	4	64.0	20.0	196.0
34	4¼	72.3	22.3	218.6
36	4½	81.0	24.8	243.1
38	4¾	90.3	27.3	267.6
40	5	100.0	30.0	294.1
44	5½	121.0	35.8	350.9
48	6	144.0	42.0	411.7
52	6½	169.0	48.8	478.4
56	7	196.0	56.0	549.0
60	7½	225.0	63.8	625.4
64	8	256.0	72.0	705.8
68	8½	289.0	80.8	791.6
72	9	324.0	90.0	882.3
80	10	400.0	110.0	1,078.4
88	11	484.0	131.0	1,284.3
96	12	576.0	156.0	1,509.8
104	13	676.0	182.0	1,784.3
112	14	784.0	210.0	2,058.8
120	15	900.0	240.0	2,352.9
128	16	1,024.0	272.0	2,666.6
136	17	1,156.0	306.0	3,000.0
144	18	1,296.0	342.0	3,352.9
152	19	1,444.0	380.0	3,725.4
160	20	1,600.0	420.0	4,117.6

## AUTHOR BIOGRAPHY



Azzahra Nirwana Islami was a student in the Department of Marine Engineering, Faculty of Marine Technology, Institut Sepuluh Nopember, Surabaya, who specialized in the Marine Manufacturing and Design. She was born in Malang, December 14<sup>th</sup> 1996. She is the first daughter of three siblings. She completed her 12 years of formal education in different cities in Indonesia, then graduated at SMA Negeri 4 Malang before entering university as a sophomore class of 2015. During her first years in university, she became a part of UKM Shorinji Kempo and participated in several regional competitions in Surabaya. She was also a member and staff of Design, Documentation, and Decoration of the event Marine

Icon in 2016 and 2017. She started to volunteer as the staff of Internal Affair Division in the Marine Manufacturing and Design staff in her second year of university. During her second year of volunteering, she participated in the AutoCad Training as a trainer for basic skill learning AutoCad for the sophomore class of 2018 held by Marine Manufacture and Design Laboratory. She did one month of job training at PT Adiluhung Sarasanegara Madura and also two months at PT Najatim Dockyard Surabaya. Throughout her study, she has been interested in the technical designing aspect of the marine industry. For further information, reach to [Azzahranirwana14@gmail.com](mailto:Azzahranirwana14@gmail.com)